


5-2018

## TUMOR IMMUNOTHERAPY: MECHANISMS OF ACQUIRED RESISTANCE AND CHARACTERIZATION OF IMMUNE RELATED TOXICITIES

Ashvin Jaiswal

Follow this and additional works at: [https://digitalcommons.library.tmc.edu/utgsbs\\_dissertations](https://digitalcommons.library.tmc.edu/utgsbs_dissertations)

 Part of the [Genetic Processes Commons](#), [Immunity Commons](#), [Immunopathology Commons](#), [Immunoprophylaxis and Therapy Commons](#), [Medical Biochemistry Commons](#), [Medical Biotechnology Commons](#), [Medical Genetics Commons](#), and the [Medical Immunology Commons](#)

### Recommended Citation

Jaiswal, Ashvin, "TUMOR IMMUNOTHERAPY: MECHANISMS OF ACQUIRED RESISTANCE AND CHARACTERIZATION OF IMMUNE RELATED TOXICITIES" (2018). *The University of Texas MD Anderson Cancer Center UTHealth Graduate School of Biomedical Sciences Dissertations and Theses (Open Access)*. 832.

[https://digitalcommons.library.tmc.edu/utgsbs\\_dissertations/832](https://digitalcommons.library.tmc.edu/utgsbs_dissertations/832)

This Dissertation (PhD) is brought to you for free and open access by the The University of Texas MD Anderson Cancer Center UTHealth Graduate School of Biomedical Sciences at DigitalCommons@TMC. It has been accepted for inclusion in The University of Texas MD Anderson Cancer Center UTHealth Graduate School of Biomedical Sciences Dissertations and Theses (Open Access) by an authorized administrator of DigitalCommons@TMC. For more information, please contact [digitalcommons@library.tmc.edu](mailto:digitalcommons@library.tmc.edu).

**TUMOR IMMUNOTHERAPY: MECHANISMS OF ACQUIRED  
RESISTANCE AND CHARACTERIZATION OF IMMUNE  
RELATED TOXICITIES**

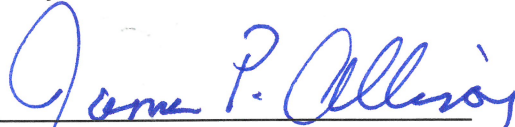
by

**Ashvin R. Jaiswal, B. Pharm., M.S.**

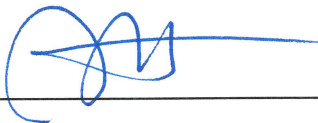
APPROVED:

  
\_\_\_\_\_

Michael A. Curran, Ph.D.  
Advisory Professor

  
\_\_\_\_\_

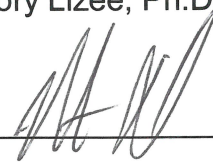
James P. Allison, Ph.D.

  
\_\_\_\_\_

Willem Overwijk, Ph.D.

  
\_\_\_\_\_

Gregory Lizee, Ph.D.

  
\_\_\_\_\_

Michael Davies, M.D., Ph.D.

APPROVED:

\_\_\_\_\_

Dean, The University of Texas  
MD Anderson Cancer Center UTHealth Graduate School of Biomedical Sciences

**TUMOR IMMUNOTHERAPY: MECHANISMS OF ACQUIRED RESISTANCE  
AND CHARACTERIZATION OF IMMUNE RELATED TOXICITIES**

A

DISSERTATION

Presented to the Faculty of

The University of Texas

MD Anderson Cancer Center UTHealth

Graduate School of Biomedical Sciences

in Partial Fulfillment

of the Requirements

for the Degree of

DOCTOR OF PHILOSOPHY

by

**Ashvin R. Jaiswal, M.S.**

Houston, Texas

May, 2018

## Copyright

*Part of the abstract and chapter-3 have been previously published in “\*Bartkowiak T, \*Jaiswal AR, Ager C, Chin R, Chen CH, Budhani P, Reilley MJ, Sebastian, MM, Hong DS and Curran MA, Activation of 4-1BB on liver myeloid cells triggers hepatitis via an interleukin-27 dependent pathway. Clinical Cancer Research, (2018).”*

\*equal contribution

Authors of articles published in AACR journals are permitted to use their article or parts of their article in the following ways without requesting permission from the AACR. All such uses must include appropriate attribution to the original AACR publication. Authors may do the following as applicable: “Submit a copy of the article to a doctoral candidate's university in support of a doctoral thesis or dissertation”.

<http://aacrjournals.org/content/authors/copyright-permissions-and-access>

## Dedication

I would like to dedicate this work to my family for their continuous support. My father, Rameshlal, and my mother, Suman, have been instrumental in believing in me and supporting my passion for science. To my wife, Sapana, and my daughter, Anika, for continuous support and inspiration. Without their support I would not be able to spend long nights to finish this work. I am thankful to my brothers (Sachin and Gajanan), my sister-in-law, Shweta, and my mother-in law, Snehlata for their love and encouragement.

## Acknowledgements

I would like to thank all of my advisors and collaborators at MD Anderson who have mentored me to grow as a scientist. Firstly, I would like to express my sincere gratitude to my advisor Dr. Michael Curran, for his enthusiasm, guidance, and unrelenting support throughout this process. His advice on both research as well as on my career have been invaluable. He has also encouraged and provided me the research environment to grow as an independent scientist. I want to extend my special gratitude to Dr. David Hong who helped me acquire knowledge of clinical studies. He provided me valuable suggestions and helped me understand the clinical aspects of my research work. I am very fortunate to have Dr. James P. Allison, Dr. Willem Overwijk, Dr. Michael Davies, Dr. Steven Ullrich, and Dr. Gregory Lizee on my dissertation committee. They not only provided me with insightful comments and encouragement but also widened my research perspective with tough questions.

I appreciate the guidance and expert opinions of our collaborators Dr. Pratip Bhattacharya, Dr. Eric Davis, Dr. Michael Davis, Dr. Jennifer Wargo, and Dr. Cristina Ivan, who helped me with multiple aspects of the study and provided valuable suggestions.

I would like to acknowledge all of the current and past members of the Curran lab: Todd, Casey, Priya, Anupallavi, Arthur, Natalie, Raven, Chao-Hsien, Renee, Pratha, Krishna, Midan, Dhvani, Courtney, Brittany, and Rachel. I am thankful to coworkers and friends Shivanand, Prasanta,

Rashika, Felix, Spencer, Naveen, Bharat, Sangeeta, Welby, Derek, Stephen, Colm, Nana-Ama, and all of the graduate students. The support from the faculty members of Immunology Graduate Program, staff members of Department of Immunology, and office of Graduate School of Biomedical Sciences (GSBS) were enormous.

Finally, I am thankful to my friends, Kunal, Rahul, Sudarshan, Swapnil, Ujwal and Ashok for their guidance and support, and for being part of every up and down of my graduate school life. You all are like family thousands of miles away from home.

Thank you all.

# **TUMOR IMMUNOTHERAPY: MECHANISMS OF ACQUIRED RESISTANCE AND CHARACTERIZATION OF IMMUNE RELATED TOXICITIES**

**Ashvin R. Jaiswal, M.S.**

**Advisory Professor: Michael A. Curran, Ph.D**

Tumor immunotherapy has shown very promising clinical benefit across an array of cancers; however, two major challenges remain unresolved in the field. First, many patients do not respond to therapy at all or relapse after a period of remission. Second, there are often dose-limiting immune related adverse effects associated with immunomodulation.

In order to understand the mechanisms employed by tumors to evade immunotherapeutic responses, we established a murine model of melanoma designed to elucidate the molecular mechanisms underlying immunotherapy resistance. Through multiple in vivo passages, we selected a B16 melanoma tumor line that evolved complete resistance to combination blockade of CTLA-4, PD-1, and PD-L1, which cures ~80% of mice bearing the parental tumor. Using gene expression analysis, and immunogenomics, we determined the adaptations engaged by this melanoma to become completely resistant to triple combination T cell checkpoint blockade. Acquisition of immunotherapy resistance by these melanomas was driven by the coordinated upregulation of the glycolytic, oxidoreductase, and mitochondrial oxidative phosphorylation pathways to create a metabolically hostile microenvironment wherein T cell functions are suppressed. Together these data indicate that by adapting a hyper-metabolic phenotype,



melanoma tumors can achieve resistance to T cell checkpoint blockade allowing them to escape host immune control.

Increasing the potency of antitumor immunity with immunotherapy disrupts the tightly controlled state of immunologic homeostasis in the body which can lead to reactivation of peripherally-tolerized T cell responses with the potential to mediate uninvited toxicities. Agonist antibodies targeting the T cell co-stimulatory receptor 4-1BB (CD137) are among the most effective immunotherapeutic agents across pre-clinical cancer models. Clinical development of these agents, however, has been hampered by dose-limiting liver toxicity. Lack of knowledge of the mechanisms underlying this toxicity has limited the potential to separate 4-1BB agonist driven tumor immunity from hepatotoxicity. The capacity of 4-1BB agonist antibodies to induce liver toxicity was investigated in wild type and genetically-modified immunocompetent mice. We find that activation of 4-1BB on liver myeloid cells is essential to initiate hepatitis. Once activated, these cells produce interleukin-27 that is required for liver toxicity. CD8 T cells infiltrate the liver in response to this myeloid activation and mediate tissue damage. Co-administration of CTLA-4 and/or CCR2 blockade may minimize hepatitis, but yield equal or greater antitumor immunity.

# Table of Contents

Copyright.....	III
Dedication .....	IV
Acknowledgements .....	V
Table of Contents .....	IX
List of Figures.....	XIV
Chapter 1: General Introduction .....	1
<b>Immunomodulatory Antibodies: Mechanisms of Resistance and Pathophysiology of Immune Related Toxicities .....</b>	<b>1</b>
1.1: Introduction .....	2
1.2: Mechanisms of resistance to checkpoint immunotherapy.....	7
1.2.1: Alteration in antigen presentation and defects in T cell recognition .....	7
a) Antigen presentation .....	7
b) Mutation load and neoantigen burden .....	9
c) TCR repertoire .....	10
d) Tumor cell intrinsic insensitivity to T cell recognition.....	11
1.2.2: Tumor microenvironment (TME) .....	13
a) Hypoxia .....	13
b) Metabolic insufficiency .....	14
c) Tumor-cell-extrinsic immunosuppressive factors .....	17
1.2.3: Enteric microbiome .....	18
1.2.4: Upregulation of alternative immune checkpoints.....	20
1.2.5: Angiogenesis and immune trafficking .....	21
1.3: Overcoming mechanisms of resistance.....	23

1.4: Pathophysiology of immune related adverse effects (IRAEs) .....	26
1.4.1: Dermatological toxicities .....	27
1.4.2: Mucosal and gastrointestinal toxicities .....	28
1.4.3: Hepatotoxicity .....	29
1.4.4: Endocrine toxicities.....	29
1.4.5: Other rare toxicities .....	30

## Chapter 2:

### **Immunotherapy Resistance\_Melanoma Evolves Complete Immunotherapy**

<b>Resistance through Acquisition of a Hyper Metabolic Phenotype .....</b>	<b>32</b>
2.1: Abstract.....	33
2.2: Introduction .....	35
2.3: Methods .....	38
2.3.1: Mice.....	38
2.3.2: Therapeutics antibodies.....	38
2.3.3: Patient cohort .....	38
2.3.4: Cell lines.....	38
2.3.5: Harvesting B16 melanoma.....	39
2.3.6: Generation of checkpoint blockade immunotherapy-resistant melanoma cells.....	39
2.3.7: Treatment strategies and monitoring tumor growth .....	40
2.3.8: RNA extraction .....	41
2.3.9: Microarray analysis.....	41
2.3.10: Bioinformatics analyses .....	41
2.3.11: Extracellular flux analyses .....	42
2.3.12: Immunofluorescence staining and imaging .....	42

2.3.13: Extraction of metabolites and NMR analysis .....	43
2.3.14: Hyperpolarized pyruvate to lactate flux imaging of tumors .....	44
2.3.15: Flow cytometric characterization of resistant tumors.....	45
2.3.16: Retroviral vectors and virus production .....	46
2.3.17: Statistical analysis .....	46
2.4: Results.....	47
2.4.1: B16/BL6 melanoma cells acquired resistance to checkpoint blockade immunotherapy through serial in vivo passage .....	47
2.4.2: Immunotherapy resistant tumors enriched genetic changes to evade immune response .....	51
2.4.3: Resistant melanoma cells acquire a hypermetabolic phenotype to evade checkpoint blockade-mediated immunotherapeutic pressure.....	56
2.4.4: Resistant melanoma tumors adapt to thrive in hostile hypoxic conditions. ....	60
2.4.5: The nutrient-depleted microenvironment of resistant tumors creates unfavorable conditions for anti-tumor immune cells to function.....	63
2.4.6: Monogenic overexpression of PGAM2 and ADH7 in parental tumors confers resistance to checkpoint blockade immunotherapy.....	70
2.4.7: Melanoma patient tumors which fail to respond to immunotherapy show enhanced expression of metabolic pathways resembling 3I-F4 .....	72
2.4.8: Nonspecific therapeutic modulation of tumor metabolism could negatively affect anti-tumor immunity .....	75
2.5: Discussion .....	79

### Chapter 3:

<b>4-1BB Induced Liver Inflammation Activation of 4-1BB on liver myeloid cells triggers hepatitis via an interleukin-27 dependent pathway.....</b>	<b>97</b>
--	-----------

3.1: Abstract.....	98
3.2: Introduction .....	99
3.3: Materials and Methods.....	101
3.3.1: Animals.....	101
3.3.2: Cell lines and reagents .....	101
3.3.3: Therapeutic antibodies .....	101
3.3.4: Immune ablation and reconstitution .....	102
3.3.5: Antibody treatment and liver enzyme analysis .....	102
3.3.6: Tumor therapy .....	102
3.3.7: Treg depletion and adoptive transfer .....	102
3.3.8: Cell isolation .....	103
3.3.9: Flow cytometry analysis.....	103
3.3.10: Immunohistochemistry.....	103
3.2.11: Immunofluorescence staining and imaging .....	104
3.2.12: Real time PCR.....	105
3.2.13: Cytometric bead array .....	105
3.2.14: Statistical analysis .....	105
3.3: Results.....	106
3.3.1: Disparate effects of CTLA-4 and PD-1 checkpoint blockade on $\alpha$ 4-1BB-mediated hepatotoxicity .....	106
3.3.2: 4-1BB agonists initiate liver pathology through activation of liver-resident myeloid cells.....	112
3.3.3: Interleukin 27 is a critical regulator of liver inflammation. ....	121
3.3.4: Regulatory T cells restrict 4-1BB agonist antibody induced liver pathology. ....	125

3.3.5: CCR2 and CXCR3 are differentially required for liver and tumor T cell trafficking.....	131
3.4: Discussion .....	137
Chapter 4:	
<b>General Discussion and Future Directions.....</b>	<b>150</b>
References:.....	157
VITA.....	206

## List of Figures

Figure 1.1 .....	6
Figure 2.1 .....	49
Figure 2.2 .....	54
Figure 2.3 .....	58
Figure 2.4 .....	61
Figure 2.5 .....	66
Figure 2.6 .....	68
Figure 2.7 .....	71
Figure 2.8 .....	73
Figure 2.9 .....	77
Supplemental Figure 2.1 .....	85
Supplemental Figure 2.2 .....	86
Supplemental Figure 2.3 .....	88
Supplemental Figure 2.4 .....	90
Supplemental Figure 2.5 .....	92
Supplemental Figure 2.6 .....	94
Figure 3.1 .....	109
Figure 3.2 .....	118
Figure 3.3 .....	123
Figure 3.4 .....	128
Figure 3.5 .....	134
Figure 3.6 .....	136
Supplemental Figure 3.1 .....	141
Supplemental Figure 3.2 .....	142
Supplemental Figure 3.3 .....	144
Supplemental Figure 3.4 .....	146
Supplemental Figure 3.5 .....	148

## **Chapter 1: General Introduction**

# **Immunomodulatory Antibodies: Mechanisms of Resistance and Pathophysiology of Immune Related Toxicities**



## 1.1: Introduction

After the breakthrough discovery of the first immunotherapeutic agent ( $\alpha$ CTLA-4) that offered a long term survival benefit in metastatic melanoma, the focus of cancer medicine shifted from targeting the tumor itself to harnessing the immune system to eliminate cancer cells. The concept of using one's own immune system to treat cancer was pioneered by Dr. William Coley, who inoculated sarcoma patients with Streptococci to stimulate anti-tumor immune responses against the infected cancer cells (1). The immunosurveillance theory coined by Dr. F. M. Burnet states that immune cells, in addition to defending the host against invasion by microorganisms, can also mediate responses against abnormal cells such as malignant cancer cells, based on their distinct antigenic qualities compared to healthy cells (2). In recent years, the concept of a cancer immunoediting theory, introduced by Dr. Schreiber, describes that immune cells not only eliminate tumor cells but also shape their immunogenicity and clonal diversity through immuno-selection (3-5). Anti-tumor immunity affects tumor growth and progression in three sequential phases: elimination, equilibrium and escape (3E) (3-5). First, immune cells try hard to eliminate cancer cells through immune mediated cell death. This is followed by the second phase where tumor cells establish an equilibrium with the immune system by hiding from immune attacks and creating an immunosuppressive tumor microenvironment (TME) (3-5). In the last stage, a highly immunosuppressive niche assists tumor cells to escape anti-tumor immune attack (3-5). T cells make major contributions in the immunosurveillance and immunoediting processes. Tumors evade immune attack

largely by escaping T cell mediated cell death. Hence, improving T cell responses has been the recent focus of the tumor immunology field.

T cell activation involves the binding of T cell receptor (TCR) to antigen, presented in the context of major histocompatibility complex (MHC) I or II, on antigen presenting cells (APCs). TCR activation also requires a second co-stimulatory signal mediated by the binding of CD28 on the T cell surface to B7-1 (CD80) or B7-2 (CD86) present on APCs(6). As a negative feedback loop, activated T cells increase CTLA-4 expression on their cell surface. Seminal work from Dr. James P. Allison and colleagues showed that CTLA-4, which also belongs to the B7 family of receptors, competitively inhibits the binding of B7 molecules to CD28 and inhibits T cell activation and proliferation (7). CTLA-4 blockade with anti-CTLA-4 antibodies blocks CTLA-4 binding to B7-1/-2, which are then freely available to bind to costimulatory CD28 molecules and provide a second stimulatory signal for T cell-mediated immune responses (6). CTLA-4 was the first immune checkpoint blockade therapy approved by Food and Drug Administration (FDA) for unresectable stage III and IV metastatic melanoma. In about 20% of melanoma patients,  $\alpha$ CTLA-4 therapy provides long term survival benefit (8-10).

Another extensively studied immune checkpoint receptor that regulates activation and effector function of CD8 T cells is the programmed death 1 (PD-1) receptor. PD-1 on T cells, after engagement by its ligands (PD-L1 and PD-L2) on tumor cells or hematopoietic cells, becomes phosphorylated (11). The cytoplasmic domains of PD-1, an immune-receptor tyrosine-based inhibitory motif (ITIM) and an immunoreceptor tyrosine-based switch motif (ITSM), when phosphorylated, recruit protein tyrosine phosphatases (SHP1 and SHP2) (12) which ultimately

dephosphorylate T cell signaling molecules, Lck and ZAP70 (11,12). Lck and ZAP70 are part of the TCR-CD28 downstream signaling cascade and dephosphorylation leads to inhibition of T cell activation and function (11). Blocking the PD-1/ PD-L1 axis has been shown to increase antitumor immune response in various preclinical tumor models. PD-1 blocking antibodies have achieved substantial success in clinic offering long term survival advantages in an array of tumor types leading to their FDA approval to treat melanoma (8,13), non-small cell lung cancer (NSCLC) (14-16), renal cell carcinoma (RCC) (17), Hodgkin lymphoma (18,19), urothelial carcinoma (20), Merkel cell carcinoma, and head and neck SCC (21,22). Similarly, PD-L1 blocking antibodies have shown promising clinical results and are gaining approval for an expanding array of indications (22). There are other T cell checkpoint receptors such as TIM3, LAG3, and VISTA, which have shown anti-tumor immune response in preclinical studies and are under clinical investigation (23).

TCR activation through co-signaling is a tightly regulated process. Along with co-inhibitory checkpoint receptors, T cells also possess co-stimulatory receptors on their surface which positively regulate T cell responses (24). CD28, a member of the immunoglobulin superfamily (IgSF), is the most well characterized co-stimulatory receptor , which up-regulates cell-survival genes and fosters expansion of antigen-specific T cells into effector and memory phenotypes (24). CD28 signaling enhances the production of interleukin-2 (IL-2), IFN- $\gamma$ , TNF $\alpha$  and other cytokines. Most of the other co-stimulatory molecules on T cells belong to the tumor necrosis factor receptor superfamily (TNFRSF) such as 4-1BB (CD137/TNFRSF9), GITR (CD357/ TNFRSF18) and OX40 (CD134/ TNFRSF4).

These molecules have structural similarities to CD28 and drive co-stimulatory functions (24). Agonist antibodies targeting 4-1BB (CD137/TNFRSF9) and OX40 have shown promising preclinical results and are under evaluation in ongoing clinical trials (25,26).

Immunomodulatory receptors (co-inhibitory and co-stimulatory) maintain immune homeostasis in the body (27). Checkpoint receptors on T cells are negative feedback mechanisms which the body uses to shut down the immune response after an infection/tumor is eliminated. Anti-checkpoint receptor antibodies or agonist antibodies targeting co-stimulatory molecules disturb immune homeostasis and can lead to immune-related adverse events (IRAEs), in dermatologic, gastrointestinal, hepatic, endocrine, and other tissues (28). Steroids are used in the clinic to manage immune related adverse events (IRAEs), but due to their immunosuppressive nature, steroids may compromise the anti-tumor immune response (27). Detailed understanding of immune resistance and the mechanisms underlying IRAEs will help facilitate design of new therapeutic strategies to overcome resistance to immunotherapy without the associated immune toxicities. This chapter reviews the current and ongoing work focused on understanding mechanisms driving resistance to immunotherapy and pathophysiology of immune related toxicities associated with immunomodulatory antibodies.

Figure 1.1

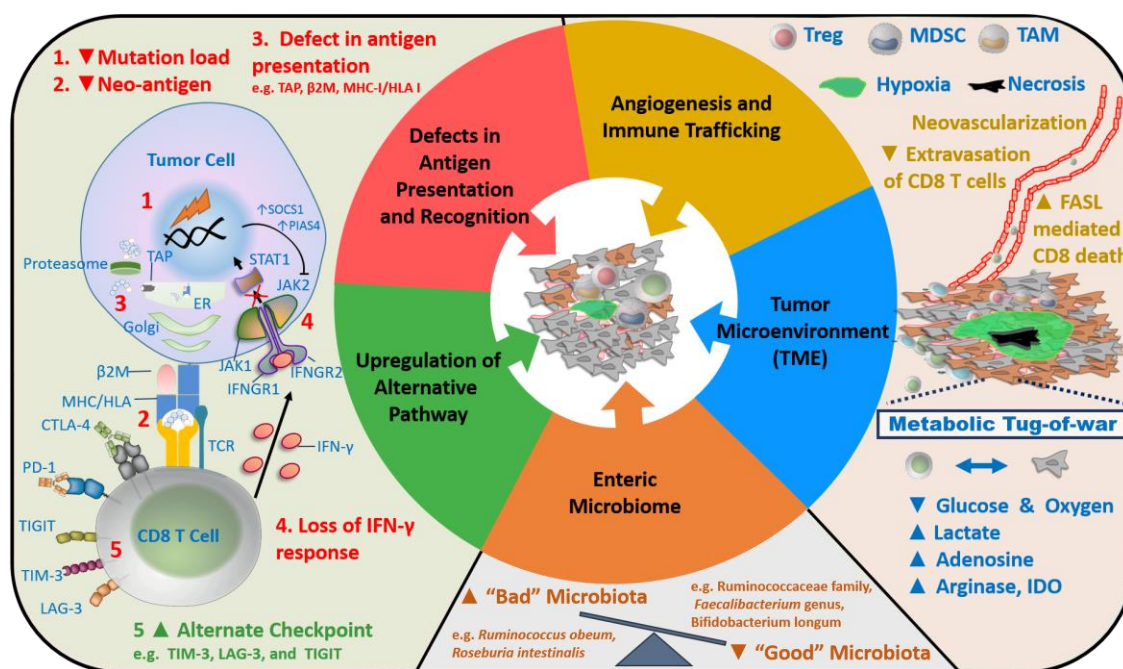


**Figure 1.1: Emerging mechanisms of resistance to checkpoint blockade immunotherapy.**  $\beta$ 2M= $\beta$ -2-microglobulin, CANX=calnexin. CTLA-4= cytotoxic T-lymphocyte-associated protein-4, ER=endoplasmic reticulum, FasL=ligand for FAS receptor, IFN- $\gamma$ =interferon gamma, IFNGR=IFN  $\gamma$  receptor, JAK=Janus kinase, LAG3=Lymphocyte-activation gene-3, PD-1= program cell death protein-1, PIAS4=protein inhibitor of activated STAT4, SOCS1=suppressor of cytokine signalling-1, STAT=signal transducer and activator of transcription, TAP=transporter associated with antigen processing, TCR=T-cell receptor, TIGIT=T cell immunoreceptor with Ig and ITIM domains, and TIM-3= T-cell immunoglobulin and mucin-domain containing-3.

## **1.2: Mechanisms of resistance to checkpoint immunotherapy**

There are large ongoing efforts to understand the mechanisms of resistance to immunotherapy. A number of escape pathways engaged by tumor cells in order to evade immunotherapeutic pressure have been described such as altering antigen presentation and recognition, creating an immunosuppressive microenvironment, upregulating alternative checkpoint receptors of effector CD8 T cells, and other pro-tumor mechanisms (Figure 1.1).

### ***1.2.1: Alteration in antigen presentation and defects in T cell recognition***

The success of the adaptive immune response relies on the recognition of antigen by T cell receptors (TCR). To prime the T cell mediated immune response, T cells have to recognize the antigen presented as a peptide on major histocompatibility complex (MHC-I or II) molecules through TCR. The intensity of the T cell mediated immune response depends on the multi-step process and quality of interaction between TCR and peptide MHC complex. Tumor cells hijack these processes at various stages to evade the immune response by downregulating or mutating antigen presentation machineries, and/or by eliminating CD8 T cells from the TME. In addition to this, tumor intrinsic genetic changes further enable tumor cells to become resistant to T cell mediated killing.

#### ***a) Antigen presentation***

The protein antigens in cancer cells undergo proteasomal degradation to produce peptides ranging from 8 to 11 amino acids in length (29). The resulting peptides are transported to the endoplasmic reticulum (ER) where they are loaded

onto MHC-I molecules (29). The peptide MHC-I complex then shuttles to the cell surface where they are recognized by TCR on CD8 T cells (29). CD8 T cells scan peptide MHC complexes on normal, infected and cancer cells. CD8 T cells eliminate infected cells that present foreign antigens and cancer cells that present neo-antigens (29). Normal cells remain safe from CD8 mediated killing since they present self-antigens (29).

MHC-I in humans is also known as human leukocyte antigen (HLA) class I. A heavy-chain and beta-2-microglobulin ( $\beta$ 2M) are crucial protein domains for the successful assembly of HLA class I complexes (30). Cancer cells are shown to alter  $\beta$ 2M to escape immune responses either by mutation, deletion or loss of heterozygosity (LOH). Giannakis et al. showed that along with  $\beta$ 2M, other genes in antigen presentation machinery (APM) were also altered in colorectal cancer (CRC) patients (31). They have identified 96 different mutations in 11% of patients which correlated with immune infiltration (31). They have also observed mutations in other APM pathways like protein folding process (CANX and HSPA5), the endoplasmic reticulum (ER) and peptide loading complexes (TAP, TAPBP, CALR and PDIA3) which also showed correlation with immune infiltration (31). Sade-Feldman et al. showed metastatic melanoma patients treated with checkpoint blockade immunotherapy (anti-CTLA-4, anti-PD1) acquired resistance through the loss of  $\beta$ 2M either by point mutations, deletions or loss of heterozygosity (LOH). In a separate validation cohort,  $\beta$ 2M LOH events were significantly enriched in about 29% of patients who did not respond to anti CTLA-4 therapy. These patients also showed a strong association between  $\beta$ 2M LOH and poor overall survival. Similarly, in the second validation cohort of patients who did not respond

to anti-PD-1 therapy,  $\beta$ 2M LOH was significantly associated with worse overall survival. Jesse Zaretsky and Antoni Ribas, in a recent study showed that acquired resistance to anti PD-1 therapy was associated with deletion in the  $\beta$ 2M component in a late-relapse patient with metastatic melanoma. Together, all the studies suggest that in order to elicit a successful response to checkpoint blockade immunotherapy, an efficient tumor antigen presentation pathway is needed. Tumor cells have the ability to alter these pathways and evade therapeutic responses.

*b) Mutation load and neoantigen burden*

Effector T cells distinguish cancer cells from healthy tissue based on the antigen presented on their surface. Healthy cells present self-antigens for which potentially reactive T cells have been tolerated. (32). On the other hand, cancer cells acquire tumor-specific mutations which results in the formation of novel protein sequences and potential MHC loading of neoantigen peptides (32). Effector T cells recognize these neoantigen peptide-MHC complexes and generate tumor specific immunity. The strength of tumor specific antitumor T cell immunity depends on the quantity and quality of mutation loads and resulting neoantigen peptides (32).

By using whole-exome sequencing, Rizvi and colleagues showed that a high nonsynonymous mutation burden is associated with improved objective clinical responses, durable clinical benefit, and progression-free survival in non-small cell lung cancers (NSCLC) treated with anti-PD-1 antibodies (33). Several other studies have highlighted the importance of neoantigens along with mutational landscapes in recognition of cancer cells by the immune system and mediating immunotherapy response (4,32,34-36). McGranahan et al. also highlight the role



of heterogeneity of intratumoral neoantigens on anti-tumor immune response following anti-CTLA-4 and anti-PD-1 therapy in advanced lung cancer and melanoma. Moreover, many tumors are non-immunogenic in nature since they have a low neo-antigenic mutational load resulting in natural (primary) resistance to immunotherapy (37). These studies together suggest that tumor cells acquire resistance to immune mediated attack by decreasing expression of mutated genes and resulting neo-antigen peptides

The mutational landscape/neoantigen burden could be used to design therapeutic strategies such as neoantigen peptide vaccination to reverse resistance. Using a peptide immunization approach, Uger Sahin and colleagues showed the beneficial effects of immunization with neoantigen peptide vaccine in combination with checkpoint immunotherapy in a preclinical B16 melanoma model. The current research focus in the field is predicting immunotherapy responses using mutational landscape/neoantigen burden, applying the knowledge to reverse resistance using therapeutic approaches such as peptide or RNA vaccination, and inducing changes in the mutational landscape of non-immunogenic tumors using chemotherapy and/or radiotherapy.

### **c) TCR repertoire**

The success of checkpoint blockade immunotherapies depends on the clonal diversity and number of tumor specific cytotoxic T cells within the tumor microenvironment. There is evidence which suggests that high mutational landscape and neoantigen burden cannot ensure the presence of cytotoxic T cells in the tumor microenvironment (38). Moreover, patients who relapsed on anti-CTLA-4 and anti-PD-1 therapy responded to adoptive T cell transfer (ACT) (39).

Together, these findings suggest that an abundance of T cells in tumor microenvironment is equally important in mediating antitumor immune responses (38,39).

Several tumor intrinsic oncogenic pathways have been identified which are involved in exclusion and elimination of tumor specific CD8 T cells from the tumor microenvironment. BRAF inhibition increases CD8 T cell infiltration in melanoma, which otherwise was inhibited by persistent tumor specific activation of mitogen-activated protein kinase (MAPK). Tumor intrinsic activation of MAPK triggers release of interleukin-8 (IL-8) and vascular endothelial growth factor (VEGF) which inhibits CD8 T cells trafficking into tumors (40). Oncogenic loss of PTEN, a tumor suppressor gene, activates PI3 kinase and increases the expression of immunosuppressive cytokines on tumor cells which, ultimately, inhibits T cell-mediated tumor killing and decreases T-cell trafficking into tumors (41). In a preclinical mouse melanoma model and in human metastatic melanoma samples, constitutive activation of the WNT/ $\beta$ -catenin signaling pathway resulted into tumor T-cell exclusion and resistance to anti-PD-L1/anti-CTLA-4 monoclonal antibody therapy (42). In addition, mouse tumor models also show that WNT/ $\beta$ -catenin activation leads to a decrease in CD103+ DCs in the tumor microenvironment which negatively impacts cytotoxic CD8 T cell abundance and clonal diversity (42). These studies suggest that tumors use intrinsic oncogenic pathways to reduce infiltration and clonal diversity of antigen-specific CD8 T cells in TME.

d) Tumor cell intrinsic insensitivity to T cell recognition

Checkpoint blockade immunotherapy increases cytolytic cytokines like interferon- $\gamma$  (IFN $\gamma$ ), granzymes, perforin, and tissue necrosis factor  $\alpha$  (TNF- $\alpha$ ) on

effector CD8 T cells (43,44). Effector CD8 cells deliver these cytolytic cytokine loads to target tumor cells and induce T cell mediated cell death (44). T cell derived IFN $\gamma$  restrains cancer cell growth directly by inducing anti-proliferative and pro-apoptotic effects, as well as indirectly by enhancing tumor antigen presentation through MHC-I upregulation, which ultimately increases recruitment of antitumor immunity. However, persistent exposure to IFN $\gamma$  can drive STAT1-related epigenomic and transcriptomic changes in cancer cells and augment alteration in interferon-stimulated genes (45). Gao and colleagues have shown that loss in IFN $\gamma$  pathways drives the resistance mechanisms to anti-CTLA-4 therapy. Melanoma patients who failed to respond to anti-CTLA-4 therapy accumulated copy number alterations and genomic loss of IFN- $\gamma$  pathway genes such as IFNGR1, IRF1, JAK2, and IFNGR2 (46). In preclinical studies, anti-CTLA4 therapy could not deliver therapeutic benefit to B16 murine melanoma tumors lacking IFNGR1 (46), while the wild type cell line is known to be anti-CTLA-4 sensitive (47). Sucker et al. showed that human melanoma patients who have a mutation in JAK1/2 are resistant to IFN- $\gamma$  induced cell death (48). The loss of IFN- $\gamma$  pathway genes, such as JAK1 and JAK2, are shown to be also associated with resistance to anti-PD-1 therapy (49). Tumor cell escape of interferon mediated cell death by down regulating interferon pathways additionally results in downregulation of IFN-induced PD-L1 expression on tumor cells (45). PD-L1 negative tumors could also fail to respond to anti-PD-1 and anti-PD-L1 therapy. Therefore, genetic defects in the IFN- $\gamma$  pathway could represent one of the mechanisms of acquired resistance to checkpoint therapies (46,49).

### **1.2.2: Tumor microenvironment (TME)**

A tumor is not just a mass of cancerous cells, but consists of a complex of cancerous and noncancerous cellular structures along with their extracellular milieu, which together create the tumor microenvironment (TME). Tumor cells influence the microenvironment by releasing extracellular signals, depleting nutrients, creating a state of hypoxia, promoting angiogenesis, and recruiting tumor promoting cells like cancer associated fibroblasts (CAF) or suppressive myeloid stroma (myeloid derived suppressor cells (MDSC)). The tumor microenvironment creates unfavorable conditions for effector T cells to function, which could also potentially mediate acquired resistance to checkpoint immunotherapy (Figure 1.1).

#### **a) Hypoxia**

Tumor cells create a state of hypoxia by depleting oxygen from the tumor microenvironment, often by increasing mitochondrial oxidative phosphorylation which induces expression of the hypoxia-inducible factors (HIFs) transcription factor family. HIF-1 $\alpha$  and HIF-2 $\alpha$ , in turn, induce hypoxia responsive genes in tumor cells and help them adapt to the self-created hypoxic condition. The role of hypoxia is well characterized in tumorigenesis and angiogenesis. Emerging research also suggests its role in mediating resistance to immunotherapeutic drugs (50). In hypoxic conditions, tumor cells also switch to glycolytic metabolism, releasing lactic acid and creating an acidic tumor microenvironment. The low oxygen and acidic pH decrease T cell activation, proliferation and cytotoxicity (50-54). Hypoxic tumors secrete miR-210, which ultimately inhibits cytotoxic T cell mediated killing of target cells. Additionally, T cells induce HIF-1 $\alpha$  in response to

hypoxia, which induces cell intrinsic immunosuppressive changes in T cells (50,55).

Hypoxia induces the production of immunosuppressive cytokines like interleukin-10 (IL-10), interleukin-6 (IL-6), transforming growth factor- $\beta$  (TGF- $\beta$ ) and Arginase by myeloid derived suppressor cells (MDSC), Tumor associated macrophages (TAM), cancer associated fibroblasts (CAF), and stromal cells. Through its effect on multiple cell types in the TME, hypoxia reduces the therapeutic benefits of immunotherapy. Thus, targeting hypoxia in combination with immunotherapy has shown synergistic effects in preclinical studies (56,57). Prostate tumors are considered non-immunogenic (immunologically cold) tumors and they fail to respond to checkpoint immunotherapies. We have recently shown that the hypoxia-activated prodrug TH-302 not only ablates hypoxia but also sensitizes TRAMP-C2 prostate tumors to checkpoint immunotherapy (56). A combination of TH-302 and T cell checkpoint blockade therapy showed synergistic survival benefit in highly aggressive prostate adenocarcinoma (56). Scharping et al. also showed beneficial effects of ablating hypoxia in a B16 melanoma model when combined with anti PD-1 therapy (57).

#### *b) Metabolic insufficiency*

Tumor cells create a hostile microenvironment for immune cells to function. Tumor cells deplete the microenvironment of glucose, oxygen, glutamine, and tryptophan while enriching it with lactate. The combination of low glucose and high lactate creates unfavorable conditions for cytotoxic CD8 T cells where they lose their metabolic fitness and associated effector functions. However, regulatory T

cells thrive under low glucose and high lactate conditions and become more immune suppressive (58).

Under conditions of chronic antigen stimulation such as cancer and chronic virus infection, CD8 T cells have demonstrated exhaustion even in the absence of immune checkpoint molecules, which raises the argument on the role of other T cell intrinsic pathways in executing CD8 effector functions (59,60). After antigen encounter T cells differentiate into effector phenotypes where they proliferate, activate, and carry out effector function through producing cytokines and delivering them to target cells. T cell activation, proliferation and execution of cytotoxic effector functions are energy demanding processes requiring metabolic fitness. T cells switch to glycolytic metabolism to meet these metabolic demands (61-63). After resolving infections or eliminating tumors, these cells go back to mitochondrial oxidative phosphorylation and fatty acid oxidation, which also play important roles in generating T cell memory (64,65). However, recent work from Delgoffe and colleagues also emphasizes the importance of mitochondrial mass in regulating effector CD8 T cell function (66, 67). Tumors create a chronic metabolic deficiency in the microenvironment in which infiltrating CD8 T cells lose PPAR-gamma coactivator 1 $\alpha$  (PGC-1 $\alpha$ ), which controls mitochondrial biogenesis (66). The persistent loss of mitochondrial function and mass causes T cells to adapt an overall phenotype of metabolic insufficiency resulting in loss of effector functions. Wherry and colleagues also showed the importance of PGC-1 $\alpha$  driven metabolism, especially glycolysis and mitochondrial metabolism, in T cell effector functions in a chronic virus infection model (LCMV)(67).

There is a metabolic tug-of-war between tumor cells and the immune compartment where tumor cells out-compete immune cells for available nutrients, causing starved CD8 T cells to lose effector function (68). As a compensatory mechanism in a glucose low environment, effector T cells induce AMPK activation which reduces energy expenditure by suppressing mammalian target of rapamycin complex 1 (mTORC1) (69). AMPK also promotes glutaminolysis as an alternative source of ATP production through the TCA cycle and mitochondrial oxidative phosphorylation (69). Interestingly, in tumor cells, intergenic AMPK activity inhibits cellular metabolic pathways that support tumor development, and loss of AMPK activity promotes tumor growth (70). Drs. Ping-Chih Ho and Susan Kaech showed that in a glucose-poor microenvironment, reprogramming of glycolytic metabolite phosphoenolpyruvate (PEP) could improve T cell effector functions (62). In T cells, PEP suppresses sarco/ER Ca<sup>2+</sup>-ATPase (SERCA), which leads to antigen-specific-TCR-mediated activation of Ca<sup>2+</sup>- NFAT signaling, ultimately increasing T cell effector functions (62). Kristen Pollizzi and Jonathan Powell showed that knocking out T cell-specific Tsc2 increases their glycolytic capacity, making them highly cytotoxic and short lived effector T cells. This cytotoxic short lived effector T cell phenotype, however, comes at the expense of losing memory potential, since Tsc2 knockout T cells lose mitochondrial oxidative phosphorylation (71,72). Increasing T cell-specific PEP and inhibiting Tsc2 could be potential therapeutic targets to break T cell metabolic insufficiency in the hostile tumor microenvironment (62,72,73).

In contrast to effector T cells, immune suppressive regulatory T cells not only manage to survive in the unfavorable tumor microenvironment, but also

harness their immune suppressive functions. Alessia Angelin and Ulf Beier have shown that in the low glucose and high lactate tumor microenvironment, FoxP3 alters the metabolism of regulatory T cells, which helps them to adapt to metabolically challenging conditions to maintain immunosuppressive function and impair tumor immunity (58). Ongoing work of Watson et al. showed that regulatory T cells take up lactate through monocarboxylate transporter 1 (MCT1) and utilize it for ATP production which gives them a survival advantage in an LDH high tumor microenvironment (74).

*c) Tumor-cell-extrinsic immunosuppressive factors*

Tumors create an immunosuppressive milieu to escape immunotherapeutic pressure by recruiting pro-tumor cells like myeloid-derived suppressor cells (MDSC), Treg, and cancer associated fibroblasts (CAF), polarizing macrophage to an immunosuppressive M2 phenotype and secreting immunosuppressive cytokines and enzymes like arginase, VEGF, indoleamine-2,3-dioxygenase (IDO) and IL-8.

Tumor cells and MDSCs produce indoleamine-2,3-dioxygenase (IDO), an enzyme involved in tryptophan catabolism, generating the immunosuppressive metabolite, Kynurenine (75). Further depletion of tryptophan, which is an essential amino acid, inhibits T cell expansion and function. This indicates that tumors escape immunotherapeutic pressure possibly by inducing IDO (76). In a preclinical B16 melanoma model, combining IDO inhibitors with anti-CTLA-4 or anti-PD-L1 therapy showed synergistic survival benefits (76-78). Similarly, catabolism of arginine, which is mediated by the enzyme Arginase, is also an immunosuppressive mechanism (79). Arginase is expressed by tumor cells,



MDSCs, tumor associated macrophages (TAM), stromal cells, and fibroblasts (78,79). Arginase expression in the TME suppresses T cell proliferation and activation (78). It also repolarizes macrophages to the suppressive M2 phenotype (78). This suggests that the expression of tryptophan- and arginine-depleting enzymes creates an immunosuppressive milieu in the TME and contributes to resistance to immunotherapy (76,78).

### **1.2.3: Enteric microbiome**

The intestinal microbiota maintains symbiosis with the host immune system, and the inner lining of gut plays an important role as a barrier between them. Any dysbiosis caused by repeated antibiotic medication could enhance the frequency of some cancers, suggesting a relationship between the microbiome and carcinogenesis (80). This gut microbiome is also known to influence immune surveillance(81) and pathophysiology of immune-related diseases like obesity (82), diabetes (83), inflammatory bowel disease (84), experimental autoimmune encephalomyelitis (85), multiple sclerosis (85,86), arthritis (86), and psoriasis (86). Gut microbiota not only influence the development and progression of gastrointestinal (GI) tract cancers like colorectal cancer (87,88) but also influence non-GI cancers like breast cancers (89,90). Once barriers are breached, gut microbes can further influence tumor immune responses by eliciting proinflammatory or immunosuppressive tumor milieu.

lida *et al.* showed that tumor bearing mice that lacked microbiota do not respond to drugs that modulate the innate immune system (CpG - cytosine, guanosine, phosphodiester link oligonucleotides) and chemotherapeutic agents

(e.g. oxaliplatin, a platinum compound). Viaud *et al.* found that cyclophosphamide treatment induces the translocation of certain species of Gram-positive bacteria into secondary lymphoid organs and promotes an antitumor adaptive immune response. More recent evidence suggests that the gut microbiome plays a role in influencing response to checkpoint blockade antibodies. Sivan *et al.* and Vétizou *et al.* have shown that resistance to anti-CTLA-4 and anti-PD-L1 therapy was mediated by stool microbiota. Vétizou *et al.* show that mice treated with antibiotics or housed in specific pathogen-free conditions failed to respond to anti-CTLA-4 therapy. When antibiotic-treated or germ-free-housed mice were given *Bacteroides fragilis*, resistance to anti-CTLA-4 therapy could be reversed. Sivan *et al.* illustrated that fecal transfer of *Bifidobacterium* improved survival in response to anti-PD-L1 antibody by augmenting dendritic cell functions and ultimately enhancing CD8+ T cell function in the TME. In more recent studies, Gopalakrishnan *et al.* and Matson *et al.* showed that melanoma patients could be distinguished as responders or non-responders to anti-PD-1 therapy based on the composition of their gut microbiome (91-93). Patients who responded to anti-PD-1 therapy had greater abundance of “good” bacteria in the gut while non-responder patients showed an imbalance in the composition of gut flora, which correlated with impaired immune function (91-93). Gopalakrishnan *et al.* analyzed the oral and gut microbiome of 112 melanoma patients who were undergoing anti-PD-1 therapy and observed that anti-PD-1 responders had significantly different diversity and composition of the gut microbiota compared to non-responders. They also examined fecal microbiome from 43 patients and found that abundance of bacteria of the Ruminococcaceae family was higher in responding patients. When

*BRAF<sup>V600E</sup>/PTEN<sup>-/-</sup>* (BP-1) melanoma tumor bearing germ free mice were implanted with fecal microbiome from anti-PD-1 responding patients, mice showed improved systemic and antitumor immunity. Matson *et al.* also showed significant differences in the composition of fecal microbiota of 16 patients who responded to anti-PD-1 or anti-CTLA-4 therapy compared to 26 non-responders. The bacterial species more abundantly found in the responders included *Bifidobacterium longum*, *Collinsella aerofaciens*, and *Enterococcus faecium*. When fecal microbiome from patients who responded to immunotherapy were transferred to B16 melanoma-bearing germ free mice, mice showed improved tumor control, increased T cell responses, and greater efficacy of anti-PD-L1 therapy. Routy *et al.* show that non-small cell lung cancer, renal cell carcinoma, and urothelial carcinoma patients who had a prior exposure to antibiotics had poor response to anti-PD-1 therapy. The antibiotic treatment disturbed the specific “good” bacterial clades (*Akkermansia*, *Faecalibacterium*, and *Bifidobacterium*), driving resistance to anti-PD-1 therapy. Together these studies suggest that composition and diversity of gut microbiota are critical factors mediating response to immunotherapy, and imbalance in gut flora composition could drive resistance to therapy.

#### **1.2.4: Upregulation of alternative immune checkpoints**

Persistent tumor antigen availability exhausts T cells in the TME, and exhausted T cells upregulate multiple inhibitory receptors like CTLA-4, PD-1, PD-L1, TIM3, LAG3 and VISTA. Paradoxically, these receptors also represent activated T cells, and evidences suggest that these receptors are regulated by distinct non-redundant mechanisms. We have shown earlier that anti-CTLA-4

blockade therapy increased PD-1 expression on tumor infiltrating T cells leading to acquired resistance to CTLA-4 therapy (94,95). We and others have shown that combining anti-CTLA-4 therapy with anti-PD-1 therapy provides synergistic survival benefit (8,9,94,96). This suggests that alternative checkpoint molecules mediate resistance to therapy, and targeting multiple checkpoint molecules might increase survival rates. In genetically engineered mouse models of lung adenocarcinomas and stage IV lung adenocarcinoma patients, Kayoma *et al.* have shown that upregulation of T-cell immunoglobulin and mucin domain-3 (TIM-3) on TIL was a mechanism of adaptive resistance to anti-PD-1 therapy(97). Similarly, in a murine HNC tumor model and human HNSCC tumors, TIM3 was upregulated in a PI3K/Akt-dependent manner during PD-1 blockade and sequential addition of anti-Tim-3 antibodies demonstrated significant antitumor activity. Gao and colleagues have shown that anti-CTLA-4 therapy increases level of PD-L1 and VISTA on TIL and macrophages as a compensatory inhibitory pathway in prostate and melanoma patients (95). These studies support an idea of a circuit of compensatory alternative checkpoint signaling as a potential escape mechanism to checkpoint blockade therapy.

### **1.2.5: Angiogenesis and immune trafficking**

To meet the continuously growing energy demand, tumors create a proangiogenic milieu, which signals tumor associated blood vessel formation (neovascularization). Tumor associated blood vessels and the immunosuppressive proangiogenic milieu limits the beneficial effects of cancer immunotherapies. Vessels development in normal tissue is a tightly controlled process, regulating blood supply to the tissue and helping in immune surveillance

through extravasation of lymphocytes. On the other hand, tumor blood vessels are developed abruptly so they harness structural abnormalities including heterogeneous distribution, tortuosity, dilation, and inadequate perivascular coverage. Abnormal tumor vasculature limits the extravasation of tumor-specific CD8 T cells and also affects their survival, proliferation and effector function. Additionally, tumor vasculature promotes immunosuppressive microenvironments by allowing infiltration of suppressive cells like tumor associated macrophages (TAMs), myeloid derived suppressor cells (MDSC) and regulatory T cells (Treg) (98). Vascular endothelial growth factor (VEGF), which is a master regulator of tumor angiogenesis, also functions as an immunosuppressive factor. VEGF promotes expression of the death mediator Fas ligand (FasL, also called CD95L) on tumor vasculature which is known to induce receptor mediated death of CD8 T cells and to increase infiltration of Treg (98). VEGF also regulates the expression of adhesion molecules like intercellular adhesion molecule-1 (ICAM-1) and vascular cell adhesion molecule-1 (VCAM-1) which negatively affect T cell infiltration and function (99,100). Elevated VEGF in the TME inhibits T cell immune responses (101), suppresses DC maturation (102), and promotes Treg suppressive function (98,103). Additionally, VEGF also recruits MDSCs, which serve as an extra source of immunosuppressive cytokines and chemokines in TME (104-108). Moreover, therapeutically blocking the VEGF/VEGFR2 signaling pathway could reverse immunosuppression in TME (101,103). In preclinical studies, Schmittnaegel et al. and Allen et al. showed that targeting tumors with a combination of checkpoint blockade immunotherapy and antiangiogenic treatments produced synergistic antitumor responses (109,110). This suggests

that tumor proangiogenic process is immunosuppressive in nature and one of the mechanisms driving resistance to immunotherapy (109,110).

### **1.3: Overcoming mechanisms of resistance**

From above, it is clear that tumors use multiple evasion mechanisms to drive resistance to immunotherapy. The resistance mechanisms could be primary or acquired during therapy. These mechanisms also vary among different tumor types and patients, which makes it important to identify patient-specific mechanisms to therapeutically target them. There are various efforts to use the knowledge of tumor evasion mechanisms to predict immunotherapy response and apply the knowledge gained to target patient-specific resistance mechanisms.

Characterizing the tumor mutational landscape along with MHC class-I prediction algorithms to predict the neoantigen burden has shown promise in the clinic to formulate patient-specific vaccines. Tumors with higher mutational load correlate with more tumor specific CD8 T cell infiltration and are more likely to respond to checkpoint therapy. Immune phenotyping using flow cytometry or CyTOF and immunogenomics are also identifying tumors with high immune infiltrate (immunologically “Hot” tumors), as being more likely to respond to immunotherapy. The immunologically “cold” tumors could be then targeted to increase their immune infiltrates and make them sensitive to therapy. Immune phenotyping has also yielded important information about the functional status of anti- and pro-tumor immune infiltrates such as alternative checkpoints molecules on T cells, arginase and IDO.

The majority of approaches focus on therapeutically targeting one of the resistance mechanisms in combination with immunotherapy to overcome resistance associated with treatment. The knowledge obtained (111,112) from mutational profiling of tumors is used to design personalized neoantigen vaccines to increase the immune infiltrates in resistant tumors. The most extensively studied and successful strategies to target immunotherapy resistance across various tumor types are combining antibodies against two immune checkpoint molecules (47,94). Combining  $\alpha$ PD-1 and  $\alpha$ CTLA-4 therapies elicit long term survival benefits in melanoma, which can last for years (8,9,113).

Cancer neoantigen vaccines have shown promising results in early clinical studies breaking resistance to checkpoint immunotherapies (NCT02113657) (26,114-116). Radiation therapy can increase mutational burden in cancer cells, and combination therapy has been shown to increase the T cell response and shows promise results in early clinical trials (NCT01449279) (117,118). Another successful strategy to improve neoantigen burden and turn immunologically “cold” tumors into “hot” tumors is combining oncolytic viruses with immunotherapy (NCT03153085, NCT02879760, NCT02798406 and NCT03259425) (119). Prime examples of targeting the immunosuppressive tumor microenvironment are targeting immunosuppressive myeloid cells with phosphoinositide 3-kinase  $\gamma$  Inhibitor (IPI549- NCT02637531) (120), CSF1R Inhibitor (PLX3397- NCT02452424) (121), Indoleamine 2,3-dioxygenase inhibitors (Indoximod- NCT02073123 (77) and Epacadostat-NCT03291054) (122,123), STING agonists (NCT03172936) (124) and arginase inhibitors (INCB001158-NCT02903914)

(125). Drugs targeting tumor hypoxia (Evoxofamide –TH-302 and Metformin) have shown synergistic pre-clinical benefit when combined with immunotherapy (56,57) and are under clinical investigation (NCT03098160 and NCT03048500). Targeting tumor metabolism can be self-defeating since it can also negatively impact anti-tumor immunity. However, in CT26 colon carcinoma tumors, treatment with a combination of glutaminase inhibitor (CB-839) and anti-PD-1 or anti-PD-L1 enhanced the anti-tumor activity (126) and is under clinical evaluation (NCT02771626).

Several preclinical studies have demonstrated that composition and diversity of microbiota can mediate resistance to immunotherapy, and that feeding the “good” bacteria improves the efficacy of therapy (80,81,84-88,91-93). This approach is now under clinical evaluation (NCT03353402). Anti-angiogenic treatment can have a substantial effect on anti-tumor immunity and has shown potential synergy when used with immunotherapy (109,110). This approach is also currently being tested in the clinic (NCT0285425 and NCT03167177).

There are ongoing efforts to understand the mechanisms that regulate anti-tumor T cell responses and resistance to immunotherapeutic pressure, including translation of preclinical insight to the clinic and taking clinical observations back to the bench. To expand the number of patients who can benefit from immunotherapy, a comprehensive understanding of primary, adaptive, and acquired resistance to immunotherapy is required. Overall, targeting resistance mechanisms with therapeutic agents has shown promising preclinical results and is being evaluated in the clinic.



#### **1.4: Pathophysiology of immune related adverse effects (IRAEs)**

Increasing the efficacy of T cell checkpoint modulating antibody immunotherapy either by improving benefit as a monotherapy or by combining with therapeutic agents targeting resistance could also lead to immune related adverse effects (IRAEs). This leads to host-specific T cell response targeting dermatologic, gastrointestinal, hepatic, endocrine, and other tissues. Steroids are used in the clinic to manage these immune related adverse events (IRAEs), but steroids are immunosuppressive and may compromise the anti-tumor response. Detailed understanding of these mechanisms will help design new therapeutic strategies to overcome resistance to immunotherapy without inviting unwanted immune related side effects.

Checkpoint proteins are critical players in preventing autoimmunity by constraining hyperactive responses through central (during T cell development in thymus) and peripheral tolerance (tissue specific self-antigen outside the thymus). Genetic polymorphisms in checkpoint proteins break self-tolerance and can lead to various autoimmune diseases. Polymorphisms in checkpoint proteins such as CTLA-4, PD-1 and PD-L1 are associated with various autoimmune toxicities such as thyroiditis (127,128), Graves' disease (127,128), diabetes mellitus (127,129,130), rheumatoid arthritis (128), celiac disease (129,131), myasthenia gravis (132), and systemic lupus (127,133-135). Tumors escape immune attack by exploiting the co-inhibitory immune checkpoint axis on T cells in order to make them anergic, exhausted, and incapable to complete anti-tumor effector functions.

Targeting these molecules with therapeutic antibodies that block co-inhibitory immune checkpoint molecules, such as CTLA-4, PD-1, TIM3 and PD-L1 reactivate T cells and restore their capacity to mediate antitumor activity. T-cell-specific anti-tumor immune responses can also be reactivated with agonist antibodies targeting co-stimulatory molecules such as: 4-1BB (CD137, TNFRSF9, tumor necrosis factor receptor superfamily member 9), OX40 (CD134, TNFRSF4, tumor necrosis factor receptor superfamily member 4) and glucocorticoid-induced tumor necrosis factor receptor (GITR). However, a disruption of immunomodulatory receptors (checkpoint receptors and co-stimulatory receptors) can break T cell tolerance and lead to hyperactive immune responses against self-tissues and organs such as skin, gastrointestinal, hepatic, pulmonary, mucocutaneous, and endocrine systems. The hyperactive immune system exerts collateral damage on self-tissues, which is termed 'immune-related adverse events' (IRAEs). This section discusses pathophysiology of organ specific IRAEs associated with immunomodulatory antibodies.

#### **1.4.1: Dermatological toxicities**

The most common lesions associated with immunomodulatory antibodies are rash, vitiligo, and alopecia areata. The most commonly reported rashes are maculopapular, papulopustular, Sweet's syndrome, follicular, and urticarial dermatitis. Meta-analysis conducted on 57 case reports and 24 clinical trials showed that 44% of the patients on  $\alpha$ CTLA-4 therapy (Ipilimumab and tremelimumab) had reported some form of dermatological toxicity (136). A pooled analysis on melanoma patients who received  $\alpha$ PD-1 therapy showed skin related toxicities in 35-39 % of patients (137). In a study comparing safety and efficacy of

$\alpha$ CTLA-4 and  $\alpha$ PD-1, 25-31 % patients on Pembrolizumab ( $\alpha$ PD-1) and 4% of patients on ( $\alpha$ CTLA-4) reported Vitiligo (138,139). The histopathologic features of dermatitis are represented by infiltration of CD4 T cells and eosinophils in the dermis. Immune related dermatitis in the clinic is treated with corticosteroids (139,140).

#### **1.4.2: Mucosal and gastrointestinal toxicities**

Diarrhea and colitis are the most common side effects associated with immunomodulatory antibody treatment, which, if not managed, can lead to severe complications such as intestinal perforation (141). Diarrhea and colitis are more common with anti CTLA-4 compared to PD1/PD-L1 blockade (138,142,143). More than 30% of patients who received Ipilimumab reported grade  $\geq 2$  diarrhea (138,143) and about 10% of patients also experience severe grade colitis and diarrhea (143). On the other hand, 5-10% of patients on PD-1 (Nivolumab and Pembrolizumab) therapy reported colitis (138,144,145). Histological features of CTLA-4 mediated colitis are characterized by neutrophilic inflammation, lymphocytic inflammation, or combined neutrophilic and lymphocytic inflammation (142,146). Lymphatic inflammation is characterized by increases in CD8 effector T cells in intestinal epithelium and CD4 effector cells in lamia propria (142,146). Immune modulatory antibody-induced diarrhea is managed by corticosteroids, with budesonide for grade I-II colitis (141) and anti-TNF $\alpha$  antibody (infliximab) for severe colitis (141,146).

### **1.4.3: Hepatotoxicity**

Most immunomodulatory antibodies cause asymptomatic increases in serum alanine aminotransferase (ALT) or aspartate aminotransferase (AST) enzymes, which is often attributed to hepatitis. These enzyme elevations could also be due to viral infections (hepatitis A, B or C), presence of a tumor, or liver metastasis, which makes it difficult to distinguish immune-related hepatitis. Less than 5% of patients reported elevated transaminase levels on anti CTLA-4 in four different studies, and transaminitis was resolved without administration of immunosuppressive medications when  $\alpha$ CTLA-4 therapy was temporarily withheld (143,147-149). Advanced hepatocellular carcinoma (HCC) patients on Nivolumab (anti PD-1) therapy showed elevated AST in 10% and ALT in  $\geq 17\%$  of patients (150). Anti PD-L1 (MPDL3280A) antibody treatment in non-small cell lung cancer (NSCLC) resulted in transaminitis in less than 5% of patients (151). Clinical development of 4-1BB agonist antibodies, in contrast, has been hampered by hepatic inflammation since about 15% of patients on Urelumab (4-1BB agonist antibodies) had grade  $\geq 2$  hepatitis (152,153). The early clinical trials of Urelumab were terminated and withdrawn due to an unusually high incidence of grade 4 hepatitis (152,153). Steroids are commonly used to manage immune related hepatitis. As 4-1BB induced hepatitis is triggered by myeloid cells, steroids might not be very effective in managing hepatitis in this setting (25).

### **1.4.4: Endocrine toxicities**

Immune-related toxicities affecting endocrine glands are more common in anti-CTLA-4 therapy compared to PD-1/PD-L1 blockade and are mainly characterized by development of hypophysitis and thyroid dysfunction (140,154-

157). Hypophysitis, or inflammation of the pituitary gland, affects up to 10% of patients on anti-CTLA-4 therapy and 1-6% of patients on PD-1/PD-L1 blockade (140,154-157). Hypophysitis can affect the entire endocrine system including the pituitary-hypothalamic axis, pituitary–thyroid axis, pituitary–gonadal axes, and pituitary–adrenal axes (140,154-157). This makes hypophysitis difficult to diagnose since symptoms can be nonspecific. Diagnosis involves biochemical screening of various endocrine hormones such as prolactin (PRL), thyroid-stimulating hormone (TSH), thyroxine (T4), luteinising hormone (LH), follicle-stimulating hormone (FSH), adrenocorticotrophic hormone (ACTH), and cortisol (28,139). Pituitary hormone inefficiency is treated with glucocorticoid replacement therapy, and in some patients, there is need for life-long therapy (140,154-157). Pituitary endocrine cells ectopically express CTLA-4 on their surface (158). Anti CTLA-4 antibodies bind to pituitary endocrine cells and serve as sites for complement activation which leads to an inflammatory cascade (158,159). Caturegli *et al.* also highlight the role of T cell mediated inflammation in CTLA-4 induced Hypophysitis (160).

Thyroiditis followed by hypothyroidism is also reported with anti- CTLA-4, PD-1 and PD-L1 therapies, which is managed by thyroid hormone replacement therapy. In some incidences, Grave’s disease, which may arise due to development of anti-TSH antibodies, has been reported on anti CTLA-4 therapy.

#### **1.4.5: Other rare toxicities**

Pneumonitis, or inflammation of lung parenchyma, is more common with PD-1/PD-L1 blockade (16,144). It has been reported in about 10% of patients who

received either PD-1 or PD-L1 antibodies (16,144). Immune related pneumonitis can be life threatening and resulted in three treatment related death in early Nivolumab studies (161). Although low grade immune-related pneumonitis could be managed with systemic steroids, severe cases require other forms of immunosuppression such as infliximab, or cyclophosphamide (139,162). Elevation of pancreatic enzymes lipase and amylase has been reported in response to both CTLA-4 and PD-1 blockade. Similarly, uveitis, nephritis, and neurotoxicities have been reported in patients receiving both anti-PD-1 and anti-CTLA-4 therapy (139,143,163-168). Most immune related rare toxicities do not have required lab tests outside of clinical trials, which makes it challenging to manage them in clinic. Steroids are generally the first choice to manage immune related uveitis, nephritis, pancreatitis, cardiotoxicities and neurotoxicities (139).

Mechanisms underlying immune-related adverse events (IRAEs) are still largely undefined. Research in the field of tumor immunotherapy focuses on improving the efficacy of therapies to expand clinical benefit across different tumor types while eliminating unwanted side effects. The second chapter of the dissertation focuses on understanding the molecular mechanisms of acquired resistance to triple ( $\alpha$ CTLA-4,  $\alpha$ PD-1 and  $\alpha$ PD-L1) combination of checkpoint immunotherapy. The third chapter of the dissertation focuses on characterizing mechanisms of immune related hepatotoxicity associated with 4-1BB agonist antibodies.

## **Chapter 2: Immunotherapy Resistance**

### **Melanoma Evolves Complete Immunotherapy Resistance through Acquisition of a Hyper Metabolic Phenotype**

## 2.1: Abstract

Despite the success of T cell checkpoint blockade antibodies in treating an array of cancers, a majority of patients still fail to respond to these therapies, or respond transiently followed by a relapse of the malignancy. The molecular mechanisms which drive the lack of response to checkpoint blockade, whether pre-existing or evolved when on therapy, remain unclear. In order to address this critical gap in clinical knowledge, we established a murine model of melanoma designed to elucidate the molecular mechanisms underlying immunotherapy resistance. Through multiple *in vivo* passages, we selected a B16 melanoma tumor line that evolved complete resistance to combination blockade of CTLA-4, PD-1, and PD-L1, which cures ~80% of mice bearing the parental tumor. Using gene expression analysis, and immunogenomics, we determined the adaptations engaged by this melanoma to become completely resistant to T cell checkpoint blockade immunotherapy. Acquisition of immunotherapy resistance by these melanomas was driven by the coordinated upregulation of the glycolytic, oxidoreductase, and mitochondrial oxidative phosphorylation pathways to create a metabolically hostile microenvironment wherein T cell functions are suppressed. We have observed and validated the upregulation of these pathways in a cohort of melanoma patients resistant to dual checkpoint blockade. Additionally, we employed MRI imaging to visualize in real time the metabolic changes in resistant tumors of mice. Clinical application of this technique could provide a much-needed non-invasive tool to predict sensitivity of patients to immunotherapy. Together these data indicate that melanoma tumors can evade by adapting a hyper



metabolic phenotype, melanoma tumors can evade T cell immunity and achieve resistance to T cell checkpoint blockade.

## 2.2: Introduction

T cell checkpoint blockade immunotherapies such as anti-cytotoxic-lymphocyte antigen-4 ( $\alpha$ CTLA-4) and anti-programmed-death-1 and its ligand ( $\alpha$ PD-1/ $\alpha$ PD-L1) antibodies have shown long term survival benefits across several tumor types including melanoma (10,47,113,169), renal cell carcinoma (RCC), bladder cancer, hematological malignancies and non-small cell lung cancer (NSCLC). Despite these advances, a significant percentage of patients show intrinsic or naturally acquired resistance to immune checkpoint blockade antibodies, causing patients to have limited or no response to therapy. Moreover, there is no biomarker which can accurately predict clinical response to checkpoint blockade immunotherapy. Many non-immunogenic tumors such as pancreatic, and prostate cancers have shown little or no response to immune checkpoint antibodies. This study addresses two major goals of the field; first, to increase the number of patients who could benefit from immune checkpoint blockade antibodies and second, to identify prognostic biomarkers that could be use predict response to checkpoint blockade immunotherapy.

In order to extend the curative potential of immunotherapy to a larger subset of patients, we must first understand the cellular and molecular mechanisms that tumors engage to escape immunotherapy and drive relapses. Several efforts are ongoing to understand the mechanisms of acquired resistance to checkpoint immunotherapy and extend this knowledge to identify prognostic biomarkers. Immune escape mechanisms that tumors engage to hide from immune attack have been extensively studied (3-5,170,171) even before the approval of the first

checkpoint blockade antibody. Until now, most of the research addressing checkpoint blockade therapy resistance mechanisms focused on the upregulation of alternative immune checkpoint proteins such as TIM3 (97,172) and VISTA (95). Mutational load (49,111,173), neoantigen burden (173), and copy number loss of components of the antigen presentation machinery (112,174) by tumor cells have also been previously described as mechanisms driving resistance to  $\alpha$ PD-1 and  $\alpha$ CTLA-4 monotherapies. Despite these advances, the basis for partial or lack of response and mechanisms of resistance to different checkpoint blockade immunotherapies remains to be elucidated. Additionally, little is known about the transcriptomic states of tumor cells that can influence sensitivity to the immune system and whether this intrinsic signaling can play an important role in checkpoint blockade resistance. To address this critical gap in knowledge, we established a novel mouse model of melanoma. The model relies on the 'cancer immunoediting' theory (5), which states that the immune system, while protecting the host from tumor development, can exert evolutionary pressure which simultaneously drives selection of select for immune-resistant tumor strains. We therefore used the '*in vivo* serial passage approach' originally developed by Fidler et. al. to select melanoma clones with increasing metastatic potential to the lung (e.g. B16-F10) (175-177), in this case selecting melanoma clones with increasing resistance to checkpoint blockade immunotherapy. Based on gene expression profiling of immunotherapy resistant clones, we hypothesized that tumor cells evade response to immunotherapy by the coordinated upregulation of aerobic glycolysis, oxidoreductase, and mitochondrial mediated oxidative phosphorylation pathways,

which creates a hostile metabolic microenvironment in which cytotoxic CD8 T cells are rendered dysfunctional.

To experimentally validate the roles each of the identified metabolic pathways, gene expression analysis was followed by a seahorse flux assay (glycostress and mitostress assay) and NMR metabolomics analysis which confirm the upregulation of glycolysis and mitochondrial oxidative phosphorylation. In hypermetabolic, resistant tumors, CD8 T cell function was profoundly suppressed. We have also validated upregulation of these pathways in a cohort of melanoma patients who failed dual checkpoint blockade therapy. Overall, our data demonstrate that these resistant tumors upregulate glycolysis, oxidoreductase and mitochondrial mediated oxidative phosphorylation to evade the response to anti-CTLA-4, anti-PD-1 and anti-PD-L1 immunotherapies.

## **2.3: Methods**

### **2.3.1: Mice**

Four to eight week old Male C57BL/6J (000664) and Rag1 knock out mice were purchased from The Jackson Laboratory (Bar Harbor, Maine, USA). The mice were cared for in a pathogen-free facility at our institution, which is fully accredited by the Association for Assessment and Accreditation of Laboratory Animals Care International. All animal experiments were performed according to the protocols approved by the Institutional Animal Care and Use Committee.

### **2.3.2: Therapeutics antibodies**

Anti CTLA-4 (9H10), anti-PD-1 (RMP1-14), anti-PD-L1 (10F.9G2) anti CD-40 (FGK4.5) and anti-VEGF (DC101) were purchased from BioXCell (West Lebanon, NH, USA) and administered intraperitoneally.

### **2.3.3: Patient cohort**

Surgical samples were acquired from metastatic melanoma patients treated with anti-CTLA-4 (ipilimumab) and/or anti-PD-1 (pembrolizumab or nivolumab) at the UT MD Anderson Cancer Center between April 2014 and September 2015 on IRB protocol 2012-0846 prior to therapy or at time of progression (Table 2.1). Clinical response was evaluated by RECIST 1.1 (173,178).

### **2.3.4: Cell lines**

The B16/BL6 cell line was originally obtained from I. J. Fidler (MD Anderson Cancer Center, Houston, TX). The B16-sFlt3L-Ig (FVAX) and B16-tdTomato cell lines have been described previously (94). The cells were maintained in RPMI media with 10% Fetal Bovine Serum (FBS).

### **2.3.5: Harvesting B16 melanoma**

To harvest the mouse tumors, tissues were treated with 0.25 mg ml<sup>-1</sup> collagenase A (Sigma-Aldrich (St. Louis, MO, USA) and 25 U ml<sup>-1</sup> DNase (Roche Diagnostics, Indianapolis, IN, USA) for 20 min at 37°C; the dissolved cells were then passed through a plastic mesh. The resulting dissociated cells were collected by centrifugation and washed twice in phosphate-buffered saline (PBS). The cells were then cultured and/or used for flow cytometry analysis and/or flow sorting.

### **2.3.6: Generation of checkpoint blockade immunotherapy-resistant melanoma cells**

We initially implanted 15 mice with  $2.5 \times 10^4$  B16/BL6-td cells subcutaneously and treated then with a combination of triple T cell checkpoint blockade inhibitors. Specifically, on days 3, 6, and 9, post implantation, the mice were vaccinated with  $1 \times 10^6$  irradiated (150 Gy) FVAX cells on the contralateral flank and treated with a combination of anti-CTLA-4 (100 µg of 9H10), anti-PD-1 (250 µg of RMP1-14), and anti-PD-L1 (100 µg of 10F.9G2). Non-responder mice, who developed tumors regardless of treatment, were euthanized when tumors reached 200-500 mm<sup>3</sup> and their tumors were harvested. Tumors from all non-responder mice were pooled and a cell line (3I-F1) was generated. The cell line (3I-F1) was then used to in a new set of 15 mice (second cycle) followed by the same immunotherapy regimen. For the second cycle and all subsequent cycles, only  $1 \times 10^4$  were implanted. The decrease in tumor cell number compared with the initial challenge was designed to distinguish true resistance from experimental variation. We repeated the serial passages until  $\geq 90\%$  of the animals became resistant to the therapy. B16 melanoma cell lines were called 3I-F1, 3I-F2, 3I-F3,

and 3I-F4 (Resistant), respectively. For the untreated control group, we implanted 5 mice with parental tumor cells and with tumor cells from each cycle of selection.

### **2.3.7: Treatment strategies and monitoring tumor growth**

Wild type mice were subcutaneously implanted with  $2.5 \times 10^4$  B16/BL6-td or 3I-F4 cells and treated with a combination of triple checkpoint blockade inhibitors. Specifically, on days 3, 6, and 9, mice were vaccinated with  $1 \times 10^6$  irradiated (150 Gy) FVAX cells on the contralateral flank and treated with a combination of anti CTLA-4 (100  $\mu$ g of 9H10), anti PD-1 (250  $\mu$ g of RMP1-14), and anti PD-L1 (100  $\mu$ g of 10F.9G2). TNF superfamily agonist antibodies, anti 41BB (150  $\mu$ g of 3H3) and anti CD40 (100  $\mu$ g of FGK4.5) were given intraperitoneally on days 3, 6 and 9. Anti-VEGF (100  $\mu$ g of DC101) was administered intraperitoneally on days 6, 9 & 12. Metformin (50 mg/kg; every other day) and 2DG (500mg/kg; daily) were given intraperitoneally beginning one day post tumor challenge. For metformin drinking water cohorts, mice were given 1g/L metformin drinking water post tumor implantation. LDH inhibitor (4mg/kg), IPI549 (15mg/kg) and Oxphos inhibitors (5mg/kg) were prepared in polyethylene glycol (PEG) base as per manufacturer's instructions and given through oral gavage every day post tumor implantation. On days 3, 4, 5, 6 and 7 post tumor challenge, TH302 (50mg/kg) was given intraperitoneally and STAT3 ASO (50mg/kg) was given subcutaneously on the contralateral flank. Tumors were measured every other day and a death event was counted when tumor volume reached  $1000 \text{ mm}^3$  or a mouse dies because of metastasis.

### **2.3.8: RNA extraction**

Tumors were harvested from mice and sorted using flow cytometry based on the td-tomato fluorescence into tumor cells and cells of the tumor microenvironment (non-tumor), which included both CD45 positive and CD45 negative populations. Total RNA was extracted using the RNeasy Mini Kit (Qiagen, MD).

For human patients, the presence of tumor was confirmed by a pathologist, and total RNA was extracted from the tumor tissue using the RNeasy Mini kit. (Qiagen, MD)

### **2.3.9: Microarray analysis**

Tumor cells and non-tumor cells of the microenvironment were sorted by flow cytometry and RNA was isolated from both as described above. Microarray analysis was done on both tumor cells and microenvironment from two independent RNA samples from parental tumors and four independent RNA samples from 3I-F4 tumors. Each RNA sample was isolated from tumors pooled from three mice. Microarray analysis was also done on RNA isolated from patients' tumor biopsies. Microarray analysis was conducted using MouseRef-8 and HumanHT-2 bead chip arrays (Illumina) respectively.

### **2.3.10: Bioinformatics analyses**

Microarray data was normalized as per manufacturer's instructions and processed in R (version 3.4.1). Low intensity probes that were not significantly expressed above the background level (detection  $p\text{-value} \geq 0.05$  in at least one of the samples) were excluded. Differential expression between resistance and



parental for tumor, and respectively for microenvironment was determined by a fold-change in absolute value equal or greater to 1.1 and a p-value obtained from the moderated t-statistic from LIMMA package less than 0.05. To support visual data exploration, we employed R to generate volcano plots, as well as heatmaps making use of the heatmap.2 function of gplots library.

Gene set enrichment analysis (GSEA) and ingenuity pathway analysis (IPA) were applied to the data sets as an unbiased bioinformatics analysis in order to compare resistant tumors with parental tumors and responder patients with non-responder patients.

### ***2.3.11: Extracellular flux analyses***

Resistant and parental cell lines were seeded at a density of 25,000 cells per well 24 hr prior to the assay. Oxygen consumption rate (OCR) and extra cellular acidification rate (ECAR) were measured as per the manufacturer's protocols on an XF96 Analyzer (Seahorse Biosciences).

### ***2.3.12: Immunofluorescence staining and imaging***

In order to image hypoxia, mice were administered Pimonidazole (Hypoxyprobe, Burlington, MA) intravenously thirty minutes prior to euthanasia so that hypoxia could be imaged in tumor sections by immunofluorescence staining with anti-pimonidazole adduct FITC conjugated antibody (Hypoxyprobe, Burlington, MA). Mouse tissues were collected and embedded in Tissue-Tek® OCT Compound (Sakura, Torrance, CA). The embedded tissues were then flash frozen in liquid nitrogen and sectioned at the MD Anderson Histology Core. The sectioned tissue was fixed with acetone for 10 min, permeabilized with the FoxP3

staining kit (eBioscience, San Diego, CA) for 10 min, and blocked with Superblock (Thermo Fisher) for 15 min at room temperature. The samples were stained with antibodies in 2% bovine serum albumin, 0.2% Triton-X100 in PBS at room temperature for 30 min and, after being washed in PBS, mounted with Prolong® Gold anti-fade reagent (Invitrogen, Carlsbad, CA). Fluorescence microscopy was performed using a TCS SP8 laser-scanning confocal microscope equipped with lasers for 405nm, 458nm, 488nm, 514nm, 568nm, and 642nm wavelengths (Leica Microsystems, Inc., Bannockburn, IL).

### **2.3.13: Extraction of metabolites and NMR analysis**

Cells were trypsinized and washed twice with phosphate buffer saline (PBS) and flash frozen in liquid nitrogen. Tumors from mice with and without immunotherapy treatments were collected on day 12-16 post implantation and flash frozen on liquid nitrogen. Cells were counted and tumor tissues were weighed before extraction of metabolites. Cells and tumor tissues were homogenized. The homogenized tissues/cells were added with 2:1 methanol and ceramic beads. The tissues/cells were then vortexed for 40 – 60 seconds followed by freezing in liquid nitrogen and thawing on ice. Water soluble proteins and other biopolymers were precipitated in methanol solvent leaving the small molecular weight metabolites in the solution which were then extracted using ultra-centrifuge. The remaining residual solvent was removed by overnight lyophilization.

The lyophilized sample was dissolved in 800 µl of <sup>2</sup>H<sub>2</sub>O and centrifuged at 10,000 rpm. The 600 µl of sample was added with 40 µl of 8 mM 4,4-dimethyl-4-silapentane-1-sulfonic acid (DSS) before acquisition on NMR. The NMR data

were collected on Avance Bruker spectrometer operating at 500 MHz proton ( $^1\text{H}$ ) resonance frequency, equipped with cryogenically cooled triple resonance ( $^1\text{H}$ ,  $^{13}\text{C}$ ,  $^{15}\text{N}$ ) TXI probe. All one dimensional (1D)  $^1\text{H}$  NMR spectra were acquired with suppressed solvent (water) signal achieved by pre-saturation during longitudinal relaxation time. The inter-scan delay of 6 seconds is used to rule out the longitudinal relaxation related signal attenuation. The 900 radio frequency (r.f) pulse of 12  $\mu\text{s}$ , spectral width of 8,000 Hz and 256 transients were used to acquire the 1D  $^1\text{H}$  NMR. All spectra were processed in topspin 3.1 and metabolites are assigned with the help of Chenomx and Human Metabolomics Database (HMDB). The intensities of metabolites were taken with respect to NMR reference compound of 0.5 mM 2, 2 Dimethyl-2-Silapentane-5-sulfonate-d6 (DSS) appearing at 0 ppm. And then all the intensities (area under the curve) of the metabolites were normalized to the cell numbers and tumor mass. The normalized intensities were used to calculate the Z score expressing relative expression of metabolite in resistant tumors/cell lines compared to parental tumors/cell line.

#### **2.3.14: Hyperpolarized pyruvate to lactate flux imaging of tumors**

Hyperpolarization is a process that uses microwave irradiation to transfer electron polarization to nuclei at temperatures as low as  $\sim 1.3$  K leading to an increased signal intensity of nuclei ( $^{13}\text{C}$ ,  $^{29}\text{Si}$  etc.) of about 10,000 compared to the conventionally observed signal. The mixture of 20  $\mu\text{l}$   $1\text{-}^{13}\text{C}$ , 10  $\mu\text{l}$  of 15 mM trityl radical OX63 and 0.4  $\mu\text{l}$   $\text{Gd}^{2+}$  was hyperpolarized for an hour with microwave irradiation at 94 GHz at low temperature 1.5 K in Oxford Hypersense instrument. The hyperpolarized pyruvate was dissolved at high temperature in 4 ml of TRIS/EDTA buffer at physiological pH 7.8 to a final concentration of 80 mM of

pyruvate. 200 µl of the solution was injected into the mice via tail vein injection which was in horizontal bore 7 T Bruker MR Scanner (179).

The anatomical proton image and  $^{13}\text{C}$  Magnetic Resonance Spectroscopy (MRS) were acquired using surface transceiver  $^{13}\text{C}$ - $^1\text{H}$  coil (Doty Scientifics). Anatomical images of coronal, axial and sagittal were acquired with  $T_2$  weighted Rapid Imaging with Refocused Echo (RARE) sequence to determine the size and location of tumor in mice models. The  $^{13}\text{C}$  enriched urea phantom was used as spectroscopic reference as well as being used to locate the tumor. The single pulse Fast Low Angle Shot (FLASH) was used to acquire 1D  $^{13}\text{C}$  magnetic resonance spectroscopy (MRS) with repetition time of 2 seconds, flip angle  $20^\circ$ , image size 2048 X 90 and single slice of thickness 5-10 mm and acquired over a period of 180 seconds (179).

### ***2.3.15: Flow cytometric characterization of resistant tumors***

Following density gradient separation, samples were fixed using the Foxp3/Transcription Factor Staining Buffer Set (eBioscience) and then stained with up to 18 antibodies at a time from Biolegend, BD Biosciences, eBioscience, and Life Technologies. Flow cytometry data was collected on a custom 5-laser, 18-color BD LSR II cytometer and analyzed using FlowJo Version 7.6.5 (Treestar)(25,26).

For metabolic characterization of CD8 T cells, fluorescently labeled glucose (NBDG) was intravenously injected in tumor bearing mice 30 minutes prior to sacrificing mice for tumor harvest.

### **2.3.16: Retroviral vectors and virus production**

Murine PGAM2 and ADH7 cDNAs were cloned into the pMG-rtNGFr retroviral vector. This vector resembles pGC-IRES except that for a truncated form of rat p75 nerve growth factor receptor (rtNGFr) is used for selection (30). Recombinant virus production and infection were performed as described (180).

### **2.3.17: Statistical analysis**

All statistics were calculated using Graphpad Prism Version 6 for Windows. Statistical significance was determined using a two-tailed Student's t test applying Welch's correction for unequal variance. Graphs show mean  $\pm$  standard deviation unless otherwise indicated. P-values less than 0.05 were considered significant.

## 2.4: Results

### 2.4.1: B16/BL6 melanoma cells acquired resistance to checkpoint blockade immunotherapy through serial *in vivo* passage

In current preclinical tumor models it is difficult to distinguish between mice that are sensitive (responders) and resistant (non-responders) to immunotherapy. Moreover, current tumor models do not allow for easy separation of tumor cells from non-tumor microenvironment for downstream genome and transcriptomic analysis. To understand tumor intrinsic molecular mechanisms of resistance to checkpoint immunotherapy, we generated B16 melanoma clones that have developed resistance to the combination of  $\alpha$ CTLA-4,  $\alpha$ PD-1, and  $\alpha$ PD-L1 immunotherapy through serial *in vivo* passaging for increasing resistance. After four *in vivo* passages, we selected a B16 melanoma tumor line 3I-F4 (Resistant) that had evolved almost 100% resistance to combination co-inhibitory blockade, which could initially cure 80% of the mice (Fig. 2.1A & 2.1B). The tumor became increasingly aggressive after each subsequent passage and grew progressively, even in the presence of strong immunotherapeutic pressure. This model not only allowed us to enrich the genetic signature of resistance, but also provided the opportunity to separate tumor cells away from tumor microenvironment before analysis since B16 melanoma clones were transduced to express the fluorescent protein td-Tomato.

To ensure that the resistant clones generated were not simply more proliferative, we compared *in vitro* and *in vivo* proliferation of B16/3I-F4 (Resistant) and B16/BL6 (Parental). Using IncuCyte™ confluency assay (Fig. 2.1C) we found no significant difference in proliferation between the parental and resistant tumor

cells. We also compared *in vivo* tumor growth and survival of mice with parental and resistant tumors in both normal C57/BL6 (WT) and B6.Rag<sup>-/-</sup> mice. Parental and resistant tumors without immunotherapy showed no significant difference in tumor growth kinetics and survival in both WT (Fig. 2.1D & Fig. 2.1A) and B6.Rag<sup>-/-</sup> mice (Fig. 2.1E & Fig. 2.1B). In the presence of immunotherapy, however, WT mice with parental tumors showed reduced tumor growth and significant survival benefit (Fig. 2.1D). In B6.Rag<sup>-/-</sup> mice, however, both parental and resistant line grew at the same rate even in the presence of triple checkpoint blockade demonstrating that resistance depends on adaptive immunity and is not due to enhanced cell proliferation.

Figure 2.1

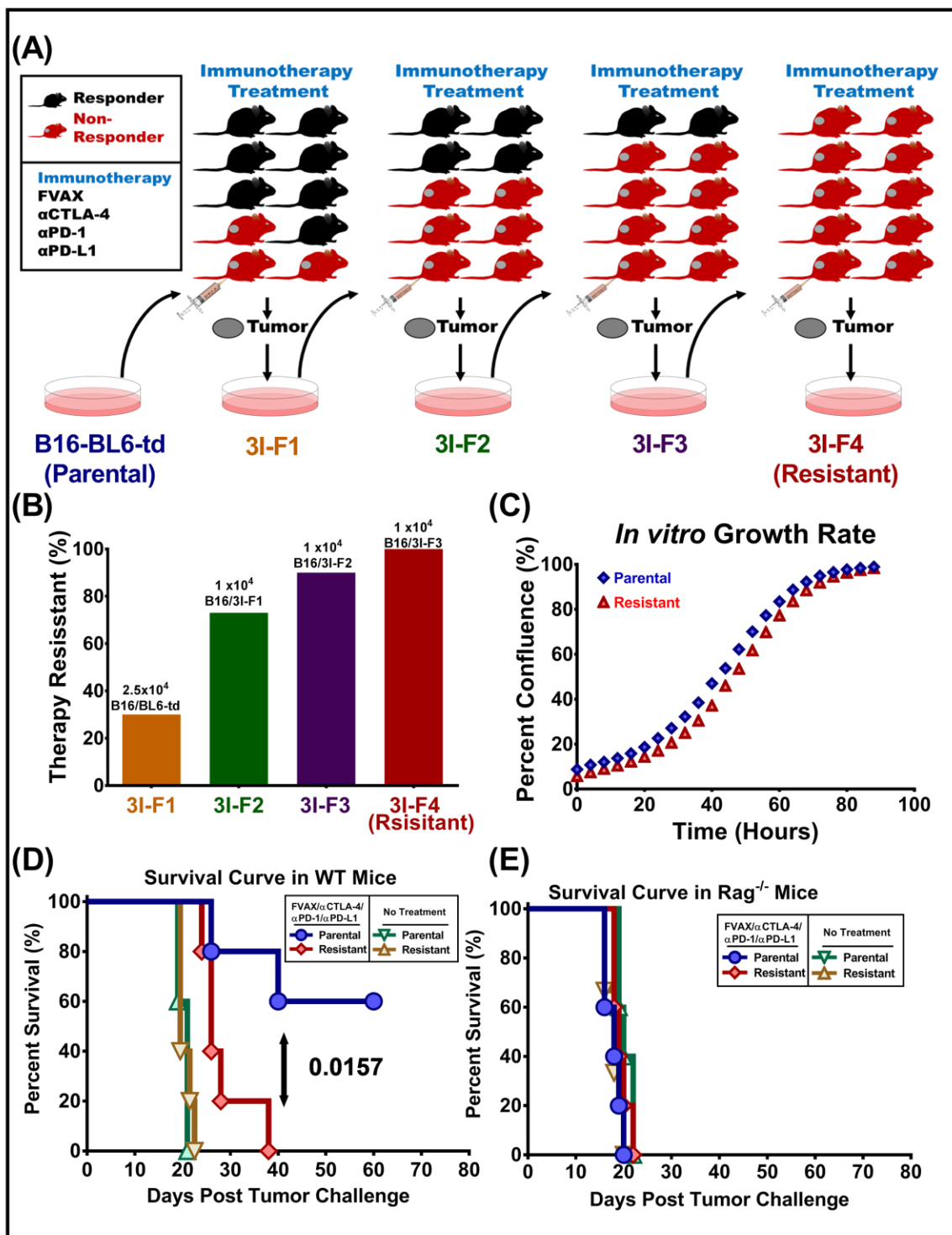




**Figure 2.1: Generation and characterization of checkpoint blockade immunotherapy resistant tumor cells through serial *in vivo* passage.** (A) Experimental model for evolution of immunotherapy resistant B16 cell line. Tumor cells were harvested and cultured from non-responder mice and tumor cell lines were generated. Through serial *in vivo* passage the immunotherapy resistant cell line (3I-F4) was generated. (B) A bar graph shows percentage of mice who did not respond to immunotherapy after each *in vivo* passage. Data labels on the bars indicate name and number of tumor cells implanted for the respective passages. (C) The *in vitro* growth kinetics of the resistant tumor cell line compared to parental tumor cell line were determined using the IncuCyte™ confluency assay. (D) Survival of mice challenged with  $2.5 \times 10^4$  parental or resistant tumor cells with and without immunotherapy treatment in (D) wild type and (E) Rag-/- mice. Statistical significance was calculated using a Student's *T* test. ns, not significant; \* $P < 0.05$ , \*\* $P < 0.01$ , \*\*\* $P < 0.001$ , \*\*\*\* $P < 0.0001$ .

### ***2.4.2: Immunotherapy resistant tumors enriched genetic changes to evade immune response***

We next sought to identify the acquired genetic changes within resistant tumors which drove the evolution of their resistance to the resistance to immunotherapy phenotype. We harvested resistant 3I-F4 tumors and separated the tumor cells away from non-tumor flow sorted to separate tumor cells from non-tumor cells (hereafter referred to as microenvironment) using Fluorescence activated cell sorting (FACS) for independent gene expression profiling on both populations (Fig. 2.2A). We observed substantial genetic diversity of expression when comparing gene arrays between resistant and parental tumor cells, however, top candidate genes generally clustered in metabolic pathways in particular, glycolysis, oxidative phosphorylation, oxidative stress, and hypoxia (Fig. 2.2B & 2.2C).

To identify pathways that were either enriched or underrepresented in 3I-F4 tumors, we performed gene set enrichment analysis (GSEA) on both resistant tumor cell and microenvironmental data sets. Independent analysis of tumor cell and associated microenvironment gene expression gave us the unique capacity to investigate cross-communication between tumors cells and the surrounding stroma. It also gave us an opportunity to investigate the effects of these genetic adaptations by resistant tumor cells on anti-tumor immunity in the TME. The gene set 'MANALO\_HYPOXIA\_DN', representing genes that are down-regulated in response to both hypoxia and overexpression of an active form of HIF1A, was positively enriched in resistant tumor cells (Fig. 2.2E) implying an adaptation to the hypoxic state. Surprisingly, the same gene set was negatively enriched in resistant

tumors' microenvironments, which implies that tumor cells are adapting to a state of hypoxia and surrounding stroma is poorly equipped to handle the hypoxic stress (Fig. 2.2D & 2.2E). The gene set 'NFE2L2.V2', representing genes up-regulated in embryonic fibroblasts (MEF) after knock out of NFE2L2 (Nrf2) which drives response to oxidative and other stresses, was positively enriched in resistant tumors. This suggests that resistant tumor cells have better adapted to the cellular stress caused by aberrant metabolism within TME (Fig. 2.2D & 2.2E). A Gene Set Enrichment Analysis (GSEA) and an Ingenuity Pathway Analysis (IPA) also revealed other metabolic crosstalk between resistant 3I-F4 tumors and their microenvironment. The tumors resistant to immunotherapy showed increases in biological pathways involving mitochondrial oxidative phosphorylation, oxidoreductase, hypoxia response genes, and glycolysis. They also showed decreases in oxidative damage pathways, implying that these cells have adapted to the hypoxic environment. On the other hand, the tumor microenvironment showed enrichment of several hypoxia related gene sets. This implies that while 3I-F4 tumors successfully adapt to the hypoxic state, the microenvironment is unable to do so due to upregulation of the gene set normally downregulated during a successful hypoxic adaptation. As a consequence, the microenvironment suppressed anti-tumor immune function, which is reflected by the negative enrichments of gene sets involving T cell effector functions, myeloid (DC and microphages) cell activation and DC maturation (Fig. 2.2D And Supplemental Fig. 2.2). Taken together the data suggests that resistant tumors deplete nutrients in the TME and create state of hypoxia in which only metabolically adapted cancer

cells can thrive. Lack of glucose and environmental hypoxia thus hamper antitumor immunity.

Figure 2.2

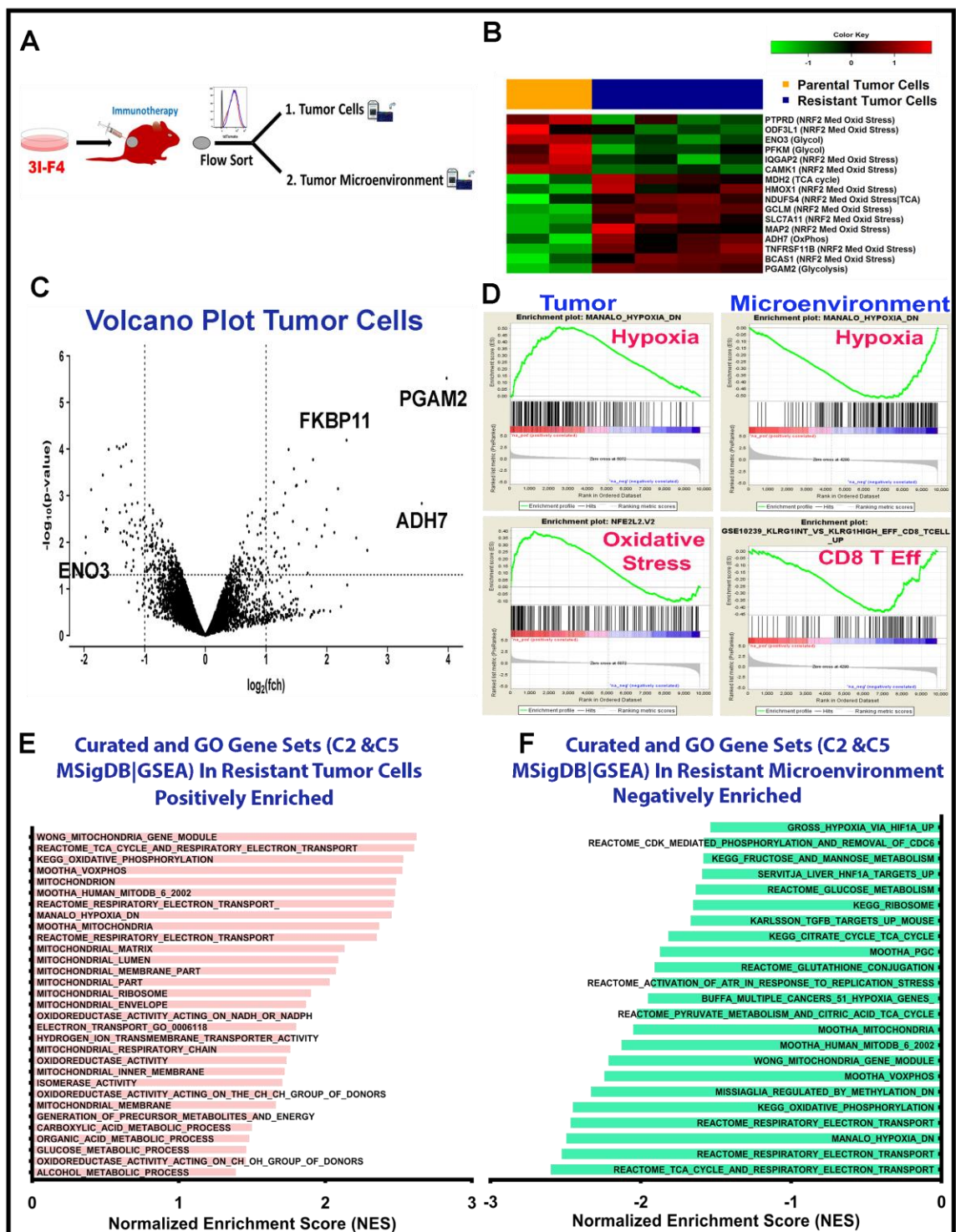


## Figure 2.2 Gene expression profiling and immunogenomics of immunotherapy resistant tumor cells

(A) Experimental schematics of the gene expression microarray. Resistant tumors and control parental tumors were FACS sorted into td-tomato positive tumor cells and td-tomato negative microenvironment. Both the populations were treated separately for microarray analysis. (B) The heat map represents fold expression change of highly upregulated and downregulated genes representing metabolic pathways. (C) A volcano plot representing log fold change in gene expression in immunotherapy resistant tumor cells compared to immunotherapy sensitive parental tumor cells. (D) Representative GSEA plots from tumors (hypoxia and oxidative stress gene sets) and microenvironment (hypoxia and CD8 T<sub>H</sub>1 gene sets). (E) Positively enriched curated (C2 MsigDB|GSEA) and GO (C5 MsigDB|GSEA) in immunotherapy resistant tumor cells compared to immunotherapy sensitive parental tumor cells. (F) Negatively enriched curated (C2 MsigDB|GSEA) and GO (C5 MsigDB|GSEA) in immunotherapy resistant tumor microenvironment compared to immunotherapy sensitive parental tumor microenvironment.

### ***2.4.3: Resistant melanoma cells acquire a hypermetabolic phenotype to evade checkpoint blockade-mediated immunotherapeutic pressure.***

To experimentally validate the metabolic adaptations of resistant tumors, we assessed their glycolytic metabolism by measuring the extracellular acidification rate (ECAR, a readout of glycolysis), and their rate of oxidative phosphorylation by measuring their oxygen consumption rate (OCR, read out of mitochondrial respiration). The immunotherapy resistant cell line, 3I-F4, had higher basal levels of both ECAR and OCAR (Fig. 2.3A & 2.3B) than the parental cell line. The maximum glycolytic capacity and mitochondrial respiration were also elevated in resistant cells compared to parental cells (Fig. 2.3A & 2.3B). Interestingly, this enhancement of both glycolysis and oxidative phosphorylation is a departure from the expected Warburg effect, in which tumor cells rely primarily on glycolysis for ATP production even in oxygen-depleted environments. In order to further validate the hypermetabolic phenotype of immunotherapy resistant tumor cells, we analyzed their cellular metabolites using nuclear magnetic spectroscopy. The resistant 3I-F4 cell line showed relative increases in lactate and other TCA cycle metabolites (Supplemental Fig. 3.3A). We also compared metabolites extracted from whole tumor lysates of resistant tumors to parental tumors with and without treatment. Consistent with the cell line data, *ex vivo* resistant tumors also showed increased relative levels of lactate and other TCA cycle metabolites under both untreated and treated conditions. (Fig. 2.3C). Interestingly, the observed increase in these metabolites was more profound in the presence of immunotherapy treatment, which suggests that treatment itself directly or indirectly triggers these metabolic changes in resistant tumors (Fig. 2.3C).

One of the major goals in the field of checkpoint blockade immunotherapy field is to define pre-treatment biomarkers that can predict response to therapy. In a previous study, increased serum LDH levels was negatively correlated with overall survival and progression-free survival in melanoma patients on anti CTLA-4 treatment (181,182), and tumors are known to be primary source of lactate in cancer patients' serum. Based on our *in vitro and ex-vivo* metabolic analyses, we hypothesized that the increase in lactate production in resistant tumors could serve as a marker to separate immunotherapy sensitive and resistant tumors by visualizing conversion of hyperpolarized pyruvate into lactate utilizing noninvasive MRI imaging. Using this approach, we showed that the rate of pyruvate to lactate conversion was significantly higher in immunotherapy resistant tumors (Fig. 2.3D & 2.3E). The *in vitro, ex vivo* and *in vivo* data suggest that checkpoint blockade immunotherapy resistant tumors acquire a hypermetabolic state where they upregulate both glycolysis and oxidative phosphorylation to evade the host immune response.



Figure 2.3

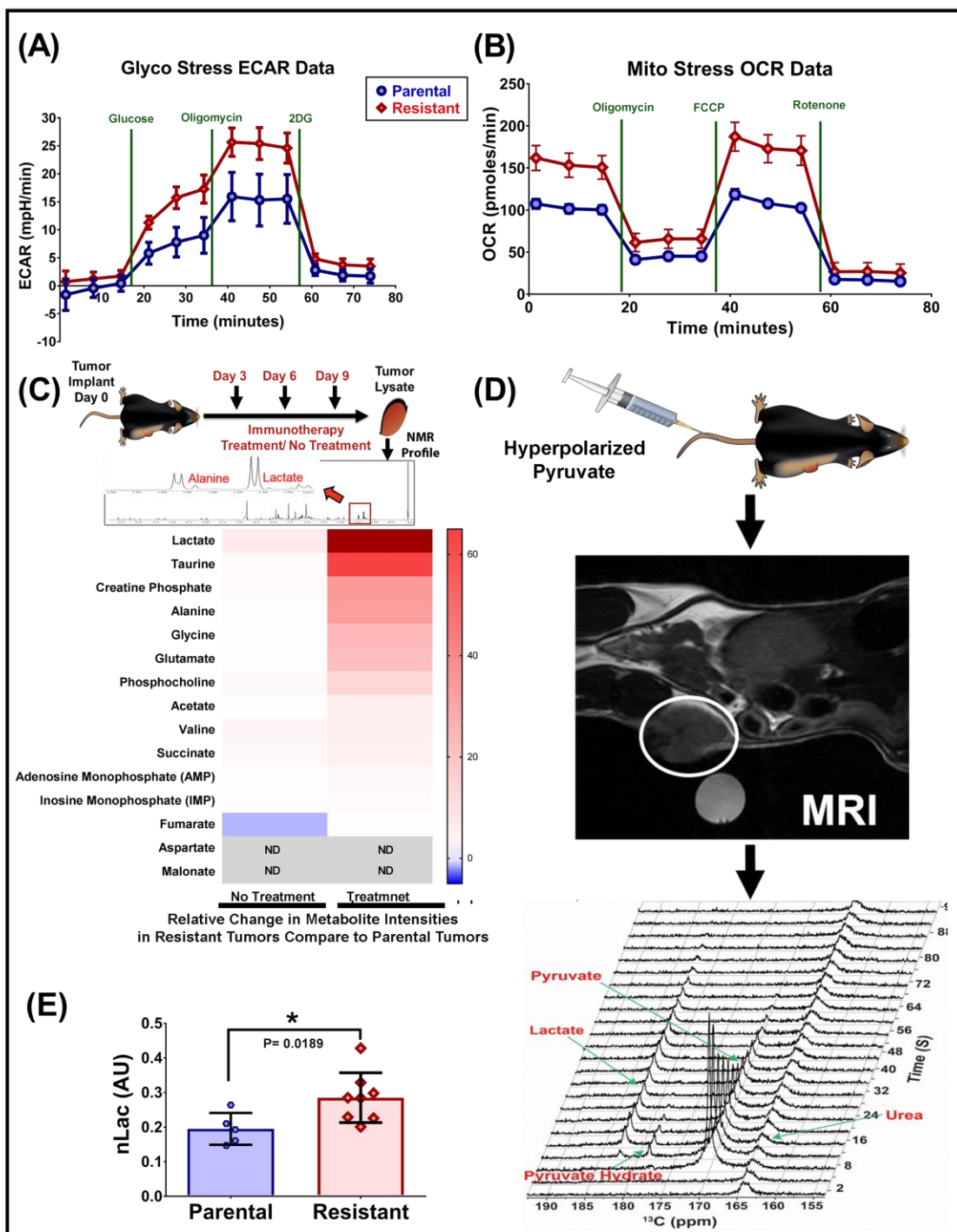


**Figure 2.3: Resistant melanoma cells acquired hypermetabolic phenotype to evade checkpoint blockade mediated immunotherapeutic pressure.**

Immunotherapy resistant 3I-F4 and immunotherapy sensitive parental cells were analyzed using seahorse flux assay. (A) Extra cellular acidification rate (ECAR), a surrogate read out for glycolysis, using glycostress assay and (B) oxygen consumption rate (OCR), a surrogate read out for mitochondrial respiration, using mitostress assay were determined. (C) Heat map depicting relative changes in metabolites' intensities from resistant to parental tumors in the presence and the absence of treatment. Tumors from mice with and without immunotherapy treatments were collected on day 12-16 post implantation and flash frozen on liquid nitrogen. The metabolites were extracted and analyzed on Avance Bruker spectrometer NMR. The intensities of metabolites were taken with respect to NMR reference compound. Heat map was then generated using Z score, which is relative intensities of extracted metabolites from resistant tumor lysates compared to parental tumor lysates. (D) A metabolic signature of resistant tumors were visualized using noninvasive MRI technique. Hyper polarized pyruvate were injected in tumor bearing mice which were then analyzed using magnetic resonance imaging (MRI) for pyruvate to lactate conversion ratio. (E) Normalized lactate to pyruvate ratio was calculated [ $nLAC = (Lactate + Pyruvate) / Lactate$ ] and used as a surrogate read out of glycolysis rate in resistant tumor compare to parental tumors. Statistical significance was calculated using a Student's *T* test. ns, not significant; \* $P < 0.05$ , \*\* $P < 0.01$ , \*\*\* $P < 0.001$ , \*\*\*\* $P < 0.0001$ .

#### **2.4.4: Resistant melanoma tumors adapt to thrive in hostile hypoxic conditions.**

We further investigated the role of hypoxia in mediating resistance to checkpoint blockade immunotherapy based on our GSEA and metabolic profile of resistant tumors. We used confocal microscopy to observe how resistant and parental tumors interact with hypoxic zones in the TME, using the Hypoxyprobe (hypoxia-specific reactive reagent Pimonidazole and anti- Pimonidazole staining antibodies) to image tumor hypoxia and td-Tomato fluorescent protein to discriminate tumor cells. There was no significant difference in the size of hypoxic regions in untreated resistant and parental tumors (Fig. 2.4A, Supplemental Fig. 2.3B); however, in response to treatment, resistant tumors exhibited more hypoxia compared to parental. In addition, td-Tomato positive cancer cells in resistant tumors were present at a higher density within hypoxic regions than their parental counterpart, which is consistent with our gene expression data showing that cancer cells in resistant tumors have adapted to an unfavorable hypoxic conditions (Fig. 2.4A, 2.4B and Supplemental Fig. 3B). An *in vitro* survival assay of resistant and parental tumors in a hypoxic chamber showed an increased growth kinetic for the resistant 3I-F4 cell line compared to parental (Fig. 2.4C) further illustrate that these cells can thrive under adverse metabolic conditions. Thus, checkpoint blockade immunotherapy-resistant 3I-F4 cells have acquired a hypermetabolic phenotype and created a hostile microenvironment in which they have genetically adapted to flourish.

Figure 2.4

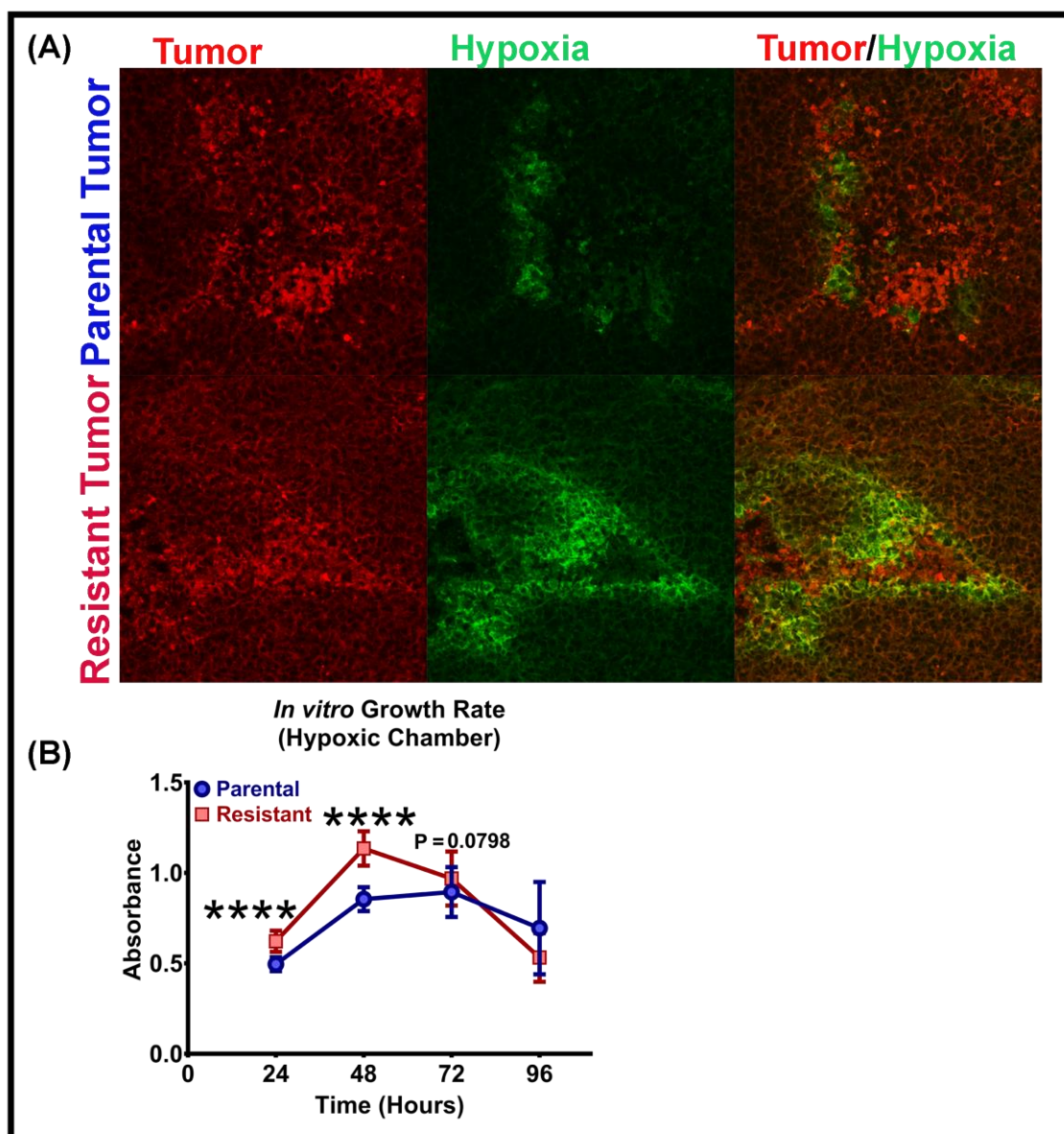


**Figure 2.4: Resistant melanoma tumors adapt to survive under hostile hypoxic conditions.** (A) Resistant and parental tumors were implanted in mice and treated on days 3, 6, and 9. Tumors were collected on day 12-14 for confocal microscopy. Hypoxia (green) was imaged using Hypoxyprobe and tumor cells (red) were visualized based on td-Tomato expression. (B) Cell survival assay (MTS) performed on resistant and parental tumors in a hypoxia chamber (1% oxygen). Statistical significance was calculated using the Student's t test. ns, not significant; \*P < 0.05, \*\*P < 0.01, \*\*\*P < 0.001, \*\*\*\*P < 0.000.

***2.4.5: The nutrient-depleted microenvironment of resistant tumors creates unfavorable conditions for anti-tumor immune cells to function***

Next, we wanted to investigate the effects of metabolic adaptation by resistant tumor cells on the composition and phenotype of immune cells in the tumor microenvironment. We performed multicolor flow cytometry analysis to study tumor immune infiltrates and found that checkpoint blockade-resistant tumors showed significantly increased CD8 T cell infiltration in response to treatment, which was similar to the response seen in immunotherapy-sensitive parental tumors (Supplemental Fig. 2.4A). However, there was a significantly higher CD8 T cell density (CD8 T cell count per mg tumor mass) in parental tumors compared to immunotherapy resistant tumors (Fig. 2.5A) when treated with triple checkpoint therapy. CD8 T cells in resistant tumors vs. parental tumors showed a significant decrease in cell proliferation as measured by Ki-67 expression under untreated conditions. In response to treatment, however, there was no difference in CD8 T cell proliferation between parental and resistant tumors (Fig. 2.5B). CD8 T cells from resistant tumors exhibited decreases in expression of the T cell cytotoxicity marker granzyme B (Fig. 2.5C), and of Glut-1, a marker for glycolytic function, (Fig. 2.5D), however, there was no significant difference in expression of activation markers such as CTLA-4, PD-1, and PD-L1 or of the cytolytic cytokine perforin or of LAP, which is a surrogate marker for a suppressive cytokine tumor growth factor- $\beta$  (TGF- $\beta$ ) (Supplemental Fig. 2.4B-F).

Effector function of cytotoxic CD8 T cells are dependent on their metabolic fitness, in particular, their glycolytic capacity. In order to test the effect of metabolic adaptation of resistant tumors on cytotoxic CD8 T cell function, we measured

glucose uptake using fluorescently labeled glucose (2NDGB) and mitochondrial membrane potential using MitoTracker Deep Red FM in tumor infiltrating T cells. CD8 T cells demonstrate reduced glucose uptake and showed high Mito FM staining in resistant tumors compared to parental tumors (Fig. 2.4 E). These data suggest that checkpoint blockade immunotherapy enhances cytotoxic CD8 T cell infiltration into resistant tumors, but their density and intra-tumor effector functions are compromised in the TME of resistant vs. parental B16 melanoma.

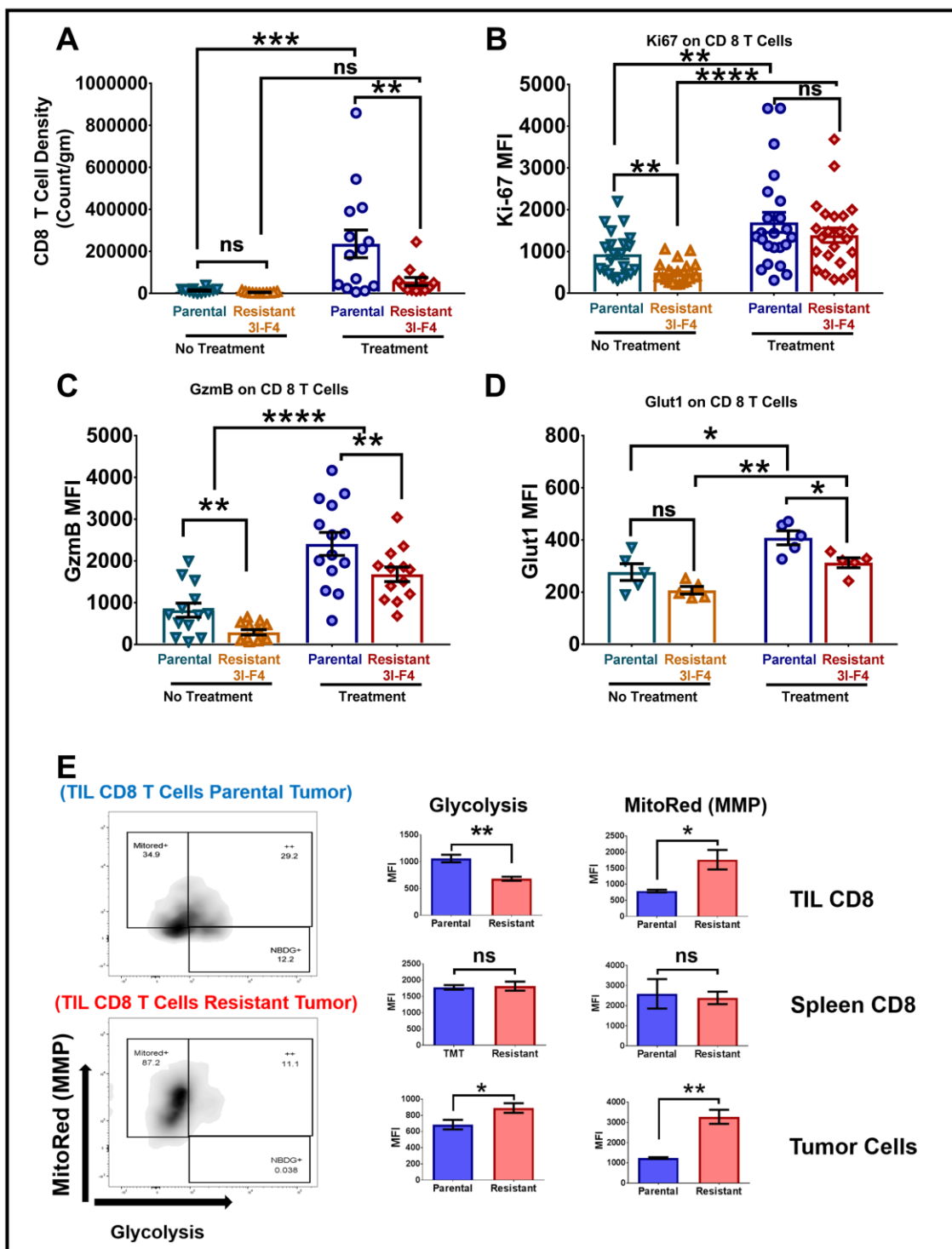
Compared to parental tumors we did not observed a significant difference in infiltration (Supplemental Fig. 5A) or proliferation (Supplemental Fig. 5A) of CD4 T effector cells in resistant tumors with and without therapy. We did not observe any significant difference in the expression of CTLA-4, PD-1, Glut-1 and LAP by CD4 T effector cells from parental and resistant tumors (Supplemental Fig. 2.5B-F). These data imply that the TME of resistant tumors may not affect CD4 T cells as adversely as it does CD8 T cells.

We also investigated the effects of metabolic adaptation of tumor cells on the tumor-supportive elements of the immune microenvironment, especially on T regulatory cells (Treg) and Myeloid Derived Suppressor cells (MDSC). There was no significant difference in either Treg infiltration or CD8:Treg ratio in resistant tumors in comparison to parental tumors, with and without therapy (Fig. 2.6A & 2.6B). We also did not observe any significant difference in proliferation of regulatory T cells in resistant tumors, as depicted by Ki67 staining (Fig. 2.6C). In resistant tumors, however, regulatory T cells significantly increased CTLA-4 expression (Fig. 2.6D) in response to therapy, which can participate in inhibiting T cell activation (183). Similarly, there was no significant difference in MDSC

infiltration and CD8: MDSC ratio in resistant tumors compared to parental tumors, however, in resistant tumors MDSC exhibited signs of enhanced-suppressive capacity. The expression of suppressive enzymes IDO and arginase was significantly increased in MDSCs from resistant tumors in response to treatment. Together, these data suggest that metabolic adaptation of immunotherapy resistant tumors creates a hostile microenvironment where antitumor CD8 T cells display decreased effector function and tumor-supportive populations such as Tregs and MDSCs become more suppressive.

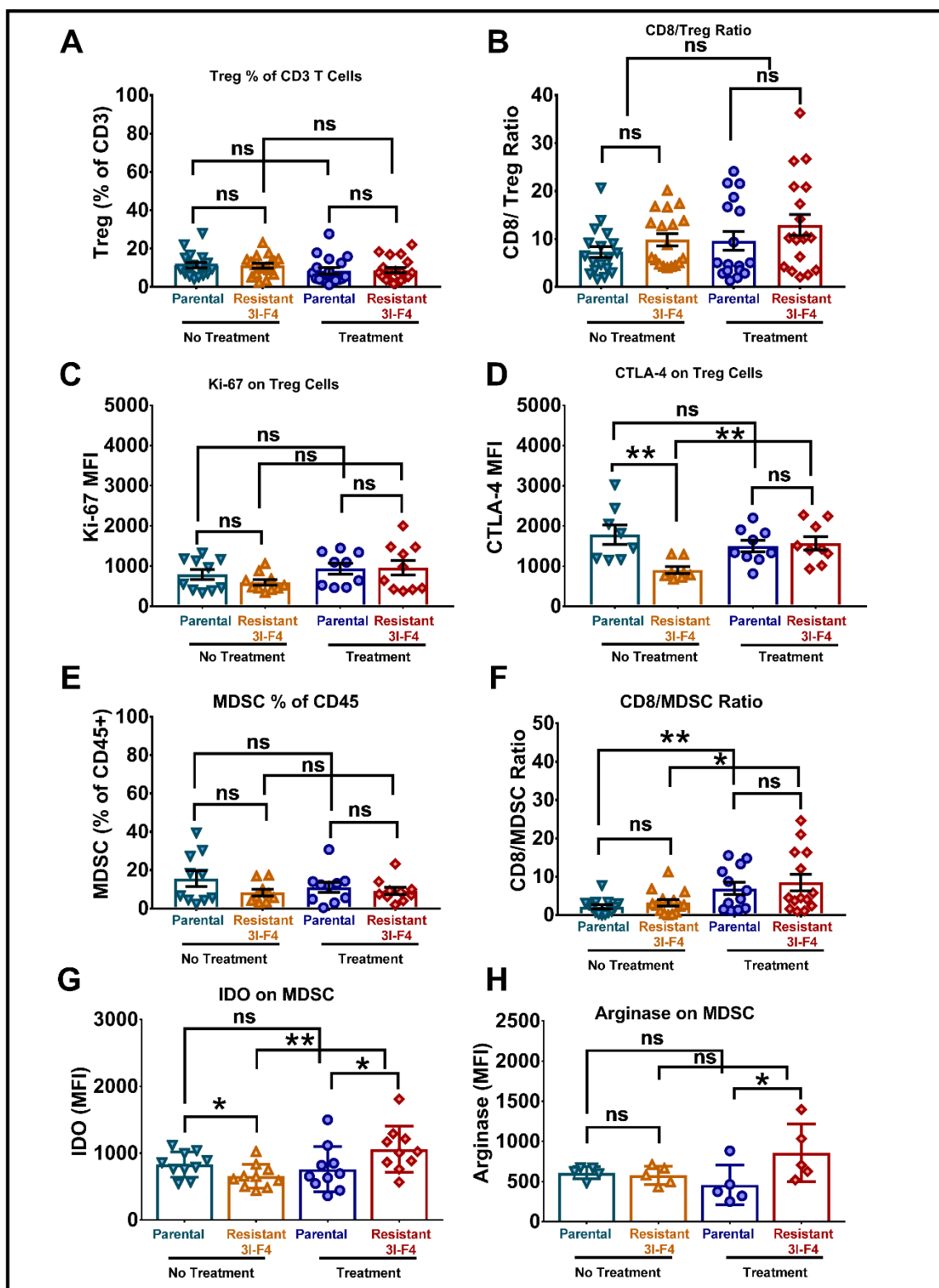


Figure 2.5



**Figure 2.5: Effects of metabolic adaptation by resistant tumors on cytotoxic T cell infiltration and function.** (A) T cell density per tumor weight was determined using flow cytometry analysis. Resistant and parental tumors were implanted in mice and treated on days 3, 6 and 9. Tumors were weighed before harvesting for flow cytometric analysis. Data are expressed as the total number of CD8 positive cells per milligram of tumor. (B) T cell proliferation analysis using multicolor flow cytometry. The data was presented as mean fluorescence intensity of Ki-67, a T cell proliferation marker. T cell function was analyzed using multicolor flow cytometry analysis. The data presented as mean fluorescence intensity of (C) Granzyme B and (D) Glut 1 receptor, T cell function and activation markers. (E) Analysis of glycolysis and oxidative phosphorylation on tumor infiltrating CD8 T cells. Resistant and parental tumors were implanted in mice and treated on day 3, 6 and 9. The tumors were harvested for flow cytometry analysis and stained with Mitored and other phenotypic markers. The mice were intravenously injected with fluorescently labeled glucose (NBDG) thirty minutes before they were sacrificed for the tumor harvest. The data is presented as mean fluorescent intensity of NBDG, and Mitored on tumor infiltrating CD8 T cells, splenic CD8 T cells and td-Tomato positive tumor cells. Statistical significance was calculated using the Student's t test. ns, not significant; \*P < 0.05, \*\*P < 0.01, \*\*\*P < 0.001, \*\*\*\*P < 0.0001.

Figure 2.6



**Figure 2.6: Effects of metabolic adaptation by resistant tumors on infiltration and function of Treg and MDSC.** (A) Regulatory T cells as a percentage of total tumor infiltrating T cells. Resistant and parental tumors were implanted in mice and treated on days 3, 6 and 9. The tumors were harvested on day 12 for multicolor flow cytometry analysis. Regulatory T cells (Treg) were gated on CD4 positive and Foxp3 positive populations. (B) CD8/Treg ratios within the tumor were calculated by dividing the number of CD8+CD3+ cells by the number of CD4+Foxp3+ cells. Proliferation and function of tumor infiltrating T regulatory cells were performed using multicolor flow cytometry. (C) Treg proliferation data was presented as mean fluorescent intensity of Ki-67, a proliferation marker. (D) Expression of CTLA-4 on tumor infiltrating Treg. The data is presented as mean fluorescence intensity of CTLA-4 by T regulatory cells. (E) Myeloid Derived Suppressor Cells (MDSC) as a percentage of total tumor infiltrating CD45+CD3- cells. MDSC were gated on CD11b+ and Gr1+ double positive populations. (F) CD8/MDSC ratios within the tumor were calculated by dividing the number of CD8+CD3+ cells by the number of CD11b+Gr1+ cells. The suppressive function of tumor MDSCs were analyzed using multicolor flow cytometric analysis and data is presented as mean fluorescent intensity of (G) Indoleamine-pyrrole 2,3-dioxygenase (IDO) and (H) Arginase. Data were pooled from  $\geq 2$  experiments with 5 mice per group. Bars represent mean  $\pm$  SD. Statistical significance was calculated using the Student's t test. ns, not significant; \*P < 0.05, \*\*P < 0.01, \*\*\*P < 0.001, \*\*\*\*P < 0.0001.

#### ***2.4.6: Monogenic overexpression of PGAM2 and ADH7 in parental tumors confers resistance to checkpoint blockade immunotherapy***

We next sought to validate the monogenic effect of candidate metabolic genes associated with acquisition of checkpoint blockade resistance identified by gene expression profiling of 3I-F4. We overexpressed PGAM2 (top hit in expression analysis; involved in glycolysis) and ADH7 (one of the top hits; gene involved in oxidoreductase pathway which decreases oxidative stress by reducing NAD to NADH) in parental cells (B16/BL6-td). We then implanted tumor cells overexpressing either PGAM2, ADH7 or empty vector in mice to monitor tumor growth and survival with or without checkpoint blockade immunotherapy. When mice were not treated with checkpoint blockade immunotherapy, PGAM2 and ADH7 overexpressing tumors did not show significant differences in tumor growth or survival (Fig. 6A & B). When treated with checkpoint blockade immunotherapy, however, PGAM2 and ADH7 overexpressing tumors became resistant to therapy (Fig. 6A & C), thus implies a role for PGAM2 and ADH7 genes in mediating metabolic changes in 3I-F4 tumors that contribute to the immunotherapy resistance phenotype.

Figure 2.7

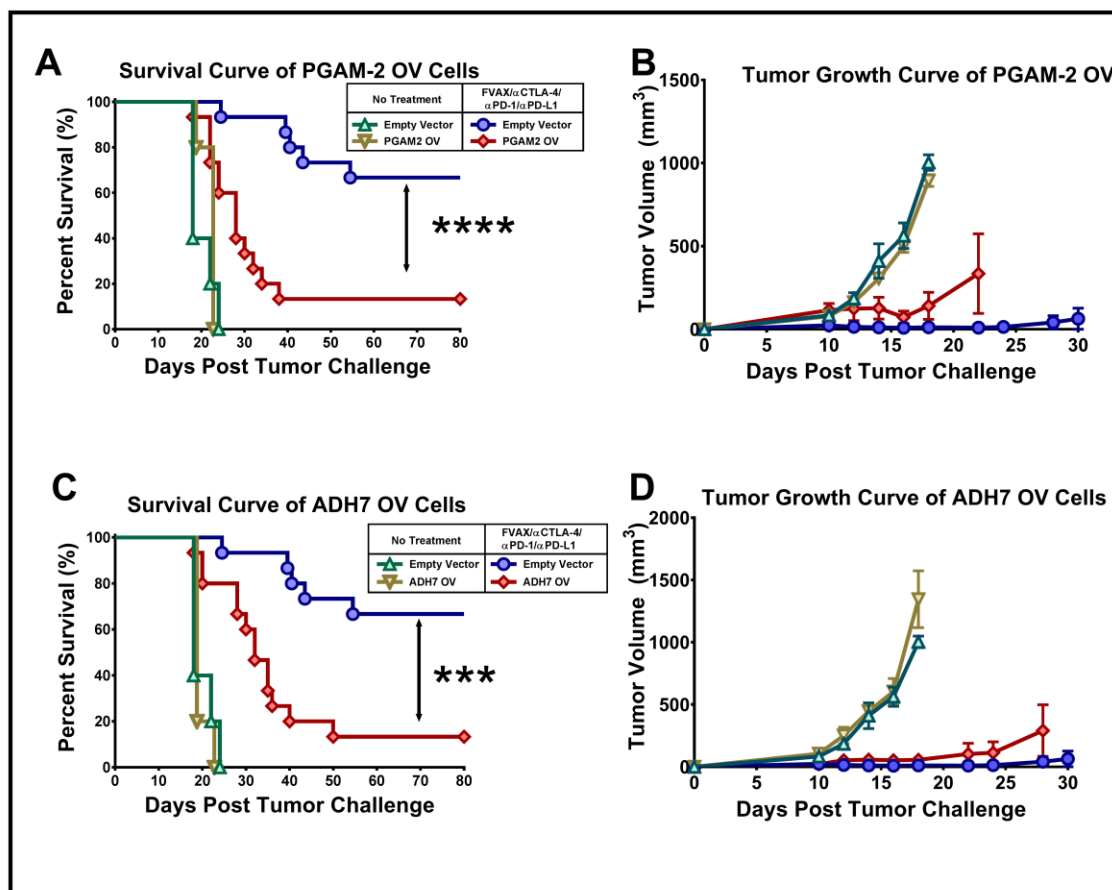


Figure 2.7: Monogenic validation of candidate genes PGAM2 and ADH7.

PGAM2 was overexpressed in the parental tumor cell line B16/BL6-td using a retroviral vector (A) Survival curve and (B) tumor growth were monitored in mice challenged with tumor cells overexpressing PGAM2 and empty vector (control) with and without immunotherapy treatment. ADH7 was overexpressed in the parental tumor cell line B16/BL6-td using a retroviral vector and survival curve (C) and (D) tumor growth were monitored in mice challenged with tumor cells overexpressing ADH7 and empty vector (control) with and without immunotherapy treatment. Statistical significance was calculated using the Student's *t* test. ns, not significant; \**P* < 0.05, \*\**P* < 0.01, \*\*\**P* < 0.001, \*\*\*\**P* < 0.000.

**2.4.7: Melanoma patient tumors which fail to respond to immunotherapy show enhanced expression of metabolic pathways resembling 3I-F4**

We sought to validate the role of metabolic adaptation in modulating the response to checkpoint immunotherapy in human patient samples. To do so, we performed gene expression analysis on mRNA samples from a patient cohort (173) consisting of metastatic melanoma patients who progressed on CTLA-4 blockade and then were treated with  $\alpha$ PD-1. Patients were biopsied prior to  $\alpha$ PD-1 therapy and responses were assessed with serial CT scan after initiation of therapy. As defined earlier (173), responders were defined by absence, stable or reduced tumor size on CT scan, and non-responders were defined by an increased tumor size or tumor control less than 6 months. There were four patients who responded and five who did not respond to therapy. GSEA and IPA analysis showed that compared to responders, non-responders enriched similar metabolic pathways to those identified in our resistant mouse models. Non-responders also showed alteration in gene expression focused on similar nodes in the glycolysis and oxidative phosphorylation pathways compared to resistant tumor models (Fig. 2.8C). These findings suggest that the murine model we generated to study checkpoint immunotherapy resistance has human relevance (Fig. 2.8B & 2.8C).

Figure 2.8

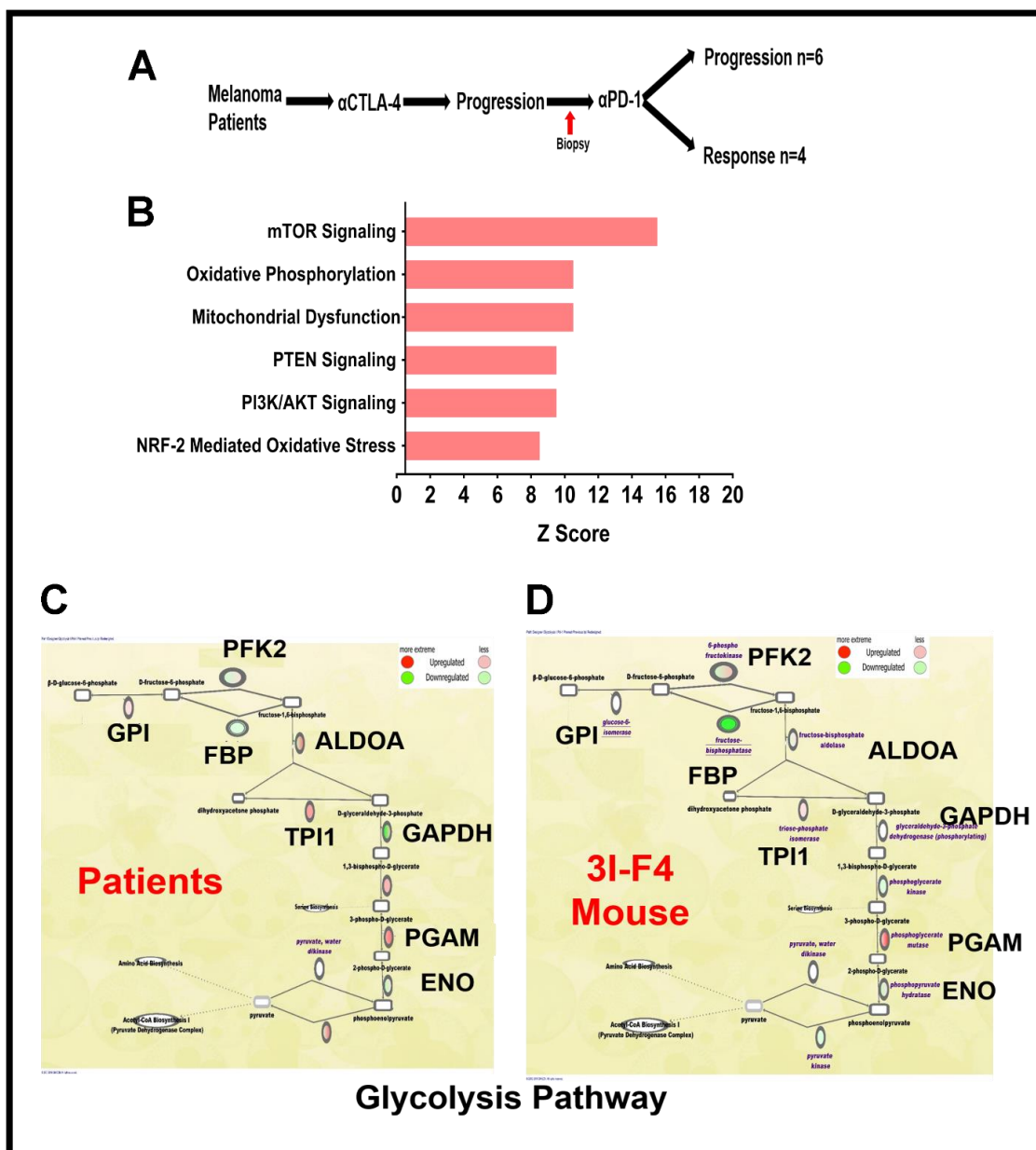




**Figure 2.7: Validation of immunotherapy resistant genetic signature in human melanoma.** (A) Metastatic melanoma patients were treated with anti-CTLA-4 and non-responders were biopsied and then treated with anti-PD-1. Patients were then evaluated for clinical benefit. Gene expression analyses was performed on 4 responders and 5 non responders. (B) Enrichment of metabolic pathways in patients who did not respond to therapy. Bioinformatics analysis was performed using GSEA and IPA analysis. (C) The glycolysis pathway was generated using IPA showing relative expression of genes in patients who did not respond to therapy compared to the responders. The red color indicates upregulation of a gene, while the green color indicates its downregulation in patients who did not respond to therapy compared to responders. (C) Similarly, the glycolysis pathway was generated in immunotherapy resistant mouse tumors showing relative expression of genes in comparison to immunotherapy-sensitive parental mouse tumors.

#### **2.4.8: Nonspecific therapeutic modulation of tumor metabolism could negatively affect anti-tumor immunity**

Based on our *in silico* and experimental findings, we hypothesized that therapeutically reversing the metabolic adaptation of tumor cells would make them sensitive to checkpoint blockade immunotherapy. Since, resistant tumors showed increases in both glycolysis and oxidative phosphorylation, we treated resistant tumors and control parental tumors with 2-Deoxy-D-glucose (2DG), a structural analogue of glucose that inhibits glycolysis, an LDHA inhibitor (GSK2837808A), a selective lactate dehydrogenase A inhibitor (58,184,185), and an oxphos inhibitor (IACS-10759) (186) which is a mitochondrial complex I inhibitor that blocks oxidative phosphorylation (Fig. 2.9A & 2.9B). Unexpectedly, all three drugs failed to provide any therapeutic advantage to resistant tumors when given in combination with immunotherapy. In the presence of 2DG and the Oxphos inhibitor (IACS-10759), even immunotherapy sensitive parental tumors lost therapeutic benefit in response to checkpoint blockade immunotherapy (Fig. 2.9A & 2.9B). Metformin (57) and TH-302(56) reduce hypoxia and are known to synergize when combined with immunotherapy. Because resistant tumors metabolically adapt to flourish in hypoxic conditions, we hypothesized that ablating hypoxia would break the immune tolerance created by resistant tumors. Contrary to our expectations, neither TH-302 nor Metformin was able to sensitize resistant tumors to checkpoint blockade immunotherapy (Fig. 2.9A & 2.9B).

We also tested if repolarizing the more suppressive tumor immune microenvironment by combining immunotherapy with STING agonist (c-di-GMP) (124), PI3K $\gamma$  inhibitor (IPI549) (120) or STAT3 ASO (AZD9150) (187) would break

immune tolerance. However, these strategies also failed to sensitize resistant 3I-F4 tumors to checkpoint blockade (Fig. 2.9A & 2.9C). We also sought to break the metabolic energy of cytotoxic CD8 T cells induced by resistant tumors by treating with TNF receptor superfamily agonist antibodies in combination with checkpoint blockade immunotherapy (188,189). When we treated resistant tumors with agonist antibodies against 4-1BB or CD40 (Fig. 2.9A & 2.9D), however, we did not see any added therapeutic benefit (188,189). While evolving the immunotherapy resistant clones, we made a visual observation that tumors increased vasculature with every increasing passage (Supplemental Fig. 2.6A & 2.6B). In our model, we did not see any increase in therapy mediated antitumor immune response when combined with  $\alpha$ VEGFR2, an antiangiogenic therapy (Fig. 2.9A & 2.9D) (110). Together, metabolic modulators (2DG, GSK2837808A, and IACS-10759), hypoxia ablating agents (TH302 and Metformin), agents targeting suppressive tumor immune cells (STING agonist, IPI549, and STAT3 ASO), TNF super family agonist antibodies ( $\alpha$ 4-1BB and  $\alpha$ CD40) and antiangiogenic therapy ( $\alpha$ VEGF) could not reverse the therapy resistance established by checkpoint blockade –resistant 3I-F4 tumors.

Figure 2.9

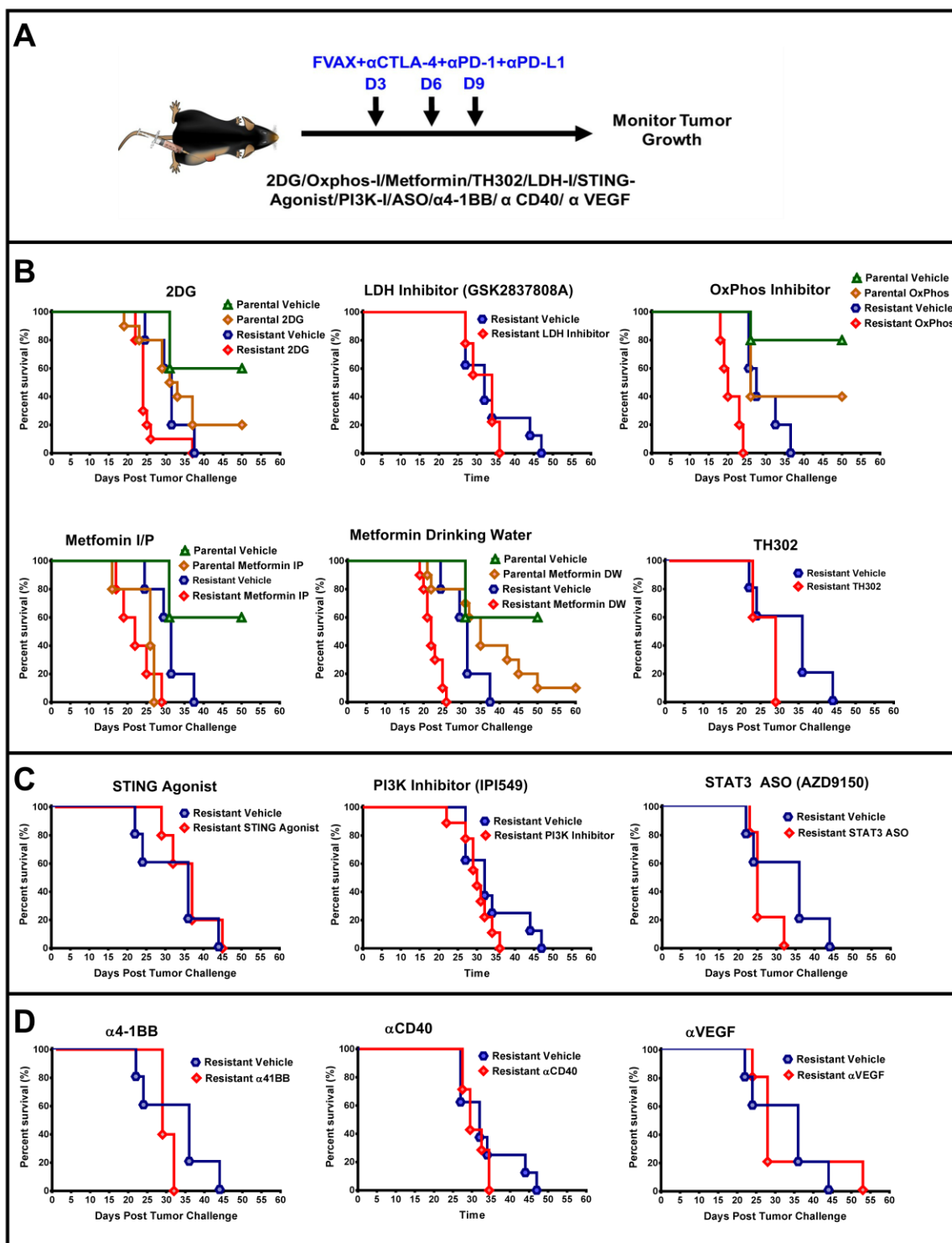


**Figure 2.9: Therapeutic modulation of tumor metabolism fail to reverse immunotherapy resistance.** (A) Experimental design and treatment strategies for tumor survival experiments. Wild type mice on day 0 were challenged with therapy resistant tumors and control parental tumors. Mice were then treated with FVAX plus  $\alpha$ CTLA-4,  $\alpha$ PD-1 and  $\alpha$ PD-L1 on days 3, 6 and 9 in combination with various therapeutic agents or control vehicle as described in the Methods section. (B) Survival graph of resistant tumors treated with metabolic modulators and hypoxia targeting drugs (glucose analogue-2DG, Lactate dehydrogenase Inhibitor-GSK2837808A, Oxidative phosphorylation inhibitor-IACS-10759, Metformin given intraperitoneally, Metformin in drinking water, and hypoxia activated prodrug-TH302). (C) Survival graph of mice treated with therapeutic agents targeting the suppressive tumor microenvironment (STING agonist, PI3 Kinase inhibitor-IPI549, and STAT3 ASO-AZD9150). (D) Survival graph of resistant tumors treated with TNF superfamily agonist antibodies,  $\alpha$ 41BB and  $\alpha$ -CD40, and antiangiogenic antibodies,  $\alpha$ -VEGFR1I.

## 2.5: Discussion

To our knowledge, we are the first to generate an immunotherapy resistant clone of B16 melanoma to conduct an unbiased investigation of acquired resistance to checkpoint blockade immunotherapy and apply the knowledge to predict treatment outcomes using noninvasive methods. The immunotherapy-resistant murine melanoma tumor increased glycolysis, oxidoreductase, and oxidative phosphorylation, which contributed to T cell dysfunction in the microenvironment and conferred resistance to checkpoint blockade immunotherapy.

Tumors resistant to immunotherapy defied Warburg theory, which states that tumor cells rely on glycolysis alone for generation of ATP and downregulate mitochondrial oxidative phosphorylation. Resistant 3I-F4 tumors showed an increase in both glycolysis and oxidative phosphorylation, which we define as a hypermetabolic state. Phosphoglycerate mutase 2 (PGAM2), a glycolytic enzyme, was found highly upregulated in immunotherapy resistant tumor cells compared to parental cells. PGAM2 converts 2-phosphoglycerate to 3-phosphoglycerate, which is an important step in glycolysis as well as anabolism (biosynthesis) of amino acids and nucleotides (190). The phosphoglycerate mutase family (PGAM) is also involved in mediating response to oxidative stress through SIRT2 binding, and protecting cells from oxidative damage by regulating NADPH homeostasis (190). The overactive glycolysis pathway in resistant tumor cells can induce oxidative stress, which may be counterbalanced by upregulation of oxidoreductase pathways. Alcohol dehydrogenase-7 (ADH7), a gene in the oxidoreductase family, is an NAD(P)<sup>+</sup>/NAD(P)H coupling agent (191,192). We believe that highly

upregulated ADH7 in resistant tumor cells offers several advantages to highly glycolytic resistant tumors (191,192). It reduces oxidative stress, generates reduced glutathione (GSH), a known scavenger of reactive oxygen species, and NAD(P)H, a substrate in mitochondrial oxidative phosphorylation (191,192). We propose that upregulation of these glycolytic nodes and oxidoreductase pathways provide metabolic advantages to tumor cells, allowing them to increase mitochondrial oxidative phosphorylation and create a state of hypoxia. The increase in oxidoreductase pathways also aides the tumor cells in adapting to and flourishing in hostile hypoxic conditions where antitumor immune cells are rendered inert.

Immunotherapy resistant tumors did not show substantial declines in the percentage of CD8 T cell infiltration, rather they increased the percentage of infiltrating CD8 T cells in response to therapy (193). These findings corroborate a previously reported study in which an increase in CD8 T cell infiltration in response to CTLA-4 and PD-1 blockade therapy was observed in a cohort of non-responder melanoma patients (174). In parental tumors, however, CD8 T cell density (CD8 T cell numbers per tumor weight) was significantly higher compare immunotherapy resistant 3I-F4 tumors. Hypermetabolic resistant tumor cells can deplete nutrients in the tumor microenvironment, increase tumor-derived lactate and create a state of hypoxia. In this hostile microenvironment, cytotoxic CD8 T cells lose their metabolic fitness (61,62,194-196) and associated effector functions. We have also seen an increase in the suppressive capacity of Treg and MDSC in resistant tumors, which also could be a result of low glucose levels and the presence of

tumor derived lactate as these conditions are known to make Treg and MDSC more immune suppressive (58,197).

There are efforts in the field to expand the therapeutic benefit of checkpoint blockade immunotherapy by understanding the mechanisms of relapse and acquired resistance. Upregulation of alternative immune checkpoint pathways such as TIM3 (97,172) and VISTA (95) were seen in patients who relapsed after PD-1 therapy. In our tumor model we did not see evidence of substantial increased expression of alternative checkpoint pathways in both our gene signature and flow cytometry analysis. We did not see any changes in the genetic expression of IFN $\gamma$  and JAK1 pathways in our resistant tumor (49,198). We did not observe downregulation of MHC class I or II complexes on the surface of resistant tumors (1,30,49). In the resistant tumor model, we rather saw an increase in both class I and II antigen presentation at both genetic and protein levels reflecting loss of environmental immune pressure.

A critical aspect of our study was the enrichment of genetic signatures of immune resistance using *in vivo* passaging. This experimental model also allowed us to separate tumor cells from the surrounding tumor microenvironment and to perform genetic analyses separately. It gave us the advantage of understanding how genetic changes can be acquired in resistant tumors in response to immunotherapeutic pressure. We could also investigate metabolic and immunological cross-communication between tumor cells and their microenvironment. This provide a number of advantages over analysis of whole tumor samples, where it is difficult to separate the biological effects of treatment on tumor cells from rest of the tumor microenvironment. *In vivo* passaging and



analysis of tumor cells separately from the tumor microenvironment, which were lacking in prior studies, facilitated both the identification of relevant genetic changes and a reduction in the signal-to-noise ratio. We believe that this tumor model could be a useful tool to screen pharmaceutical drug candidates to overcome checkpoint resistance. We also showed that this signature can be imaged *in vivo* using a novel MRI technique coupled with a hyperpolarized pyruvate probe. This technique has just been approved for human studies, (199,200) and if applied in immune-oncology (I/O), might provide the first non-invasive approach to assessing whether or not a given patient's tumor is likely to respond to checkpoint blockade.

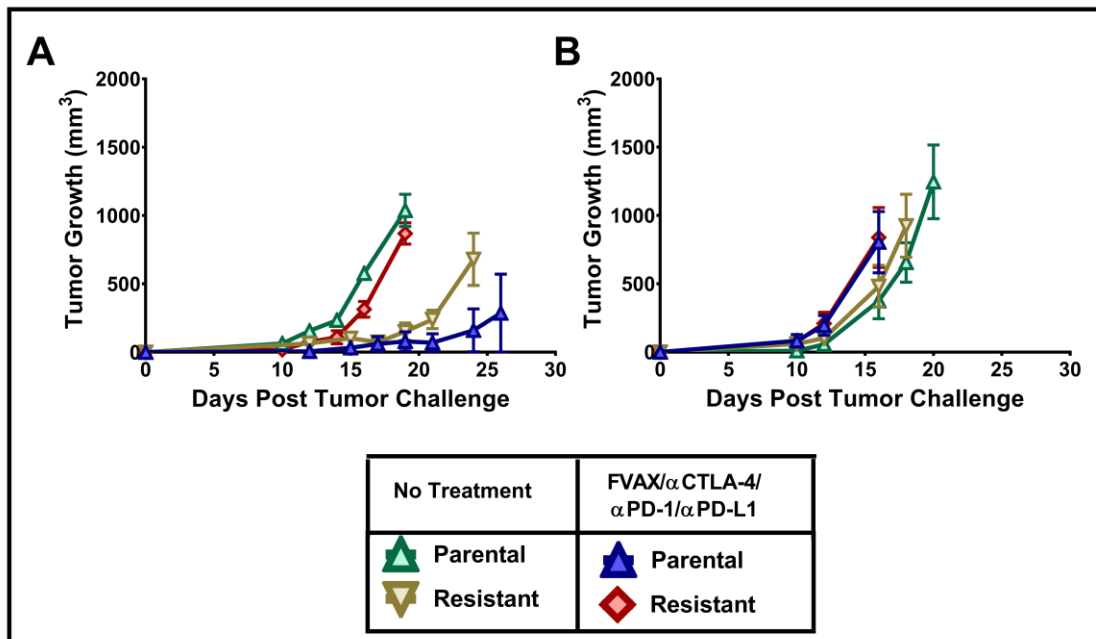
One potential limitation of our study was that the tumor model could not distinguish between mechanisms that drive resistance to each single immunotherapy since a combination of three checkpoint blockade antibodies ( $\alpha$ CTLA-4,  $\alpha$ PD-1 and  $\alpha$ PD-L1) were used to generate immunotherapy-resistant clones. The metabolic adaptation of resistant tumor cells may have been the most prominent mechanism driving resistance, even in the presence of all three checkpoint blockade antibodies, and could therefore be clinically relevant to target. While metabolic adaptation appears prominent in our system, we cannot deny other biological processes may contribute to resistance to immunotherapy such as mutational load (49,111,173), neoantigen load (173), and copy number loss (112,174). These were defined in earlier studies as mechanisms driving resistance to PD-1 and CTLA-4 monotherapy. It would be interesting to analyze the role of mutational landscape in our resistant tumor model, although this was not the focus of the current study.

We therapeutically targeted metabolic adaptation of resistant tumors with metabolic modulators 2DG, LDH inhibitor and oxphos inhibitor but failed to reverse resistance to therapy. Oxphos inhibitor and 2DG, rather, worsened the survival benefits of immunotherapy-sensitive parental tumors. While tumor cells rely on glycolysis and mitochondrial oxidative phosphorylation, both metabolic pathways are equally important to the anti-tumor immune component as well. Thus, we believe there is a metabolic tug-of-war between tumor and immune cells in the tumor microenvironment (68,201). Understanding the metabolic differences between tumor cells and the immune compartment at the molecular level would facilitate the design of therapeutic agents targeting tumor specific metabolism without affecting the immune compartment. Agents that are known to repolarize the immunosuppressive myeloid compartment such as STING agonists, PI3K Inhibitors, anti CD40 antibodies, and a STAT3 ASO failed to break immune tolerance in immunotherapy-resistant tumors. Anergic CD8 T cells could not be rescued by 4-1BB or CD40 agonist therapy either. Interestingly, therapeutic agents targeting hypoxia (TH302 and metformin) and angiogenesis (anti VEGFR11 antibodies) also could not reverse the therapy resistance in immunotherapy resistant tumors. We hypothesize that the rapid growth kinetics characteristic of B16 melanoma contributes to the complete resistance of this model, and that the above agents might require a larger therapeutic window in order to sensitize 3I-F4 tumors to checkpoint blockade.

In conclusion, B16 melanoma acquired immunotherapy resistance by coordinated upregulation of the glycolytic, oxidoreductase pathways and mitochondrial oxidative phosphorylation to create a metabolically hostile

microenvironment in which T cell function is profoundly suppressed.

## Supplemental Figure 2.1



**Supplemental Figure 2.1: Generation and characterization of checkpoint blockade immunotherapy resistant tumor cells through serial *in vivo* passage.** (A) Tumor growth was monitored in mice challenged with parental or resistant tumor cells with and without immunotherapy treatment in wild type and (B) Rag<sup>-/-</sup> mice. 25000 resistant and parental tumor cells were implanted in wild type and Rag<sup>-/-</sup> mice. The tumor growth was monitored with and without treatment. Statistical significance was calculated using a Student's *t* test. ns, not significant; \**P* < 0.05, \*\**P* < 0.01, \*\*\**P* < 0.001, \*\*\*\**P* < 0.0001.

Supplemental Figure 2.2

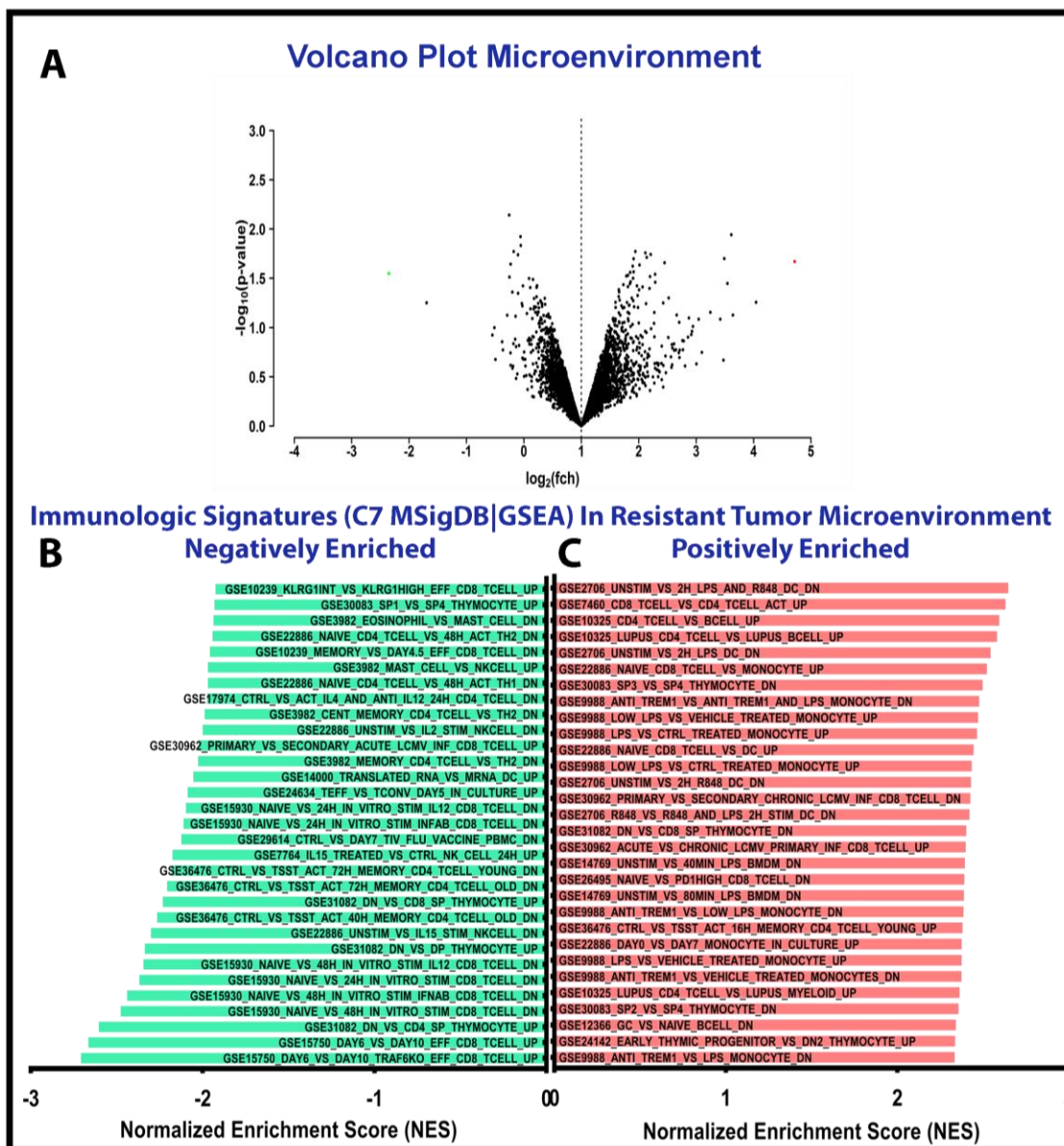


**Figure Supplemental 2.2: Gene expression profiling and immunogenomics of the immunotherapy-resistant tumor microenvironment** (A) Volcano plot representing log fold change in gene expression in immunotherapy resistant tumor microenvironment compared to immunotherapy sensitive parental tumor microenvironment. (B) Positively and (C) negatively enriched immunological gene signature (C7 MsigDB|GSEA) in immunotherapy-resistant tumor microenvironment compared to immunotherapy-sensitive parental tumor microenvironment.

Supplemental Figure 2.3

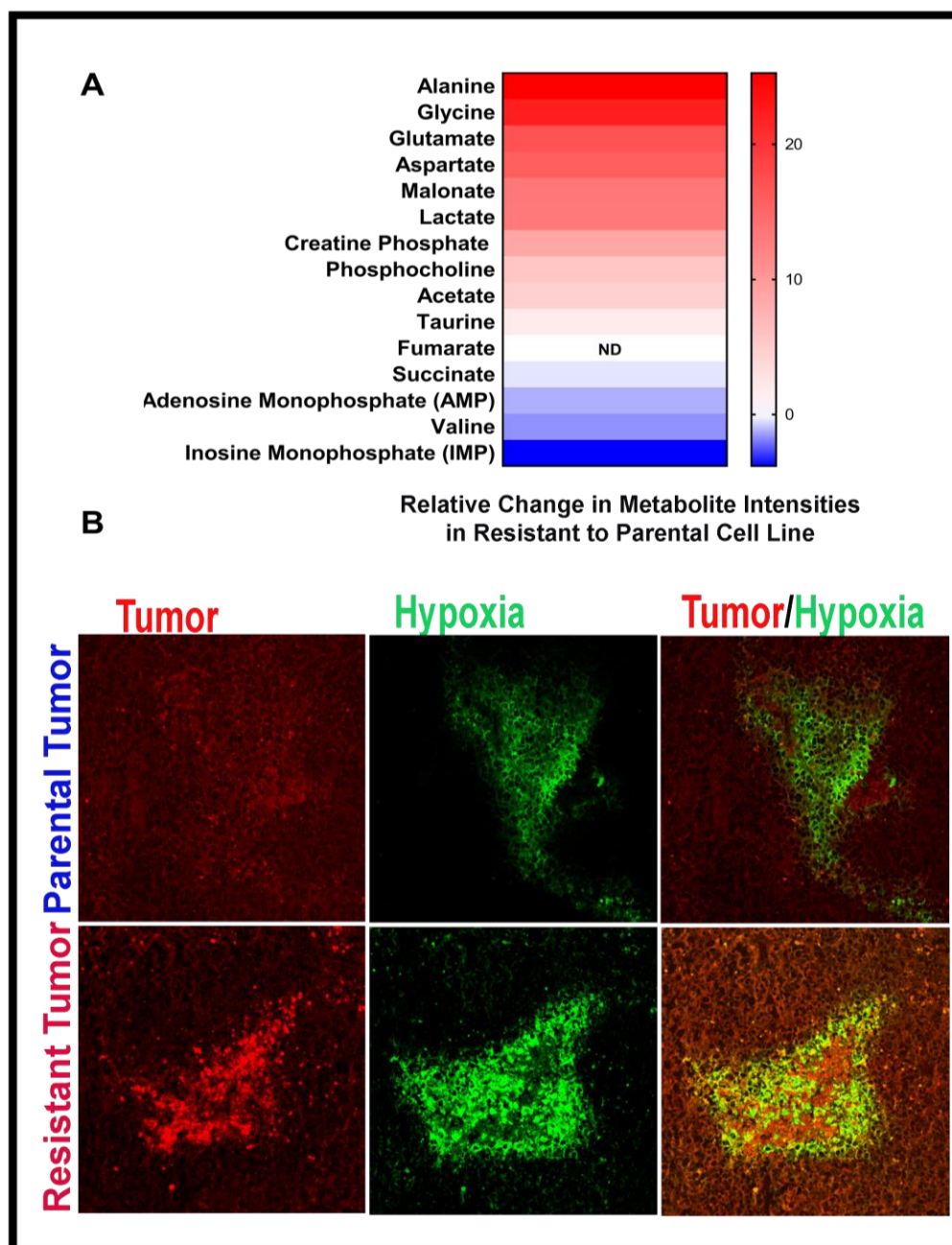
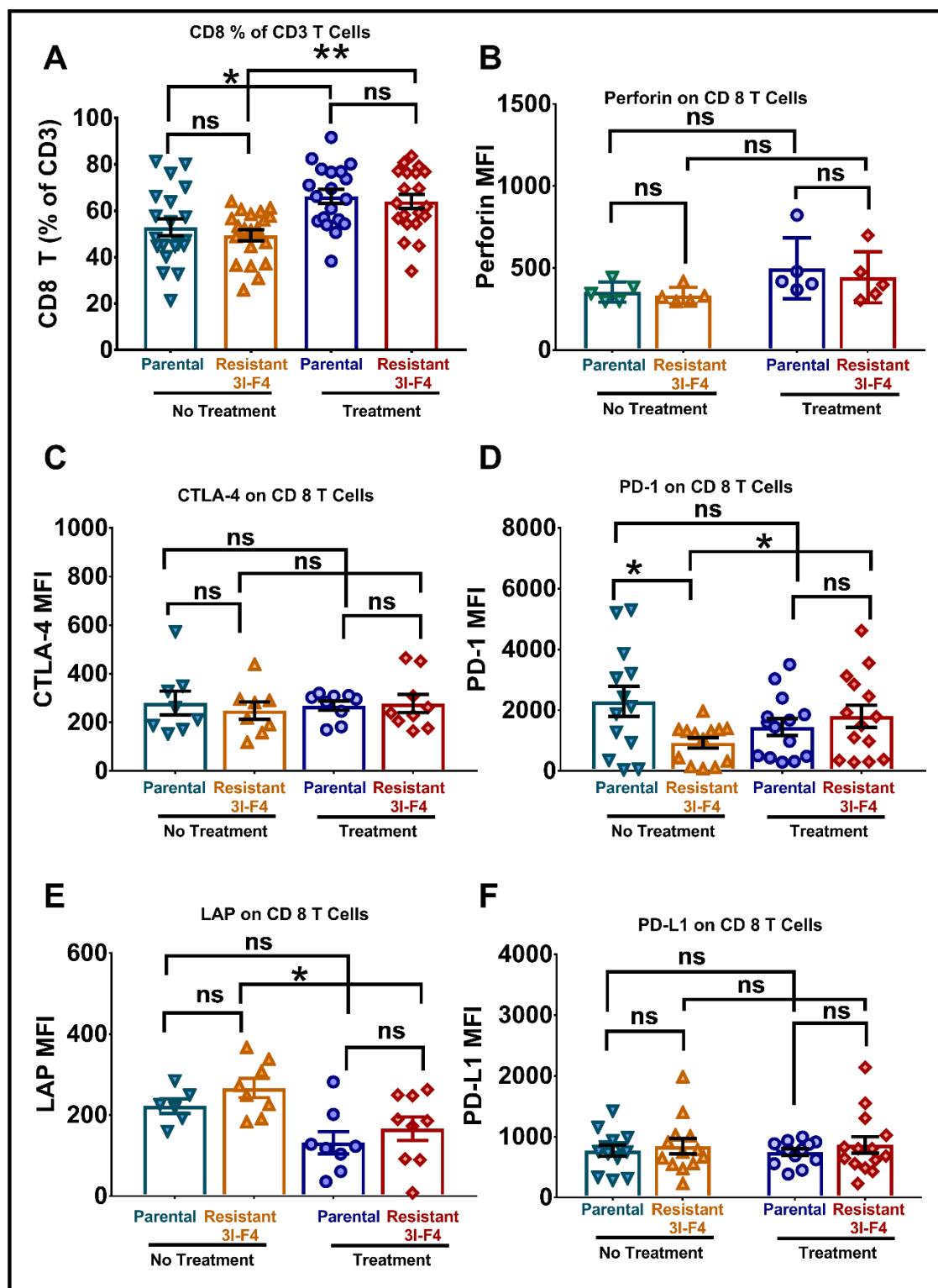


**Figure 2.3: Metabolic signature of resistant cell line using NMR profiling and hypoxyprobe staining of resistant tumors.** (A) Heat map of relative NMR metabolite intensities in resistant cell line (3I-F4) compared to parental cell line (B16/BL-td). Cell lines were washed with PBS twice and flash frozen on liquid nitrogen. The intensities of metabolites were taken with respect to NMR reference compounds. A heat map was then generated using Z score, which depicts relative intensity of metabolites in resistant cell line lysate compared to parental cell line lysate. (B) Resistant and parental tumors were implanted in mice (no treatment). Tumors were collected on day 12-14 for confocal microscopy. Hypoxia (green) was imaged using Hypoxyprobe and tumor cells (red) were visualized with td-Tomato fluorescent protein.

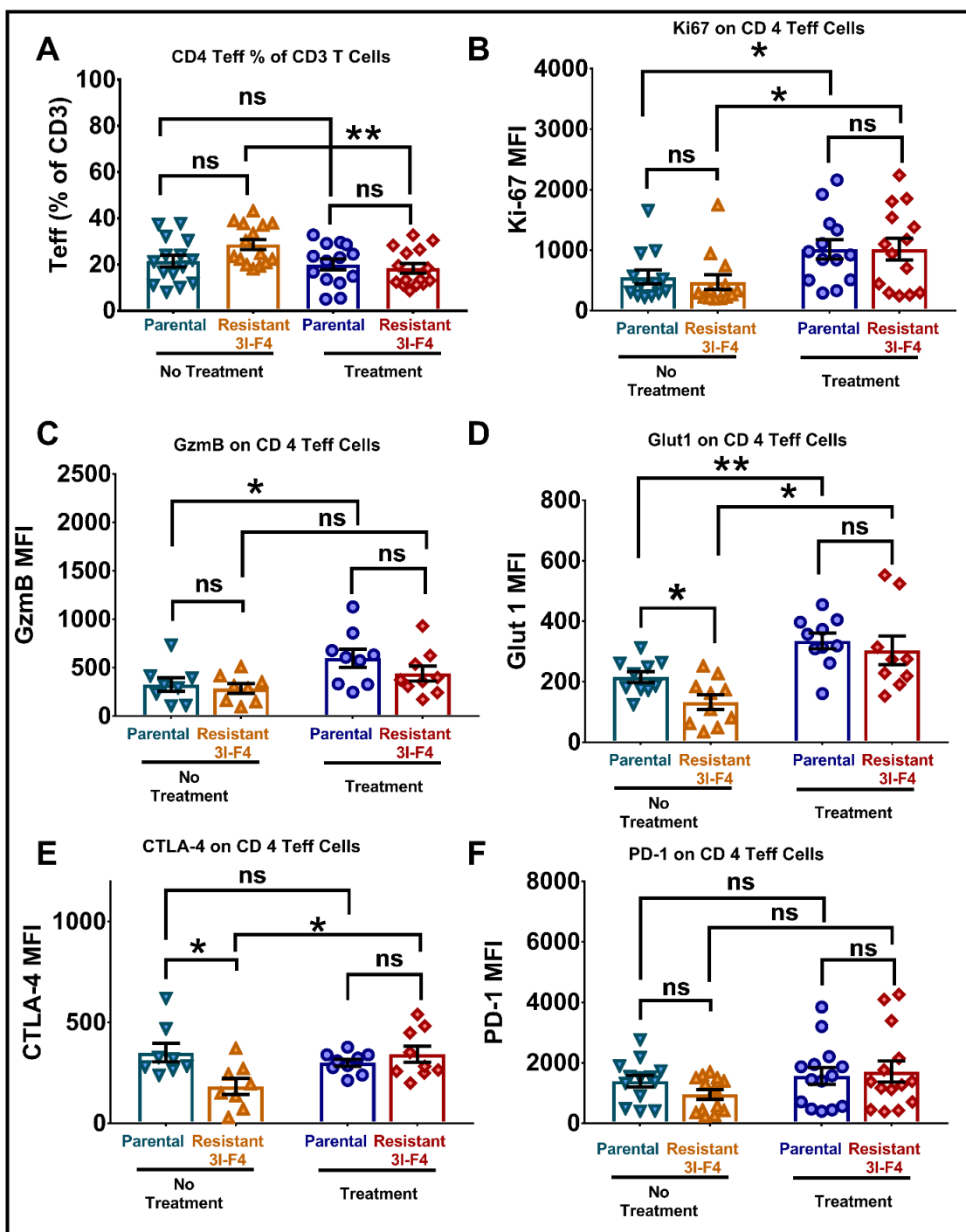


Supplemental Figure 2.4



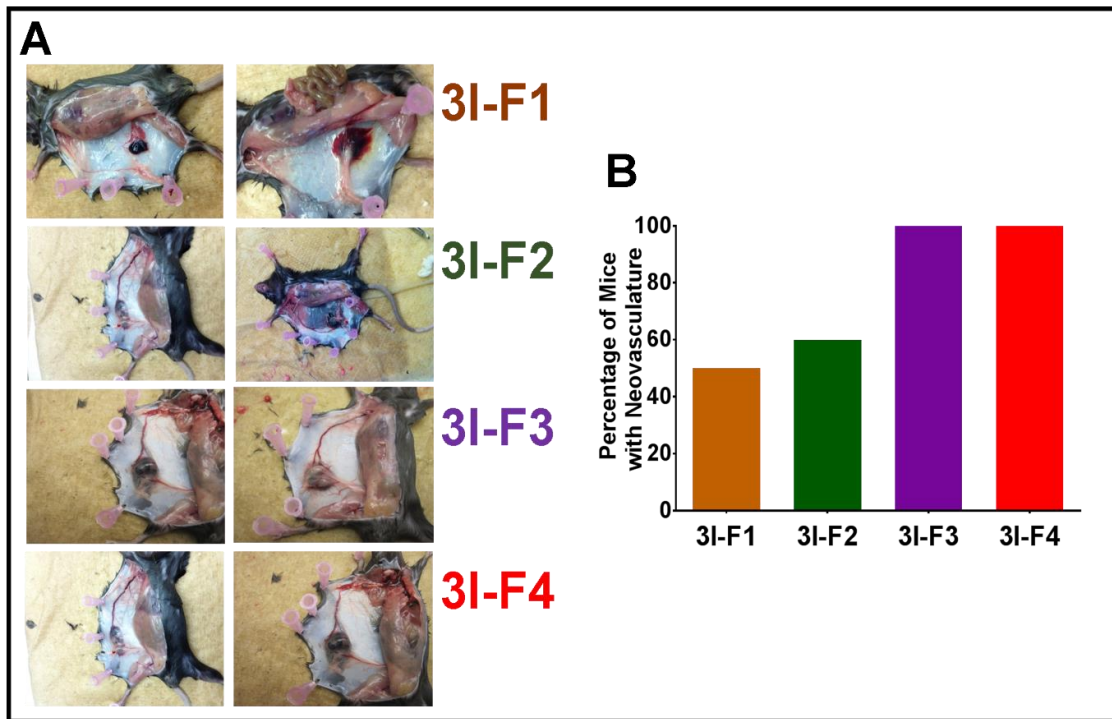
**Supplemental Figure 2.4: Effects of metabolic adaptation by resistant tumors on function of cytotoxic T cells.** (A) CD8 T cell percentage of total tumor infiltrating T cells. Resistant and parental tumor were implanted in mice and treated on day 3, 6 and 9. Tumors were harvested for flow cytometric analysis. CD8 T cells were gated on CD3+CD8+ cells. The data presented show CD8 T cells as a percentage of total CD3 T cells. T cell function was analyzed using multicolor flow cytometry analysis. The data are presented as mean fluorescent intensity of (B) perforin (C) CTLA-4, (D) PD-1, (E) LAP and (F) PD-L1. Data were pooled from  $\geq 2$  experiments with 5 mice per group. Bars represent mean  $\pm$  SD. Statistical significance was calculated using a Student's t test. ns, not significant; \*P < 0.05, \*\*P < 0.01, \*\*\*P < 0.001, \*\*\*\*P < 0.0001.

Supplemental Figure 2.5



**Supplemental Figure 2.5: Effects of metabolic adaptation by resistant tumors on cytotoxic CD4 T effector cell infiltration and function.** (A) CD4 T effector cells as a percentage of total tumor infiltrating CD3 T cells. Resistant and parental tumor were implanted in mice and treated on day 3, 6 and 9. Tumors were harvested for flow cytometric analysis. CD4 T effector cells were gated as CD4 positive and Foxp3 negative. The data presented show CD4<sup>+</sup> FoxP3<sup>-</sup> (CD4Teff) cells as a percentage of total CD3 T cells. T cell proliferation and function of tumor infiltrating CD4 T cells were performed using multicolor flow cytometry. The CD4 T cell proliferation data was presented as mean fluorescent intensity of Ki-67, a proliferation marker. T cell function data was presented as mean fluorescent intensity of (C) Granzyme B, (D) Glut 1 receptor, (E) CTLA-4, and (F) PD-1, T cell function and activation markers. Data were pooled from  $\geq 2$  experiments with 5 mice per group. Bars represent mean  $\pm$  SD. Statistical significance was calculated using the Student's t test. ns, not significant; \*P < 0.05, \*\*P < 0.01, \*\*\*P < 0.001, \*\*\*\*P < 0.0001.

## Supplemental Figure 2.6



**Supplemental Figure 2.6: Large vascular formation by resistant tumors.** (A) Representative pictures showing neo-vascular formation by resistant tumors with increasing *in vivo* passages of generating immunotherapy resistance. (B) Histogram representing percentage of total mice with large, apparent vasculature. Total 15 mice per passage were implanted with respective immunotherapy resistant tumor cell line (3I-F1, 3I-F2, 3I-F3 and 3I-F4). The mice with neo-vasculature were counted and plotted as percentage of the total number of mice for each passage.

Sample name	Lab Code	Tumor Biopsy Source	organism	Characteristics: Biopsy Timepoint	Characteristics: Treatment	characteristics: Previous Ipilimumab	characteristics: Response (PD = progressive disease; SD = stable disease; PR = partial response; CR = complete response)	Molecule	Label	Platform
9983140041_G	MC_106a	Melanoma tumor biopsy	Homo Sapiens	Pre-treatment	PD1	Yes	CR	total RNA	Biotin/Cy3	GPL19915
9983140041_H	MC_106b	Melanoma tumor biopsy	Homo Sapiens	Pre-treatment	PD1	Yes	CR	total RNA	Biotin/Cy3	GPL19915
9983140070_G	MC_38	Melanoma tumor biopsy	Homo Sapiens	Pre-treatment	PD1	Yes	PR	total RNA	Biotin/Cy3	GPL19915
9983140070_K	MC_72	Melanoma tumor biopsy	Homo Sapiens	Pre-treatment	PD1	Yes	CR	total RNA	Biotin/Cy3	GPL19915
9983140070_B	MC_108	Melanoma tumor biopsy	Homo Sapiens	Pre-treatment	Ipilimumab+PD1	No	PR	total RNA	Biotin/Cy3	GPL19915
9983140070_E	MC_27	Melanoma tumor biopsy	Homo Sapiens	Pre-treatment	PD1	Yes	PD	total RNA	Biotin/Cy3	GPL19915
9983140070_H	MC_40	Melanoma tumor biopsy	Homo Sapiens	Pre-treatment	PD1	Yes	PD	total RNA	Biotin/Cy3	GPL19915
9983140070_D	MC_19	Melanoma tumor biopsy	Homo Sapiens	Pre-treatment	PD1	Yes	PD	total RNA	Biotin/Cy3	GPL19915
9983140070_L	MC_112	Melanoma tumor biopsy	Homo Sapiens	Pre-treatment	PD1	Yes	PD	total RNA	Biotin/Cy3	GPL19915
9983140070_J	MC_43	Melanoma tumor biopsy	Homo Sapiens	Pre-treatment	PD1	Yes	PD	total RNA	Biotin/Cy3	GPL19915
9983140041_D	MC_135	Melanoma tumor biopsy	Homo Sapiens	Pre-treatment	Ipilimumab+PD1	No	PD	total RNA	Biotin/Cy3	GPL19915

Table 2.1: A patient cohort representing treatment, biopsy, clinical evaluation and gene arrays analysis.

*This chapter have been previously published in “Bartkowiak T\*, Jaiswal AR\*, Ager C, Chin R, Chen CH, Budhani P, Reilley MJ, Sebastian, MM, Hong DS and Curran MA, Activation of 4-1BB on liver myeloid cells triggers hepatitis via an interleukin-27 dependent pathway. Clinical Cancer Research, (2018).”*

*\*equal contribution*

Authors of articles published in AACR journals are permitted to use their article or parts of their article in the following ways without requesting permission from the AACR. All such uses must include appropriate attribution to the original AACR publication. Authors may do the following as applicable: “Submit a copy of the article to a doctoral candidate's university in support of a doctoral thesis or dissertation”.

<http://aacrjournals.org/content/authors/copyright-permissions-and-access>

## Chapter 3: 4-1BB Induced Liver Inflammation

**Activation of 4-1BB on liver myeloid cells triggers hepatitis via an interleukin-27 dependent pathway**



### 3.1: Abstract

Agonist antibodies targeting the T cell co-stimulatory receptor 4-1BB (CD137) are among the most effective immunotherapeutic agents across pre-clinical cancer models. In the clinic, however, development of these agents has been hampered by dose-limiting liver toxicity. Lack of knowledge of the mechanisms underlying this toxicity has limited the potential to separate 4-1BB agonist driven tumor immunity from hepatotoxicity. The capacity of 4-1BB agonist antibodies to induce liver toxicity was investigated in immunocompetent mice, with or without co-administration of checkpoint blockade, via 1) measurement of serum transaminase levels, 2) imaging of liver immune infiltrates, and 3) qualitative and quantitative assessment of liver myeloid and T cells via flow cytometry. Knockout mice were used to clarify the contribution of specific cell subsets, cytokines and chemokines. We find that activation of 4-1BB on liver myeloid cells is essential to initiate hepatitis. Once activated, these cells produce interleukin-27 that is required for liver toxicity. CD8 T cells infiltrate the liver in response to this myeloid activation and mediate tissue damage, triggering transaminase elevation. FoxP3+ regulatory T cells limit liver damage, and their removal dramatically exacerbates 4-1BB agonist-induced hepatitis. Co-administration of CTLA-4 blockade ameliorates transaminase elevation, whereas PD-1 blockade exacerbates it. Loss of the chemokine receptor CCR2 blocks 4-1BB agonist hepatitis without diminishing tumor-specific immunity against B16 melanoma. 4-1BB agonist antibodies trigger hepatitis via activation and expansion of interleukin-27-producing liver Kupffer cells and monocytes. Co-administration of CTLA-4 and/or CCR2 blockade may minimize hepatitis, but yield equal or greater antitumor immunity.

### 3.2: Introduction

The transformative efficacy of checkpoint blockade immunotherapy for the treatment of melanoma has revolutionized the field of oncology and initiated a new era of immune-targeted therapeutics (202,203). Beyond blockade of T cell co-inhibitory receptors, agonist antibodies which activate tumor necrosis factor superfamily receptors have demonstrated significant therapeutic potential both in pre-clinical models and clinical trials (204). Among these agonists, activators of the co-stimulatory receptor 4-1BB (CD137) have demonstrated exceptional potency across multiple pre-clinical tumor models, as well as the capacity to elicit objective clinical responses in patients with diverse cancers (205,206).

In addition to mediating tumor regressions, releasing the “brakes” on T cell responses with checkpoint blockade can also trigger T cell responses targeting normal self-tissues known as Immune Related Adverse Events (IRAE). These IRAE can be severe and even life-threatening, but are readily managed with timely steroid intervention (207). 4-1BB agonist antibodies, by contrast, can effectively treat autoimmunity in a variety of murine models and may even ameliorate CTLA-4 antagonist antibody-induced IRAE (208,209). Despite this, these agents induce a unique spectrum of on-target adverse events ranging from mild to moderate hematologic perturbations, up to high grade transaminitis and potentially fatal hepatotoxicity (210,211).

We sought to elucidate the underlying mechanisms by which  $\alpha$ 4-1BB antibody therapy promotes liver damage, and to explore potential avenues to uncouple augmentation of anti-tumor immunity from hepatitis. Results presented

here demonstrate that 4-1BB agonist induced hepatotoxicity initiates at the myeloid level through activation of liver-resident Kupffer cells. Moreover, we find that the inflammatory cytokine interleukin 27 (IL-27), released from these cells in response to activation, is critically required for hepatic damage. We further show that, in contrast to CD40 agonist induced acute hepatotoxicity, 4-1BB agonist antibody therapy induces a chronic hepatotoxicity characterized by dense and persistent T cell infiltration in the hepatic portal zones. This infiltrate is dominated by CD8<sup>+</sup> T cells which are the primary effectors of liver tissue injury. CD4<sup>+</sup>Foxp3<sup>+</sup> regulatory T cells (Treg), on the other hand, act to maintain tissue tolerance and limit  $\alpha$ 4-1BB-induced hepatic damage. Treg ablation severely exacerbates 4-1BB agonist liver inflammation and abrogates the capacity of CTLA-4 blockade to ameliorate transaminitis. Finally, we show that chemotaxis of immune cells into the liver is a critical step in the progression of liver injury. While hepatogenic immune responses following 4-1BB agonist therapy rely heavily on the chemokine receptors CCR2 and, less so, to CXCR3, these receptors appear to be largely dispensable for anti-melanoma immunity in the same animals. These data suggest that differential trafficking requirements for the liver and tumor microenvironments may be exploited to increase the tumor selectivity of 4-1BB agonist antibody immunotherapy.

### 3.3: Materials and Methods

#### 3.3.1: Animals

Male (6wk) C57BL/6 mice were purchased from Taconic Biosciences (Hudson, NY). *4-1BB<sup>-/-</sup>*, *EBI3<sup>-/-</sup>*, *IL27 receptor alpha<sup>-/-</sup>*, *β2M<sup>-/-</sup>*, *MHCII<sup>-/-</sup>*, *Foxp3-DTR*, *CXCR3<sup>-/-</sup>*, *CCR2<sup>-/-</sup>*, and *CCR5<sup>-/-</sup>* mice were purchased from the Jackson Laboratory (Bar Harbor, ME). All procedures were conducted in accordance with the guidelines established by the U.T. MD Anderson Cancer Center Institutional Animal Care and Use Committee.

#### 3.3.2: Cell lines and reagents

B16 melanoma, B16-Flt3-ligand (FVAX) and B16-Ova were obtained/created and cultured as described (94,180). The BV421-labeled H2-K<sup>b</sup> epitope OVA<sup>257-264</sup> (SIINFEKL)-containing tetramer was acquired from the Tetramer Core Facility at the National Institute of Health (Emory University, Atlanta GA).

#### 3.3.3: Therapeutic antibodies

T cell co-stimulatory modulating antibodies were purchased from BioXcell: 4-1BB (3H3 [Rat IgG2a], 250 µg/dose), CTLA-4 (9D9 [mouse IgG2b] or 9H10 [Syrian Hamster Ig], 100 µg/dose), PD-1 (RMP1-14 [Rat IgG2a], 250 µg/dose), and CD40 (FGK4.5 [Rat IgG2a], 100 µg/dose). All doses indicate quantity administered per injection. The mouse CTLA-4 antibody 9D9 engages the mouse IgG2b receptor which gives it a low to moderate ADCC capacity similar to the human CTLA-4 antibody ipilimumab (human IgG1). The mouse 4-1BB antibody 3H3 is more similar to the human antibody urelumab as it exhibits strong agonist activity,

while utomilumab is a weaker agonist. RMP-14 is a purely blocking antibody for PD-1 with weak Fc receptor binding similar to the human PD-1 antibodies pembrolizumab and nivolumab which are human IgG4.

### **3.3.4: Immune ablation and reconstitution**

C57BL/6 mice or 4-1BB<sup>-/-</sup> mice were sub-lethally irradiated (500 rads) using a Cesium-137 irradiator. One day later, splenic lymphocytes were isolated using CD90.2 magnetic beads (Miltenyi Biotec, San Diego, CA) and injected i.v. at 2X10<sup>6</sup> cells/mouse into irradiated hosts.

### **3.3.5: Antibody treatment and liver enzyme analysis**

Antibodies were given i.p. for 3 doses every 3 days. On day 16 after initiation of therapy mice were bled and serum levels of aspartate transaminase (AST), alanine transaminase (ALT), and alkaline phosphatase (AP) were measured by the MDACC Veterinary Diagnostic Laboratory. Mice were sacrificed, livers were perfused with PBS and harvested for immune infiltrates.

### **3.3.6: Tumor therapy**

Wild type, CCR2<sup>-/-</sup>, CXCR3<sup>-/-</sup>, or CCR5<sup>-/-</sup> mice were implanted s.c. with 3X10<sup>5</sup> B16-Ova cells on the flank as described (94,180). On days 3,6, and 9 mice received α4-1BB i.p, and a mixture of irradiated FVAX and B16-Ova s.c. on the opposite flank as described (94). On day 19, mice were sacrificed and tumors and perfused livers were harvested for analysis of immune infiltrates.

### **3.3.7: Treg depletion and adoptive transfer**

Mice bearing the diphtheria toxin (DT) receptor driven by the Foxp3 promoter (Foxp3-DTR) were administered DT at 10 µg/kg one day prior to α4-1BB

and every 3 days thereafter until sacrifice. Alternately, CD4<sup>+</sup>CD25<sup>+</sup>CD3<sup>+</sup> cells were FACS sorted from naïve spleens and 5X10<sup>5</sup> cells were injected into host mice one day prior to immunotherapy.

Myeloid cells were adoptively transferred by magnetically sorting bone marrow-derived monocytes using a monocyte isolation kit (Miltenyi Biotec, Auburn CA). Sorted cells (CD45.2) were adoptively transferred at 2X10<sup>6</sup> cells/mouse into congenically marked (CD45.1) mice before initiation of therapy.

### **3.3.8: Cell isolation**

Livers were perfused with PBS and tumors were harvested for analysis of immune infiltrate as described (212,213).

### **3.3.9: Flow cytometry analysis**

Samples were fixed using the Foxp3/Transcription Factor Staining Buffer Set (Thermo) and then stained with up to 16 antibodies at a time from Biolegend, BD Biosciences, and Thermo. Flow cytometry data was collected on an 18-color BD LSR II cytometer and analyzed in FlowJo (Treestar).

### **3.3.10: Immunohistochemistry**

Each liver lobe was collected and formalin fixed separately for ≥ 24 hours. Tissues were then paraffin embedded (FFPE), sectioned and stained for H&E and IHC for CD8 and F4/80, at the MDACC Research Histology, Pathology, and Imaging Core at Science Park.

Two sections were generated from the left lateral lobe at the widest dimension, and stained by H&E. H&E sections were evaluated by semi-quantitative scoring based on the number of inflammatory and necrotic cells in the

portal triad, central vein, or parenchyma. A score of 0 or nil indicates no inflammation; Score 1, minimal inflammation, <15 inflammatory cells around portal triad, central vein, or in parenchyma; Score 2, mild inflammation, > 15 inflammatory cells around portal triad, central vein, or in parenchyma; Score 3: moderate inflammation, > 30, inflammatory cells around portal triad, central vein, or in parenchyma, and Score 4: severe inflammation, approximately > 50 cells around portal triad, central vein, or in parenchyma.

Two sections per animal per group were stained with the following immunohistochemical stains: CD8 and F4/80. The number of CD8<sup>+</sup> and F4/80<sup>+</sup> cells in the liver, both at the perivascular zones (central vein or portal area) and in the parenchyma, were counted separately in a microscopic field at 20X magnification. Four areas with the most abundant infiltration were selected for both areas and the average number per animal was calculated as described in Peng et.al. 2015(214).

### ***3.2.11: Immunofluorescence staining and imaging***

Tissues were collected and flash frozen in liquid nitrogen. The frozen tissues were embedded in Tissue-Tek® OCT Compound (Sakura, Torrance, CA) and sectioned at the MD Anderson Histology Core. The sectioned tissues were fixed with acetone for 10 minutes, then stained with various antibodies and mounted in Prolong Gold (Invitrogen, Carlsbad, CA). Confocal imaging was performed using a TCS SP8 laser-scanning confocal microscope equipped a 20X objective (HCPL APO 20X/0.70 NA), Leica Microsystems) with lasers for excitation

at 405nm, 458nm, 488nm, 514nm, 543nm, and 633nm wavelengths. (Leica Microsystems, Inc., Bannockburn, IL).

### **3.2.12: Real time PCR**

Liver myeloid subpopulations were sorted as shown (Supplemental Fig. 3.1) at the MD Anderson Flow Cytometry and Cellular Imaging Core Facility (FCCIF). Total RNA was extracted using the RNeasy Mini Kit (Qiagen, MD) and reverse transcribed using the SuperScript IV Reverse Transcriptase kit (Thermo). Taqman real-time PCR was performed on a Via 7 Real Time PCR System (Applied Biosystem, CA) as previously described (212,213). Levels of *il27-p28*, *ifng*, and *tnfa* were expressed as the fold change using the  $\Delta\Delta C_t$  method.

### **3.2.13: Cytometric bead array**

Bone marrow derived monocytes were isolated from wildtype mice using a Monocyte Isolation Kit (Miltenyi Biotech) and were stimulated *in vitro* with  $\alpha 4$ -1BB (3H3) antibody for 48 hours. Cytokine release was quantified using a Th1/Th2/Th17 Cytometric Bead Array kit (BD) as per manufacturer's instructions.

### **3.2.14: Statistical analysis**

All statistics were calculated using Graphpad Prism Version 6 for Windows. Statistical significance was determined using a two-sided Student's T test applying Welch's correction for unequal variance. Graphs show mean  $\pm$  standard deviation unless otherwise indicated. P-values less than 0.05 were considered significant.



### 3.3: Results

#### ***3.3.1: Disparate effects of CTLA-4 and PD-1 checkpoint blockade on $\alpha$ 4-1BB-mediated hepatotoxicity***

To determine the potential for currently approved checkpoint blockade antibodies ( $\alpha$ CTLA-4,  $\alpha$ PD-1) to ameliorate 4-1BB agonist antibody induced liver pathology, mice were treated with three administrations of checkpoint antibody,  $\alpha$ 4-1BB alone,  $\alpha$ 4-1BB in combination with  $\alpha$ CTLA-4 or  $\alpha$ PD-1, or triple combination therapy. At the peak of hepatic injury, sixteen days after the initiation of treatment (Supplemental Fig. 3.1A), mice were bled and serum was analyzed for liver transaminases including alanine aminotransferase (ALT; Reference mean  $26.5 \pm 5$ ) and aspartate aminotransferase (AST; Reference mean  $43.2 \pm 9.5$ )(215). As noted previously, co-administration of  $\alpha$ CTLA-4 significantly decreased serum transaminase levels compared to  $\alpha$ 4-1BB monotherapy (209), whereas dual therapy with  $\alpha$ 4-1BB and  $\alpha$ PD-1 significantly increased transaminase levels (Fig. 3.1A) (216). The protective effect of  $\alpha$ CTLA-4 therapy was lost when given in combination with both  $\alpha$ 4-1BB and  $\alpha$ PD-1, suggesting that exacerbation of hepatitis by  $\alpha$ PD-1 dominates over the capacity of  $\alpha$ CTLA-4 to limit it. As triple combination therapy failed to alleviate hepatic damage, we sought to define the cellular mechanisms by which CTLA-4 blockade acted to limit  $\alpha$ 4-1BB hepatotoxicity.

4-1BB agonist administration drove robust CD3<sup>+</sup> T cell infiltration of the liver including > 2-fold increases in cytotoxic CD8 T cells relative to untreated animals or those receiving CTLA-4 blockade (Fig. 3.1B, Supplemental Fig. 3.1B), but did

not significantly impact infiltration of bulk CD4<sup>+</sup> T cells (CD4<sup>+</sup>CD3<sup>+</sup>) or CD4<sup>+</sup> effector T cells (CD4<sup>+</sup>CD3<sup>+</sup>FoxP3<sup>-</sup>) (Supplemental Fig. 3.2A, and B). Functionally, the majority of these infiltrating T cells bore the recently defined Eomesodermin<sup>+</sup>KLRG1<sup>+</sup> signature of the cytotoxic ThEO (CD4) and TcEO (CD8) phenotype that are critical for anti-tumor immunity by exhibiting elevated cytotoxicity compared to their Th1/Tc1 counterparts, and likely play a significant role in mediating liver damage (Supplemental Fig. 3.2 C,D,E)(213,217-219). Further, the addition of CTLA-4 blockade to α4-1BB treatment reduced the frequency of T cell infiltration into the liver versus α4-1BB alone (Fig. 3.1B). Whereas the overall CD3 density was reduced in α4-1BB/αCTLA-4 combination treated animals, no changes in the CD4 and CD8 frequencies within the infiltrating T cell pool, nor in the percentage of cells adopting the ThEO/TcEO phenotype were observed (Fig. 3.1B, Supplemental Fig. 3.2D,E). Consistent with the overall decrease in T cell infiltration, inflammatory foci (Fig. 3.1C) and clusters of CD8 T cells in the liver parenchyma also decreased when αCTLA-4 was co-administered with α4-1BB , but were exacerbated by triple combination therapy (Fig. 3.1D, E). Overall, αCTLA-4 co-administration with α4-1BB significantly decreased the severity of inflammation, necrotic regions, and CD8 T cell infiltration in liver parenchyma as indicated by a reduced pathology score (Fig. 3.1E,F).

To test whether the ability of CTLA-4 blockade to reduce liver pathology was specific for 4-1BB agonist therapy, we also tested αCTLA-4 in combination with antibodies targeting the TNF receptor CD40. Co-stimulation through CD40 induces an acute and transient hepatic injury that peaks within a week of antibody administration and declines thereafter, whereas 4-1BB agonists induced a chronic,

and persistent hepatic pathology as measured by maintained elevation of serum transaminases over the 16-day study (Fig. 3.1G). Further, in contrast to  $\alpha$ 4-1BB,  $\alpha$ CD40-induced liver damage was not ameliorated by co-administration with  $\alpha$ CTLA-4 (Fig. 3.1H).

These data suggest that 4-1BB agonist antibodies mediate chronic liver pathology through a mechanism distinct from CD40 activation. Although CTLA-4 blockade can ameliorate 4-1BB agonist induced hepatitis through reduction of T cell infiltration; this mechanism fails to impact liver injury resulting from  $\alpha$ CD40 or  $\alpha$ 4-1BB/ $\alpha$ PD-1 combination therapy.

Figure 3.1

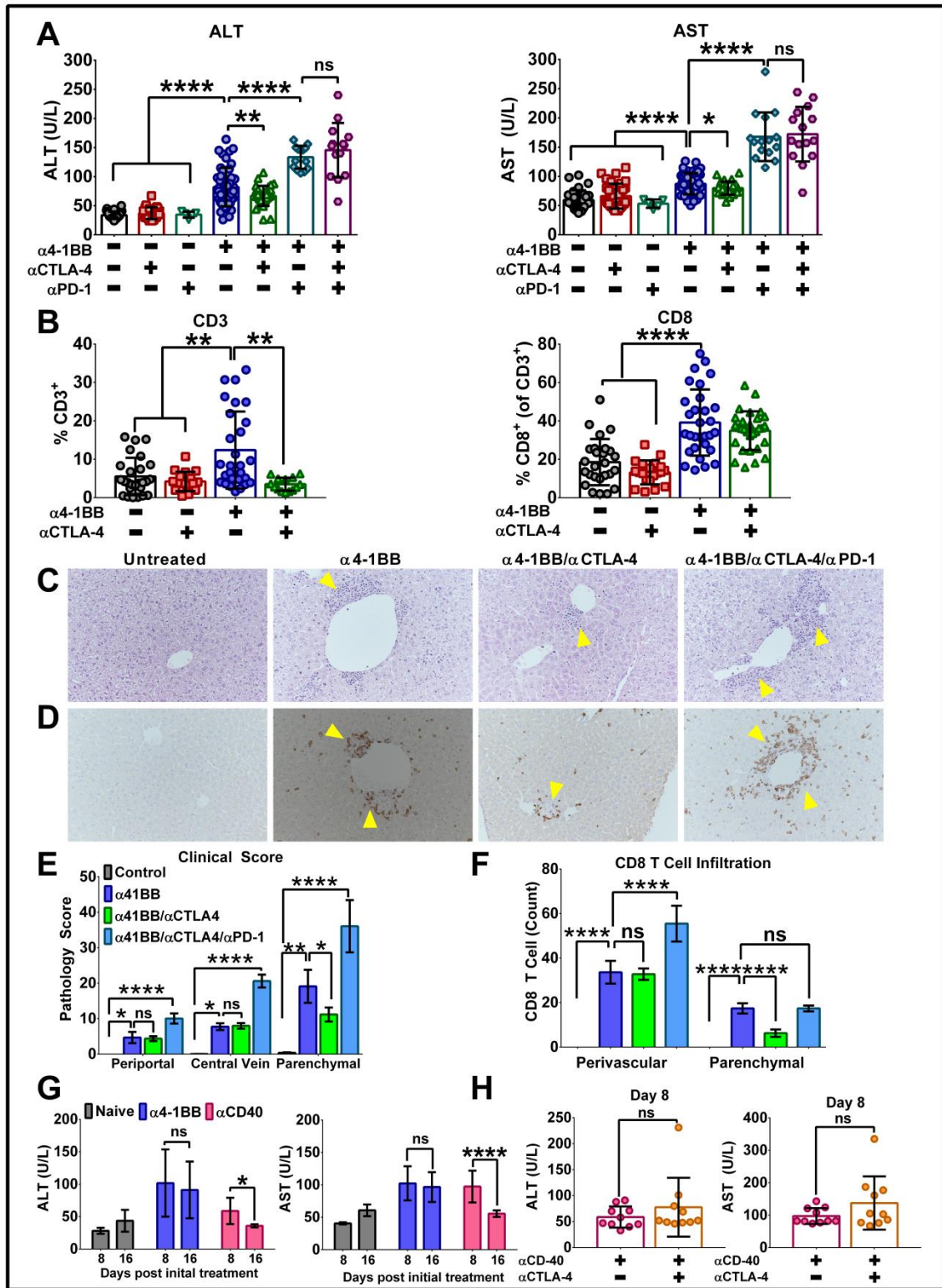


**Figure 3.1: Combination immunotherapy augments  $\alpha$ 4-1BB mediated hepatotoxicity.** Mice were administered  $\alpha$ 4-1BB,  $\alpha$ CTLA-4, or  $\alpha$ PD-1 antibodies alone or in combination within 3 day intervals (days 0, 3, and 6). Mice were bled 16 days after initiation of therapy and sacrificed to measure liver immune infiltrates by flow cytometry. A) Serum levels of alanine aminotransferase (ALT) and aspartate aminotransferase (AST) were measured upon sacrifice as units of enzyme/liter of blood. B) Immune infiltrates within perfused livers of treated mice were measured by flow cytometry. Percent of CD3<sup>+</sup> cells was calculated as a fraction of liver CD45<sup>+</sup> cells. Frequency of CD8<sup>+</sup> T cells was calculated as a percent of CD3<sup>+</sup> cells. C) Hemotoxylin and Eosin (H&E) staining or immunohistochemistry (IHC) targeting CD8 (D) was performed on sectioned liver tissues from treated mice 16 days after initiation of therapy. E) Sections were assigned a clinical score by a pathologist based on the number of inflammatory cells in the portal triad, central vein, or parenchyma and (F) CD8<sup>+</sup> infiltration was enumerated per section. G) Mice administered either  $\alpha$ 4-1BB or  $\alpha$ CD40 agonist antibodies were bled 8 or 16 days after initiation of therapy and serum levels of ALT and AST were analyzed. H) Mice were administered either  $\alpha$ CD40 agonist antibodies alone or in combination with  $\alpha$ CTLA-4 blockade. Mice were then bled at the peak of  $\alpha$ CD40-mediated liver damage (D8) in order to assess serum transaminase levels. Each point in A, and B represents an individual mouse. Micrographs in C and D were imaged at 20X magnification. Data were pooled from  $\geq 3$  experiments with 5 mice per group. Bars represent mean  $\pm$  SD. Statistical significance was calculated using a two-sided Student's T test applying Welch's

correction for unequal variance. ns, not significant; \* $P < 0.05$ , \*\* $P < 0.01$ , \*\*\* $P < 0.001$ , \*\*\*\* $P < 0.0001$ .

### ***3.3.2: 4-1BB agonists initiate liver pathology through activation of liver-resident myeloid cells.***

Given the differential liver toxicities associated with 4-1BB agonists and CD40 agonists, we sought to uncover the relative contribution of the myeloid and T cell pools to 4-1BB agonist-induced liver damage. Whereas CD40 is exclusively expressed by myeloid cells (220), 4-1BB can be expressed on both T cell, NK cell and myeloid populations (205,213,221,222), and the relative contribution of each of these to liver pathology remains undefined.

To reveal the relative contribution of the myeloid versus lymphocyte compartments to  $\alpha$ 4-1BB induced hepatotoxicity, wildtype or 4-1BB<sup>-/-</sup> mice were administered a sublethal dose of radiation sufficient to eliminate their endogenous lymphocytes. Twenty-four hours after irradiation, splenic lymphocytes from wildtype or 4-1BB<sup>-/-</sup> mice were magnetically sorted and adoptively transferred into irradiated wildtype or 4-1BB<sup>-/-</sup> hosts. In this way, ablation of the lymphoid pool, but not the radio-resistant myeloid pool, allowed us to specifically target 4-1BB on either T cells or myeloid cells. Mice then received 4-1BB agonist therapy as previously described. Mice receiving WT to WT splenocyte transfers (myeloid 4-1BB<sup>+</sup>, lymphocyte 4-1BB<sup>+</sup>) clearly manifested ALT elevation in response to 4-1BB agonist antibody treatment compared to WT to WT transfers administered isotype control antibodies or 4-1BB<sup>-/-</sup> mice receiving 4-1BB<sup>-/-</sup> cells in conjunction with  $\alpha$ 4-1BB (Fig. 3.2A), while AST elevation, which is always less affected by  $\alpha$ 4-1BB, showed modest elevation as well (Supplemental Fig. 3.3A). Wildtype mice that received splenocytes from 4-1BB<sup>-/-</sup> mice (myeloid 4-1BB<sup>+</sup>, lymphocyte 4-1BB<sup>-</sup>) were not significantly protected against ALT elevation, but did show reduced

elevation of AST. On the other hand, 4-1BB<sup>-/-</sup> mice receiving splenocytes from wildtype mice (myeloid 4-1BB<sup>-</sup>, lymphocyte 4-1BB<sup>+</sup>), were fully protected from ALT elevation and showed no significant elevation of AST relative to mice lacking 4-1BB only on T cells. Thus, when 4-1BB was absent from the myeloid compartment, α4-1BB could no longer trigger hepatotoxicity suggesting a requirement for myeloid 4-1BB activation to initiate a liver inflammatory cascade. The absence of 4-1BB on T cells did not appear deterministic for liver inflammation, but the modest reductions in transaminases relative to WT mice suggested a contributory role for 4-1BB on T cells as well.

Given our prior data, we investigated the role of myeloid cells in initiating α4-1BB induced liver pathology. We found that, in comparison to untreated livers, α4-1BB therapy increased the frequency of F4/80<sup>+</sup> macrophages within the liver parenchyma which was significantly reduced by combining αCTLA-4 with α4-1BB (Fig. 3.2B, C, D). Interestingly, combination therapy favored accumulation of F4/80<sup>+</sup> cells within the perivascular space compared to infiltration into the tissue parenchyma (Fig. 3.2D). The expanded liver macrophages consist of tissue-resident Kupffer cells, defined by expression of the adhesion receptor F4/80, that remain relatively quiescent within healthy liver, are replenished by bone marrow-derived myeloid precursors or via low-level homeostatic proliferation, and are functionally and phenotypically distinct from circulating CD11b<sup>+</sup>F4/80<sup>-</sup> monocytes (223). Further, Kupffer cells can be sub-classified into populations of CD11b<sup>+</sup>CD68<sup>-</sup> myeloid cells specialized for cytokine production, CD11b<sup>-</sup>CD68<sup>+</sup> phagocytic macrophages and CD11b<sup>+</sup>CD68<sup>+</sup> cells with intermediate phagocytic activity and cytokine expression (224). In naïve mice, we were only able to detect



clear 4-1BB expression on monocytes by flow cytometry (Supplemental Fig. 3.3B); however, 4-1BB expression was detected on both F4/80<sup>-</sup> monocytes and on a small percentage of F4/80<sup>+</sup> Kupffer cells *in situ* by immuno-fluorescence (Fig. 3.2E). The Kupffer cell phenotype is sensitive to disruptive procedures used to prepare livers for flow cytometry, likely explaining the lower resolution of flow cytometry. Both methods, however, showed that 4-1BB was readily induced on Kupffer cells by inflammatory cytokines such as TNF $\alpha$  which are plentiful during  $\alpha$ 4-1BB-induced liver injury, with flow cytometry confirming the CD11b<sup>-</sup>CD68<sup>+</sup> and CD11b<sup>+</sup>CD68<sup>+</sup> sub-populations as the primary targets (Fig. 3.2E, Supplemental Fig. 3.3C). To assess the origin of these Kupffer cell populations, as well as the plasticity of infiltrating bone marrow-derived monocytes, we adoptively transferred congenically labelled bone marrow myeloid progenitor cells and administered  $\alpha$ 4-1BB to the recipient mice. In response to 4-1BB activation, these monocytes expanded in the blood and infiltrated the liver (Supplemental Fig. 3.3D). A majority of these liver-infiltrating cells remained phenotypically monocytes (CD11b<sup>+</sup>F4/80<sup>-</sup>); however, some capacity to differentiate into CD11b<sup>-</sup>CD68<sup>+</sup> and CD11b<sup>+</sup>CD68<sup>+</sup> subpopulations of Kupffer cells was observed (Fig. 3.2F). This is consistent with recent literature showing that while most Kupffer cells originate from embryonically derived erythro-myeloid progenitor (EMP) cells, some capacity of bone-marrow derived monocytes to replenish these populations does exist(225,226).

Based on these findings, we hypothesize that bone marrow-derived monocytes infiltrate the liver and, in response to 4-1BB activation, initiate a cascade of inflammatory cytokine production (Supplemental Fig. 3.3E) which triggers 4-1BB upregulation by resident Kupffer cells allowing them to respond in

turn to the agonist antibody (Supplemental Fig. 3.3C). Our data, however, does not rule out a minor contribution of 4-1BB<sup>+</sup> monocytes differentiating into resident cells with a Kupffer phenotype themselves and contributing to the response directly.

Further, all three Kupffer cell subsets showed signs of activation in response to 4-1BB agonist antibody (Fig. 3.2G). Increases in the CCR5<sup>+</sup> fraction of the CD11b<sup>+</sup>CD68<sup>-</sup> and CD11b<sup>-</sup>CD68<sup>+</sup> subpopulations by approximately 2-fold suggests that these cells are either new emigrants or derived from them, or, alternatively that they are re-distributing within sub-compartments of the liver. Both possibilities are consistent with increased infiltration into the perivascular space that we observed (227,228). CCR5 expression decreased, however, on the CD11b<sup>+</sup>CD68<sup>+</sup> subset, which may be a result of receptor downregulation by recent emigrants from the bone marrow as we observed no evidence of elevated *in situ* proliferative expansion by Ki67. Moreover, all three subsets of F4/80<sup>+</sup> cells increased MHC-II expression, further suggesting that these populations are activated by 4-1BB antibody consistent with published literature demonstrating that this activation promotes enhanced co-stimulatory capacity (213,221).

We next sought to confirm the ability of the cytokine-producing myeloid populations to mediate liver damage during the course of α4-1BB therapy, as well as to determine what effector molecules these populations produce to mobilize immune responses leading to hepatic damage. Within the F4/80 positive population, CD68<sup>+</sup> (F4/80<sup>+</sup>CD11b<sup>-</sup>CD68<sup>+</sup>), CD11b<sup>+</sup> (F4/80<sup>+</sup>CD11b<sup>+</sup>CD68<sup>-</sup>), and CD11b<sup>+</sup>CD68<sup>+</sup> (F4/80<sup>+</sup>CD11b<sup>+</sup> CD68<sup>+</sup>) cells as well as CD11b<sup>+</sup>F4/80<sup>-</sup> monocytes

were FACS sorted on day 7 from the livers of treated mice (Supplemental Fig. 3.1), and RNA was isolated from each population for quantitative real time PCR. We found that, compared to  $\alpha$ CD40 treatment which induced significant activation and IFN $\gamma$  production in CD11b<sup>+</sup>CD68<sup>+</sup> Kupffer cells, the F4/80<sup>+</sup>CD11b<sup>+</sup>CD68<sup>-</sup> and F4/80<sup>+</sup>CD11b<sup>+</sup>CD68<sup>+</sup> myeloid cells were the predominant cytokine producers with little or no contribution from the CD11b<sup>-</sup> subset within the livers of  $\alpha$ 4-1BB treated mice. Within the two CD11b<sup>+</sup>CD68<sup>-</sup> subsets, we observed approximately 20-fold increased expression of *IL-27-p28* following 4-1BB agonist therapy compared to treatment-naïve mice. In contrast, the CD11b<sup>-</sup>CD68<sup>+</sup> subset was the primary source of interferon- $\gamma$  (Fig. 3.2H). Moreover, both CD11b<sup>+</sup> subsets of Kupffer cells produced the majority of TNF $\alpha$ . Notably, the cytokine producing subsets of myeloid cells produced less IL-27 and TNF $\alpha$  in mice receiving the  $\alpha$ 4-1BB/ $\alpha$ CTLA-4 combination therapy compared to mice receiving  $\alpha$ 4-1BB monotherapy. While the CD11b<sup>-</sup>CD68<sup>+</sup> subset demonstrated roughly 50-fold increases in IL27-p28 expression relative to its baseline level during  $\alpha$ 4-1BB/ $\alpha$ CTLA-4 combination therapy, the delayed cycle within which transcripts were detected (~cycle 37 versus  $\leq$ cycle 26 for the cytokine-producing subsets) suggests that the actual quantity of transcript present in these cells was extraordinarily small.

Together, these data suggest,  $\alpha$ 4-1BB-mediated inflammatory hepatotoxicity initiates at the myeloid level via activation of tissue-resident Kupffer cells and, potentially, infiltrating monocytes. All three subsets of Kupffer cells, and to a lesser extent monocytes, showed signs of activated antigen presentation, and both CD11b<sup>+</sup> cytokine-producing subsets increased production of IL-27. Co-administration of CTLA-4 blockade reduced inflammatory cytokine production in

these subsets, consistent with the reduced transaminase elevation observed in those mice.

Figure 3.2

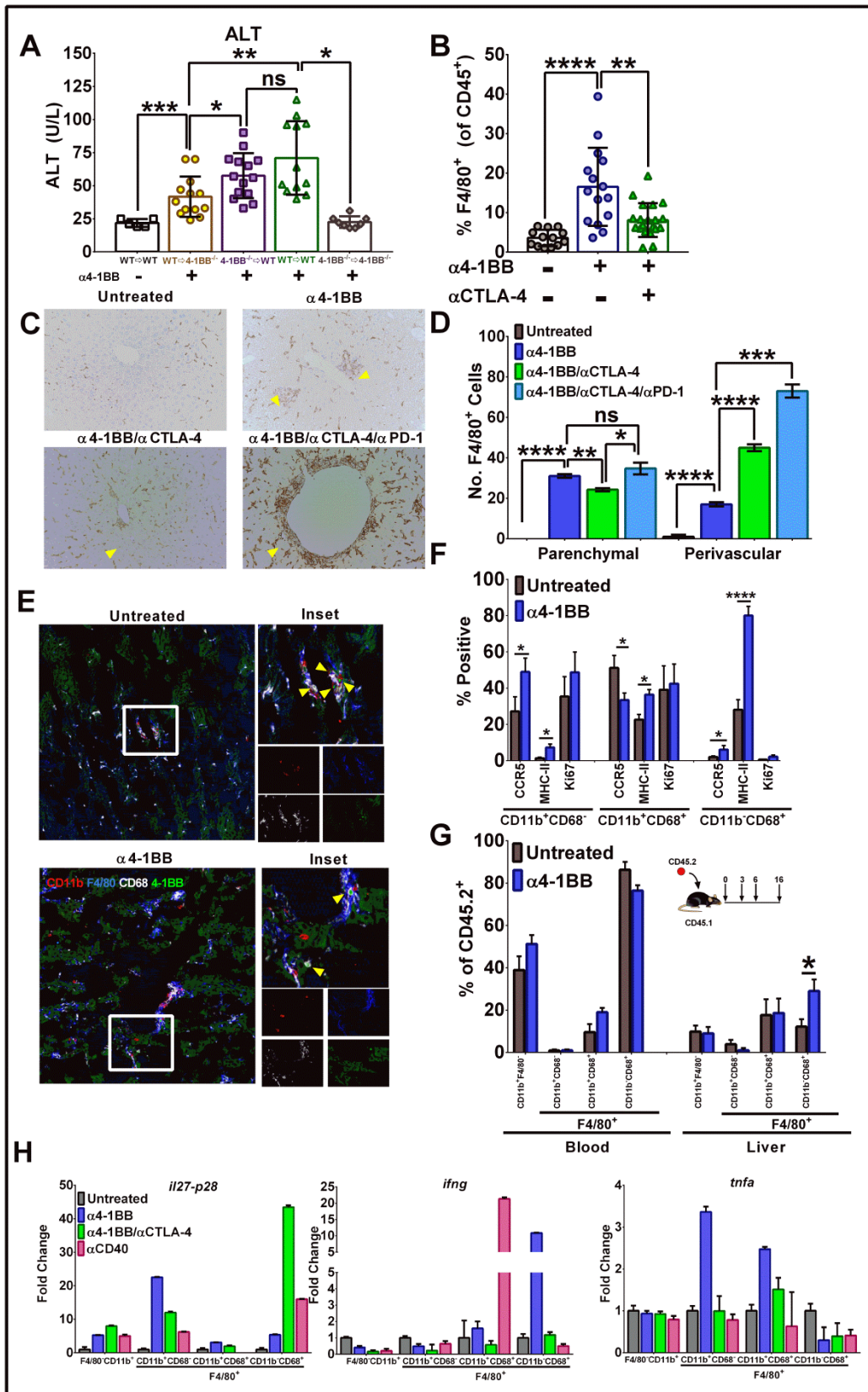


**Figure 3.2: Administration of 4-1BB agonist antibodies initiates liver pathology through activation of liver-resident myeloid cells.** A) Mice were sublethally irradiated (500 rads) before administration of  $2 \times 10^6$  CD90<sup>+</sup> splenocytes. Wildtype mice either received splenocytes from wildtype mice (WT→WT) or from 4-1BB<sup>-/-</sup> mice (4-1BB<sup>-/-</sup>→WT) and 4-1BB<sup>-/-</sup> mice received splenocytes from wildtype mice (WT→4-1BB<sup>-/-</sup>) or from 4-1BB<sup>-/-</sup> mice (4-1BB<sup>-/-</sup>→4-1BB<sup>-/-</sup>). Mice were subsequently treated with three rounds of isotype control or  $\alpha$ 4-1BB immunotherapy. Treated mice were then bled 16 days after the first administration of therapy and serum ALT was measured. B) Frequency of F4/80<sup>+</sup> myeloid infiltration into perfused livers based on flow cytometry of lymphoid-replete wildtype mice administered either  $\alpha$ 4-1BB therapy alone or in combination with  $\alpha$ CTLA-4 checkpoint blockade. Myeloid infiltration shown as the percent of F4/80<sup>+</sup> cells as a fraction of total CD45<sup>+</sup> cells. C) Immunohistochemistry staining for F4/80<sup>+</sup> was performed on sectioned liver tissues from treated mice 16 days after initiation of therapy. D) Quantification F4/80<sup>+</sup> cellular infiltrates based on IHC staining of liver sections. Individual F4/80<sup>+</sup> cells were enumerated within the liver parenchyma or perivascular space. E) Confocal imaging of myeloid immune infiltrates in naïve or  $\alpha$ 4-1BB-treated livers 16 days after initiation of treatment. F) Phenotypic characterization of congenically marked, adoptively transferred bone marrow-derived myeloid cells into perfused livers and blood based on flow cytometry of mice administered  $\alpha$ 4-1BB therapy. G) Frequency of inflammatory/activation markers based on flow cytometry of perfused livers from treated mice based on three subsets of liver-resident macrophages: CD11b<sup>+</sup>CD68<sup>-</sup> cytokine-producing Kupffer cells, CD11b<sup>+</sup>CD68<sup>+</sup> cytokine-producing/phagocytic Kupffer cells, and

CD11b-CD68<sup>+</sup> phagocytic Kupffer cells. H) Gene expression from individual myeloid populations was calculated at day 7 post treatment initiation using real-time PCR analysis with *gapdh* as the endogenous control. Each point in A and B represents an individual mouse. Micrographs in C were imaged at 20X magnification. Micrographs in E were imaged using a 20X air objective. Insets for magnified using 2X magnification. Gene expression was calculated using Taqman primers via the  $\Delta\Delta C_t$  method. Data were pooled from  $\geq 2$  experiments with 5 mice per group. Bars represent mean  $\pm$  SEM. Statistical significance was calculated using a two-sided Student's T test applying Welch's correction for unequal variance. ns, not significant; \* $P < 0.05$ , \*\* $P < 0.01$ , \*\*\* $P < 0.001$ , \*\*\*\* $P < 0.0001$ .

### 3.3.3: Interleukin 27 is a critical regulator of liver inflammation.

In addition to the above, we previously reported that IL-27 acts to polarize T cells to the cytotoxic ThEO/TcEO phenotype (213), and therefore hypothesized that it may play a role in triggering  $\alpha$ 4-1BB-induced hepatic damage. To evaluate the contribution of IL-27 to immune-mediated hepatotoxicity, mice lacking the Ebi3 subunit of IL-27 (*EBI3*<sup>-/-</sup>) or mice lacking the IL-27 receptor alpha subunit (*IL27R $\alpha$* <sup>-/-</sup>) were treated with  $\alpha$ 4-1BB therapy followed by analysis of transaminase levels. Compared to wildtype mice, *EBI3*<sup>-/-</sup> and *IL27R $\alpha$* <sup>-/-</sup> mice treated with 4-1BB agonists failed to develop liver damage as measured by serum ALT and AST (Fig. 3.3A). Remarkably, the high-grade elevation of liver transaminases resulting from triple combination  $\alpha$ 4-1BB/ $\alpha$ CTLA-4/ $\alpha$ PD-1 therapy was also nearly completely abrogated in *EBI3*<sup>-/-</sup> mice. Moreover, abrogation of the IL-27 pathway did not significantly impact basal 4-1BB expression nor TNF $\alpha$  induced expression on liver-resident myeloid populations (Supplemental Fig. 3.4A, B), suggesting that *EBI3*<sup>-/-</sup> mice were equally capable of receiving 4-1BB signal.

In mice lacking the IL-27/IL-27R pathway, CD3<sup>+</sup> T cell infiltration of the liver was reduced (Fig. 3.3B) as were both the frequency and density of cytotoxic CD8<sup>+</sup> cells (Fig. 3.3C). Further, the frequency of CD4 effector T cells appeared minimally affected by knockout of the IL-27 pathway (Supplemental Fig. 3.4C). While the percent of CD4<sup>+</sup>Eomes<sup>+</sup>KLRG1<sup>+</sup> ThEO phenotype cells (Supplemental Fig. 3.4D), and CD8<sup>+</sup> TcEO phenotype T cells were minimally affected by loss of IL-27, the total numbers of the highly inflammatory TcEO population within liver infiltrates were significantly diminished absent functional IL-27 signaling (Fig.3.3D).



Taken together, these data demonstrate a critical requirement for the inflammatory cytokine IL-27 in mediating 4-1BB agonist antibody-induced hepatotoxicity as well as for recruitment and/or expansion of hepatogenic T cells into the liver.

Figure 3.3

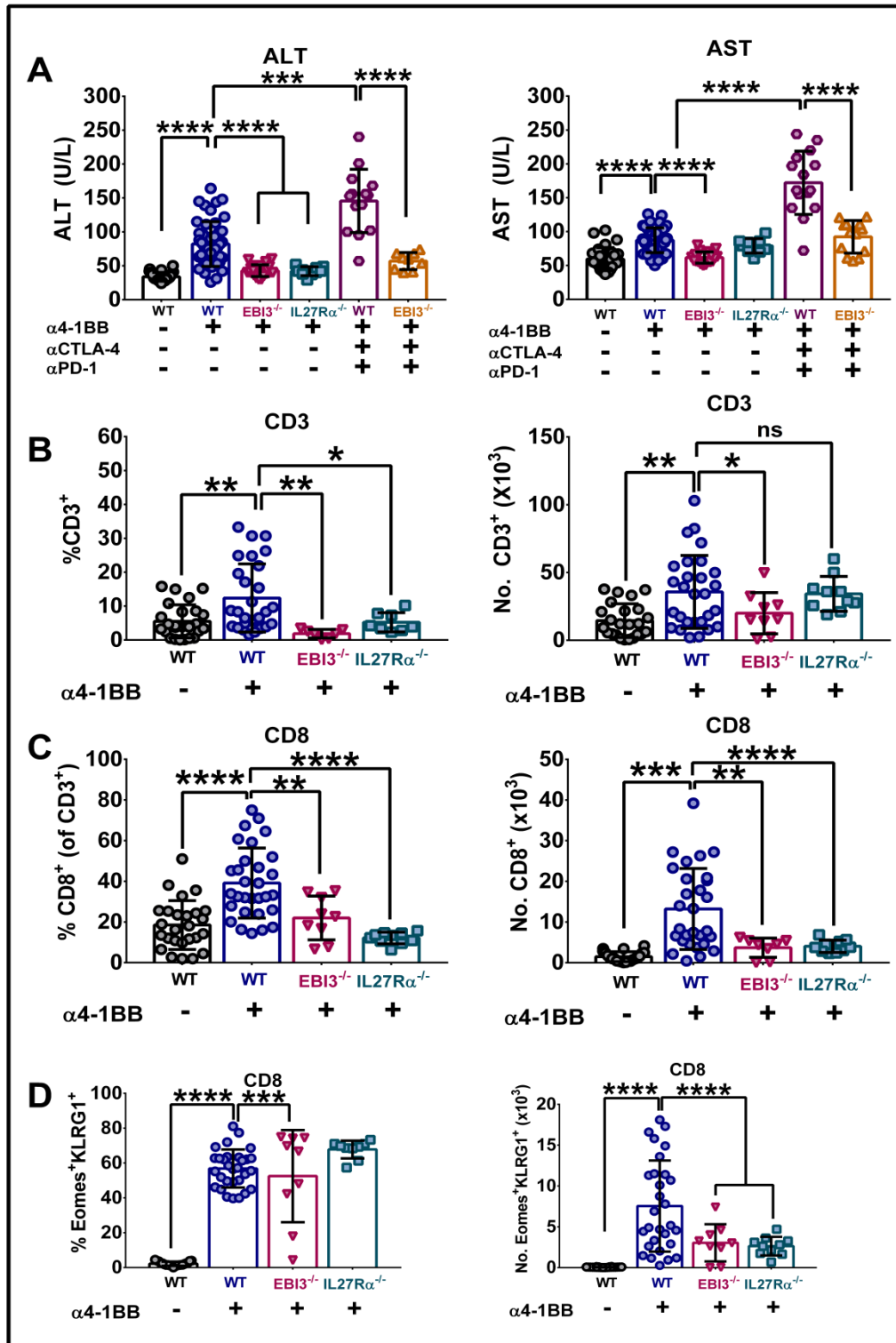


**Figure 3.3: Interleukin 27 is a critical regulator of 4-1BB agonist-induced liver inflammation.** Wildtype mice or mice lacking the Ebi3 subunit of the IL-27 cytokine complex (Ebi3<sup>-/-</sup>) or the IL-27 receptor alpha subunit (IL27Rα<sup>-/-</sup>) were treated for three rounds of α4-1BB agonist immunotherapy before analysis of serum transaminase levels and hepatic immune infiltrates 16 days after initiation of treatment. A) Serum levels of alanine aminotransferase (ALT) and aspartate aminotransferase (AST) were measured upon sacrifice as units of enzyme/liter of blood volume. B) Quantification of immune infiltrates within perfused livers of treated mice was measured by flow cytometry. Frequency of CD3<sup>+</sup> cells was calculated as a percent of total CD45<sup>+</sup> cells in the liver. C) Frequency of CD8<sup>+</sup> T cells was calculated as a percent of CD3<sup>+</sup> cells. Total numbers of cells were taken as number of CD3<sup>+</sup> or CD3<sup>+</sup>CD8<sup>+</sup> cells within perfused livers. D) Quantification of percent and total numbers of TcEO T cell infiltration within the livers of treated mice. Frequency of TcEO was calculated based on the percent of CD3<sup>+</sup>CD8<sup>+</sup> T cells expressing Eomesodermin (Eomes) and KLRG1. Each point within each graph represents an individual mouse. Data were pooled from ≥ 2 experiments with 5 mice per group. Bars represent mean ± SD. Statistical significance was calculated using a two-sided Student's T test applying Welch's correction for unequal variance. ns, not significant; \**P* < 0.05, \*\**P* < 0.01, \*\*\**P* < 0.001, \*\*\*\**P* < 0.0001.

### **3.3.4: Regulatory T cells restrict 4-1BB agonist antibody induced liver pathology**

Given the ability of myeloid cells to activate T cell responses, coupled with the capacity of IL-27 to act as an inflammatory mediator of hepatic damage with pleotropic effects on helper T cell polarization, Treg suppression, and T cell trafficking (229-231), and the prolonged inflammatory response induced by  $\alpha$ 4-1BB (Fig. 3.1G), we investigated the role of T cells in propagating  $\alpha$ 4-1BB-mediated liver damage. To assess the relative contribution of the T cell pool in mediating hepatotoxicity, we administered  $\alpha$ 4-1BB to mice lacking the  $\beta$ 2 microglobulin subunit of the major histocompatibility (MHC) I complex ( $\beta$ 2M<sup>-/-</sup>) or mice lacking all H2-A/E MHC genes (*MHCII*<sup>-/-</sup>). These mice are deficient in antigen presentation to CD8 and CD4 T cells respectively, leading to a failure of these cells to complete thymic positive selection and enter the periphery. Even though these mice exhibited similar patterns of 4-1BB expression compared to wildtype mice (Supplemental Fig. 3.5A,B), elevation of liver ALT and AST levels was completely abrogated in  $\alpha$ 4-1BB-treated  $\beta$ 2M<sup>-/-</sup> mice, confirming the role of CD8<sup>+</sup> T cells in mediating the bulk of the liver damage (Fig. 3.4A) (210). To separate the possibilities that this effect may be due to absent CD8 T cell responses and/or to defective antigen presentation, mice were sub-lethally irradiated and CD8<sup>+</sup> splenocytes from wildtype mice were transferred into  $\beta$ 2M<sup>-/-</sup> mice. We hypothesized that if the lack of CD8 T cells in these mice was the sole cause of the abrogated hepatotoxicity, then supplying wildtype CD8<sup>+</sup> T cells would reinitiate toxicity. Interestingly, supplementation of WT CD8<sup>+</sup> T cells into  $\beta$ 2M<sup>-/-</sup> mice did not abrogate the resistance of these animals to liver damage when challenged with 4-

1BB antibody (Fig. 3.4B). This suggests that not only are CD8 T cells required to effect 4-1BB agonist-induced liver injury, but that antigen presentation on MHC Class I is also necessary. This further indicates that hepatitis-inducing CD8 T cells are being activated by 4-1BB-activated myeloid cells in an antigen-specific manner. Intriguingly, impairing the CD4 response in MHCII<sup>-/-</sup> mice significantly escalated liver damage, denoted by approximately 1.5-2-fold increases in serum AST (176 vs. 87; p=0.0008) and ALT (108 vs. 84; p=0.0244) levels in MHCII<sup>-/-</sup> mice compared to  $\alpha$ 4-1BB treated wildtype mice (Fig. 3.4A).

We next hypothesized that exacerbation of hepatotoxicity in MHCII<sup>-/-</sup> mice stemmed not from dysregulation of effector T cells responses, but from elimination of Treg cells, leading to loss of immune homeostasis in the liver. We made the related observation that there was a 2-fold increase in the fraction of Foxp3<sup>+</sup> regulatory T cells in the livers of  $\alpha$ 4-1BB compared to untreated mice (Fig. 3.4C) suggesting that Treg expansion might be acting to limit hepatitis. Using flow cytometry based analysis, however, we did not see any significant difference in overall Treg infiltration in the liver of  $\alpha$ 4-1BB alone treated mice compared to combination treated mice. Interestingly, probing cellular localization using immunohistochemistry revealed increased infiltration of Treg in the liver parenchyma when  $\alpha$ CTLA-4 was co-administered with  $\alpha$ 4-1BB, which is consistent with a reduction of inflammatory foci in the liver parenchyma of mice treated with  $\alpha$ CTLA-4 and  $\alpha$ 4-1BB in combination (Fig. 1C,E). To validate a role for Tregs in limiting  $\alpha$ 4-1BB-induced liver toxicity, we treated mice expressing the diphtheria toxin (DT) receptor (DTR) under control of the Foxp3 promoter (Foxp3-DTR) in which Foxp3<sup>+</sup> regulatory T cells can be depleted upon administration of DT.

Briefly, DT was administered 2 days before  $\alpha$ 4-1BB therapy, and continued until the end of treatment for complete and sustained Treg depletion. Treg depletion was successful based on analysis of blood three days before serum analysis (Supplemental Fig. 3.5C). Consistent with our hypothesis, depletion of Tregs significantly aggravated  $\alpha$ 4-1BB induced liver damage, increasing AST and ALT levels 5-6-fold, and eliminating the ability of  $\alpha$ CTLA-4 to dampen liver damage (Fig. 3.4D). This effect was not due to administration of DT, as DT alone did not significantly impact transaminase levels. Moreover, Treg adoptive transfer prior to therapy limited transaminase elevation, suggesting that Treg cells are critical suppressors of inflammation during  $\alpha$ 4-1BB treatment. Of note, while the CTLA-4 antibodies used here are capable of depleting Tregs in the context of tumor microenvironments, they do not deplete peripheral Tregs, and may sometimes expand them, due to the low densities of the Fc $\gamma$ RIV receptor in these tissues (232).

Taken together this data suggests a critical role of CD8 T cell activation in mediating  $\alpha$ 4-1BB liver damage. Antigen presentation was also required suggesting hepatogenic CD8 T cells are liver tissue-antigen specific. Further, Treg cells play a critical role in protecting the liver from CD8-mediated injury downstream of  $\alpha$ 4-1BB.

Figure 3.4

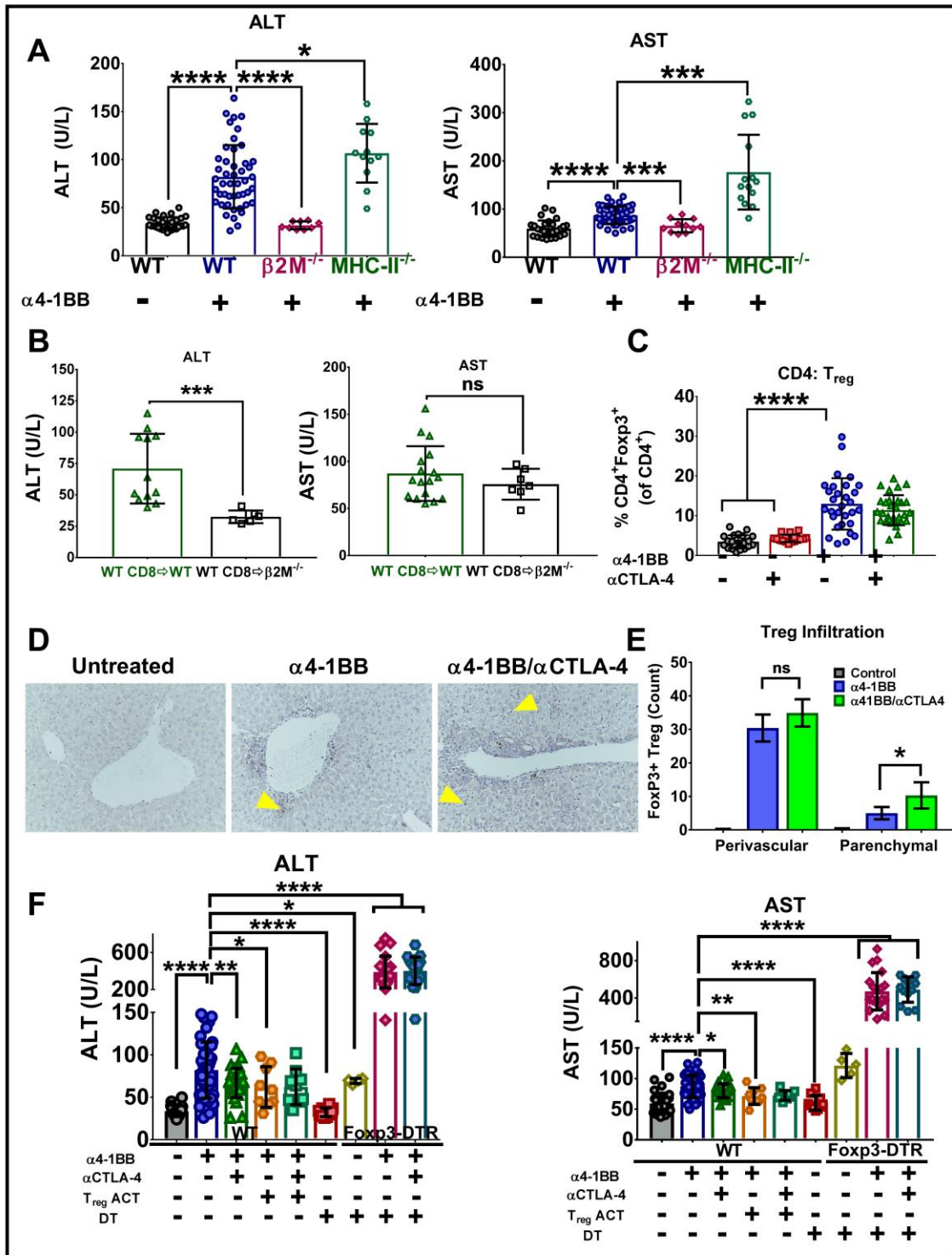


**Figure 3.4: Regulatory T cells suppress 4-1BB agonist antibody induced liver pathology.** A) Wildtype mice or mice lacking MHC Class I expression ( $\beta 2M^{-/-}$ ) or all MHC Class II alleles ( $MHC-II^{-/-}$ ) were treated for three rounds with  $\alpha 4-1BB$  agonist antibody (days 0, 3, and 6) before mice were bled for serum liver enzyme analysis 16 days after beginning treatment. Serum ALT and AST were measured upon sacrifice as units of enzyme/liter of blood. B) Mice were sub-lethally irradiated (500 rads) before administration of  $2 \times 10^6$   $CD8^+$  splenocytes. Wildtype mice or  $\beta 2M^{-/-}$  mice received splenocytes from wildtype mice (WT  $CD8 \rightarrow$  WT) or (WT  $CD8 \rightarrow \beta 2M^{-/-}$ ) respectively. Mice were subsequently treated with three round of  $\alpha 4-1BB$  immunotherapy. Treated mice were then bled 16 days after first administration of therapy and serum ALT and AST were measured. C) Frequency of regulatory T cell (Treg) infiltration into the perfused livers of mice 16 days after initiation of therapy was quantified by flow cytometry as the percent of  $Foxp3^+CD4^+$  cells as a fraction of total  $CD4^+$  T cells. D) Immunohistochemistry (IHC) targeting regulatory T cells was performed on sectioned liver tissues from mice 16 days after initiation of therapy. E) Sections were quantified for Treg infiltration in the perivascular and parenchyma area of liver and was enumerated per section. F) Mice received  $5 \times 10^5$   $CD3^+CD4^+CD25^+$  splenocytes FACS-sorted from naïve mice one day prior to treatment. Concurrently, mice expressing the diphtheria toxin receptor under control of the *Foxp3* promoter (*Foxp3-DTR*) were administered 10  $\mu g/kg$  body weight of diphtheria toxin one day prior to initiation of therapy and every three days thereafter until completion of the experiment. Data were pooled from  $\geq 2$  experiments with 5 mice per group. Bars represent mean  $\pm$  SD. Statistical significance was calculated using a two-sided Student's T test applying Welch's



correction for unequal variance. ns, not significant; \* $P < 0.05$ , \*\* $P < 0.01$ , \*\*\* $P < 0.001$ , \*\*\*\* $P < 0.0001$ .

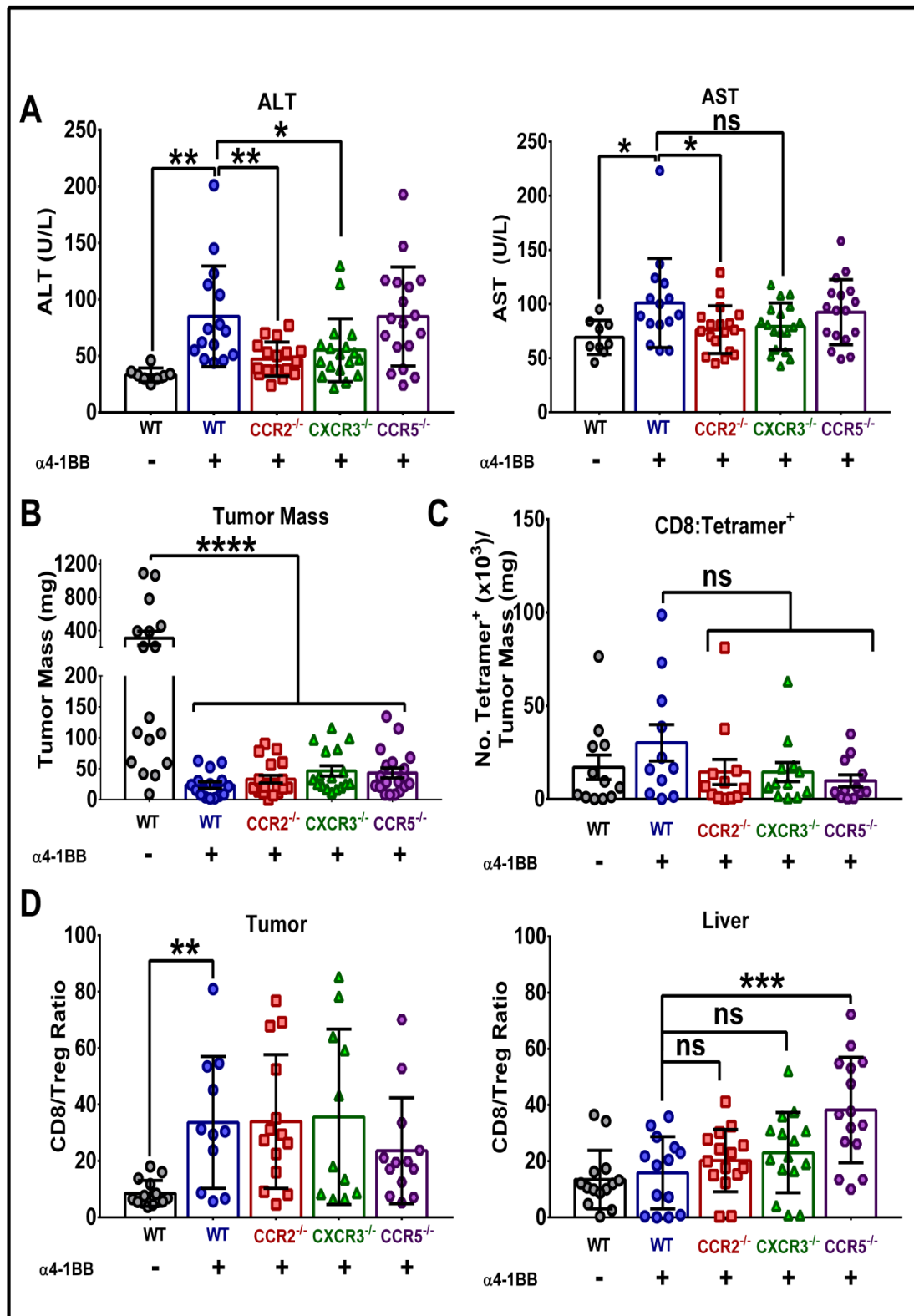
### ***3.3.5: CCR2 and CXCR3 are differentially required for liver and tumor T cell trafficking***

Given the ability of IL-27 to induce chemokine receptor expression (233,234), the reduced immune infiltrate in the liver in the absence of IL-27, and the reduced myeloid presence in mice treated with  $\alpha$ 4-1BB/ $\alpha$ CTLA-4 co-therapy, we hypothesized that 4-1BB agonist therapy might alter T cell trafficking patterns into the tissue via chemokine modulation. Given the differential expression patterns of chemokine receptors on T cells capable of homing into tumor tissue versus liver (228,235), we sought to determine whether anti-tumor immunity could be separated from hepatitis based on differential homing. We challenged either wildtype, CCR2<sup>-/-</sup>, CXCR3<sup>-/-</sup>, or CCR5<sup>-/-</sup> mice subcutaneously with  $3 \times 10^5$  murine B16 melanoma cells expressing the ovalbumin antigen (B16-Ova). Mice were then treated with 4-1BB agonist and assessed for serum transaminase elevation and infiltration. CXCR3 is critical for driving IFN $\gamma$ -dependent T cell trafficking into tumors, while CCR5 remains the predominant trafficking mechanism into the liver; however, CXCR3 can regulate liver chemotaxis in response to injury (236). CCR2, in contrast, minimally impacts T cell trafficking to liver even in the context of viral infection. Intriguingly, following 4-1BB agonist antibody therapy, CCR2<sup>-/-</sup> mice exhibited significantly reduced AST and ALT serum levels, while CXCR3<sup>-/-</sup> mice showed significantly reduced ALT levels and a trend towards lower AST levels ( $p=0.08$ ) (Fig. 3.5A). In contrast, CCR5<sup>-/-</sup> showed no significant reduction in the liver damage induced by  $\alpha$ 4-1BB. Ablation of these chemokine receptors individually failed to impact the ability of 4-1BB agonist therapy to mediate rejection of subcutaneous melanoma (Fig. 3.5B), implying either that they are not required,

or that sufficient redundancy exists to preserve responses in the tumor setting. Moreover, removing these chemokine receptor pathways did not significantly affect recruitment of antigen-specific T cells into the tumor (Fig. 3. 5C). Of note, the apparent lack of significant increase in tetramer frequency in response to  $\alpha$ 4-1BB therapy here is largely a function of the potency of 4-1BB agonists against these B16-Ova tumors. In the treated animals, both wild-type and chemokine knockout, the therapy is so effective that a significant number of mice have eradicated their tumors leaving only a small remnant of Matrigel and few, if any, antigen-specific CD8 T cells. It has been demonstrated across multiple tumor microenvironments that increased CD8/Treg ratios correlate with more successful responses to immune-based therapies (94,237,238). We found that the magnitude of elevation of CD8/Treg ratios in wildtype, CCR2<sup>-/-</sup>, CXCR3<sup>-/-</sup>, and CCR5<sup>-/-</sup> mice were not significantly different providing additional evidence that loss of a single chemokine receptor pathway does not impact anti-tumor immune responses (Fig. 3.5D, Supplemental Fig. 3.5D). Interestingly, within the liver, abrogation of CCR5 significantly increased the CD8/Treg ratio. While this may be beneficial in the tumor setting, an increased ratio within the liver may account for the maintenance of elevated transaminase elevation in the CCR5 knockout mice (Fig. 3.5A). The lack of an increase in transaminases in these CCR5 knockout mice, we hypothesize, suggests that Treg may rely on production of soluble factors such as TGF- $\beta$ , rather than on cell-contact dependent interactions to maintain liver homeostasis, and therefore can maintain tissue tolerance even when at a modest numerical disadvantage relative to effectors.

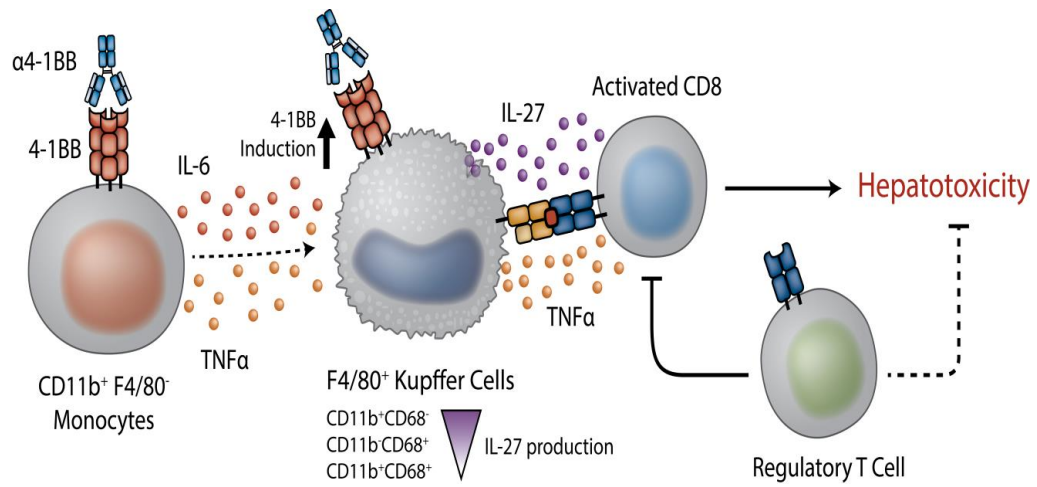
Taken together, these data suggest that immune infiltration into the liver and tumor can be uncoupled through abrogation of chemokine receptor signaling. Further, CCR2 and CXCR3 appear to be critical mediators of  $\alpha$ 4-1BB induced hepatotoxicity-mediating T cell trafficking, while disengaging these pathways does not significantly impact the ability of  $\alpha$ 4-1BB therapy to generate potent anti-tumor immunity.

Figure 3.5



**Figure 3.5: The chemokine receptors CCR2 and CXCR3 contribute to 4-1BB agonist-induced liver pathology.** Wildtype mice or mice lacking specific chemokine receptors (CCR2<sup>-/-</sup>, CXCR3<sup>-/-</sup>, or CCR5<sup>-/-</sup>) were subcutaneously implanted on the right flank with 3X10<sup>5</sup> B16 melanoma tumor cells expressing the ovalbumin antigen (B16-Ova). At three-day intervals after initial tumor challenge (days 3, 6, and 9) mice were treated with antibody immunotherapy delivered i.p. in combination with an irradiated tumor vaccine (FVAX) administered subcutaneously on the left flank. Mice were bled for serum liver enzyme analysis 16 days after treatment initiation. Mice were then sacrificed and perfused livers and tumors were extracted, weighed, and processed for FACS analysis. A) Serum ALT and AST were measured upon sacrifice as units of enzyme/liter of blood volume. B) Upon sacrifice, tumors were harvested and weighed. C) Tumor infiltration of Ova-specific CD8<sup>+</sup> T cells was determined by staining tumor infiltrating lymphocytes (TIL) with fluorescently labeled Ova<sup>257-254</sup>/K<sup>b</sup> (SIINFEKL) tetramer and antibodies to CD8. Data are expressed as the total number of tetramer positive cells per milligram of tumor. D) Quantification of CD8/Treg ratios within the tumor and liver were calculated by dividing the number of CD8<sup>+</sup>CD3<sup>+</sup> cells by the number of CD4<sup>+</sup>Foxp3<sup>+</sup> cells found within the tissue infiltrate. Data were pooled from ≥ 2 experiments with 5 mice per group. Bars represent mean ± SD. Statistical significance was calculated using a two-sided Student's T test applying Welch's correction for unequal variance. ns, not significant; \**P* < 0.05, \*\**P* < 0.01, \*\*\**P* < 0.001, \*\*\*\**P* < 0.0001.

Figure 3.6



**Figure 3.6: Mechanistic model of 4-1BB agonist antibody-mediated hepatotoxicity.**

### 3.4: Discussion

While the field of immunotherapy has experienced unprecedented growth due to the success of immune checkpoint blockade, clinical translation of the most efficacious mono- and combination therapies from pre-clinical models has been limited by immune toxicities. 4-1BB agonist antibodies are among the most effective immunotherapeutics across pre-clinical models of cancer (205). Severe off-target liver damage in early Phase I trials; however, has limited the clinical progression of highly active 4-1BB antibodies (211). Effective prophylaxis, biomarker prediction, or management of this toxicity, except through highly attenuated dosing, has proven challenging due to a lack of mechanistic understanding of underlying cellular and molecular mechanisms. Efforts at development of 4-1BB agonist antibodies with limited toxicity are ongoing; however, no 4-1BB agonist has advanced beyond early Phase II trials. In this manuscript, we sought to uncover the mechanisms driving 4-1BB agonist mediated liver pathology so that this knowledge may inform both antibody engineering and combination 4-1BB agonist trial design.

The capacity of 4-1BB activation to potentiate CD8 T cell responses is widely accepted; however, we find that activation of liver myeloid cells, not T cells, is a critical initiating step that triggers hepatotoxicity. Following  $\alpha$ 4-1BB administration, bone marrow derived monocytes infiltrate the liver and, in response to 4-1BB activation, initiate a cascade of inflammatory cytokine production that triggers 4-1BB upregulation by resident Kupffer cells, allowing these cells to subsequently respond to agonist antibody. Antigen presentation capacity



increased in multiple Kupffer cell populations based on MHC-II upregulation. In addition, the cytokine-producing CD11b<sup>+</sup> subsets increased production of IL-27 more than 20-fold. We find that this augmented IL-27 production is essential for the progression of liver inflammation, as neither *EBI3*<sup>-/-</sup> nor *IL27R $\alpha$* <sup>-/-</sup> mice showed any evidence of transaminase elevation in response to 4-1BB activation. Despite the requirement for myeloid initiation, CD8 T cells mediate the actual liver injury, as mice lacking CD8s fail to develop transaminase elevation. Prior studies indicate that mice expressing only CD8 T cells specific for an Ovalbumin-peptide/H2-Kb complex were also resistant to  $\alpha$ 4-1BB liver toxicity (210). This observation, coupled with our own  $\beta$ 2M<sup>-/-</sup> data, led us to question whether CD8 T cell activation downstream of myeloid 4-1BB activation was occurring via an antigen-dependent or independent mechanism. Mice deficient in MHC Class I antigen presentation upon transfer of wildtype CD8 T cells failed to develop liver injury in response to  $\alpha$ 4-1BB, suggesting that hepatotoxic CD8 T cells recognize uncharacterized liver-specific auto-antigens. It is likely then, that 4-1BB activation of myeloid cells leads to enhanced presentation of liver tissue antigens and secreted IL-27 further provides a critical signal 3 for liver auto-reactive CD8 T cell activation. The role of IL-27, in this context, could be direct co-stimulation of effector CD8 and/or inhibition of Treg suppressive activity. These mechanistic insights suggest IL-27 blockade as a means to reduce to 4-1BB agonist liver toxicity; however, we have previously found IL-27 to play a critical role in effector T cell polarization downstream of  $\alpha$ 4-1BB as well as in anti-tumor responses (213,239,240).

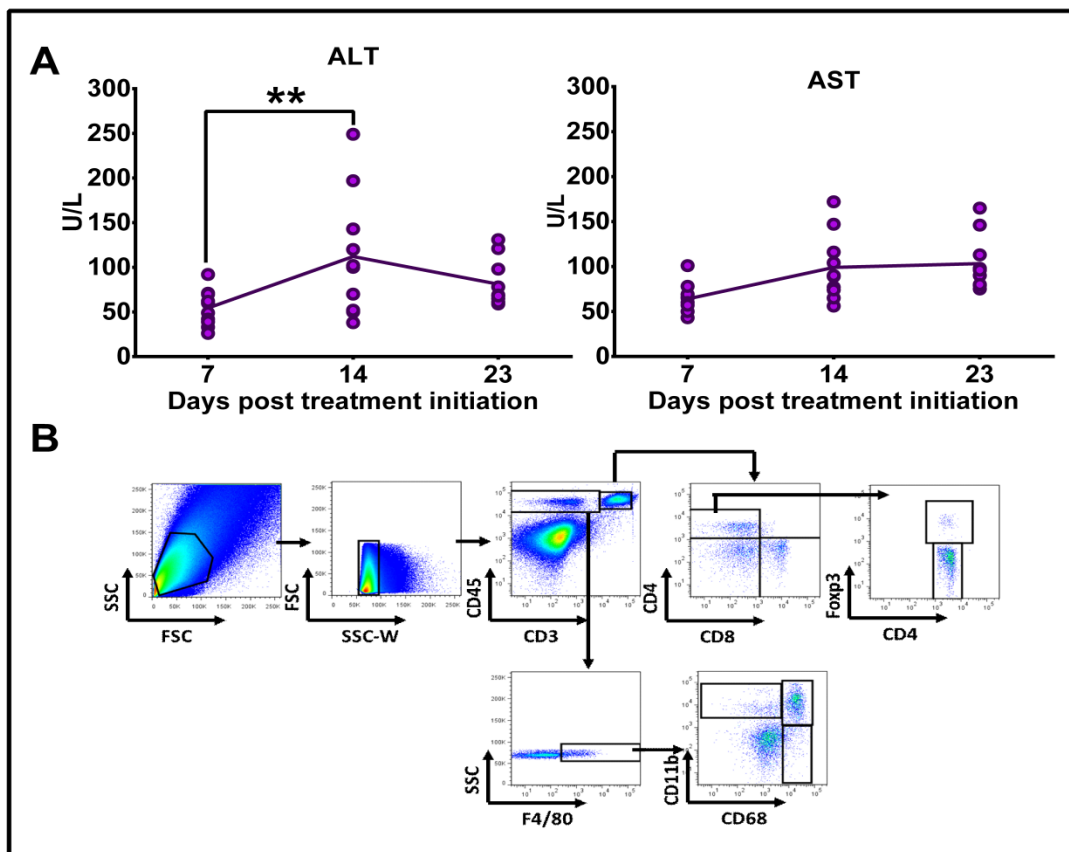
Currently the only described mechanism to reduce 4-1BB agonist liver toxicity involves combination therapy with CTLA-4 blockade (209). We confirm the

capacity of this combination to block 4-1BB agonist transaminase elevation. Given this combination also shows therapeutic synergy and the capacity to limit  $\alpha$ CTLA-4 IRAE (94,209), it remains unfortunate that no trials have tested  $\alpha$ 4-1BB/ $\alpha$ CTLA-4 in patients. In contrast, the  $\alpha$ 4-1BB/ $\alpha$ PD-1 combination has been tested in patients, but with very limited dosing regimens due to the capacity of  $\alpha$ PD-1 to worsen  $\alpha$ 4-1BB-mediated hepatitis – an effect we also validated herein (216). We hypothesized that the liver-protective effect of CTLA-4 blockade might also extend to  $\alpha$ 4-1BB/ $\alpha$ PD-1 combination therapy; however, the effect of PD-1 blockade was, in fact, dominant and that triple combination treatment engendered severe transaminitis. Differential effects of CTLA-4 and PD-1 checkpoint blockade on  $\alpha$ 4-1BB-mediated liver toxicity may be due, in part, to the expression patterns of each receptor on distinct immune populations, (high CTLA-4, moderate PD-1:Tregs, low CTLA-4, high PD-1; CD8) or on potential potency of these receptors to inhibit T cell activation/effector responses. Alternatively, PD-1 blockade may decrease the suppressive capacity of Treg, and our data suggests that CTLA-4 blockade requires the presence of (functional) Treg to ameliorate 4-1BB agonist liver toxicity(241). In the context of our model (Fig. 3.6), CTLA-4 blockade limited the accumulation of CD8 T cells and increased Treg in the liver parenchyma following 4-1BB agonist administration, and thus attenuated resulting hepatotoxicity. We also demonstrated an impact of  $\alpha$ CTLA-4 co-administration on myeloid infiltration and effector function in the liver. We observed distinct patterns of parenchymal versus perivascular infiltration of F4/80<sup>+</sup> cells in each combination setting. We hypothesize that it is the combination of accumulation of F4/80<sup>+</sup> cells in the perivascular area, coupled with a capacity to infiltrate the parenchyma which

equals or exceeds that of 4-1BB agonist alone, that explains why the triple combination induces exacerbated liver toxicity. Although perivascular infiltration increases with the  $\alpha$ CTLA-4/ $\alpha$ 4-1BB combination, parenchymal F4/80<sup>+</sup> cell density decreases, coincident with a decrease in CD8 T cells in this region and an increase in Treg. Liver damage associated with significant transaminase elevation, in general, requires infiltration and damage within the liver parenchyma itself. Perivascular accumulation can represent expansion of resident cells with progenitor capacity and/or infiltration of monocytes and their subsequent differentiation into F4/80<sup>+</sup> cells (a phenomenon for which we have demonstrated a limited capacity).

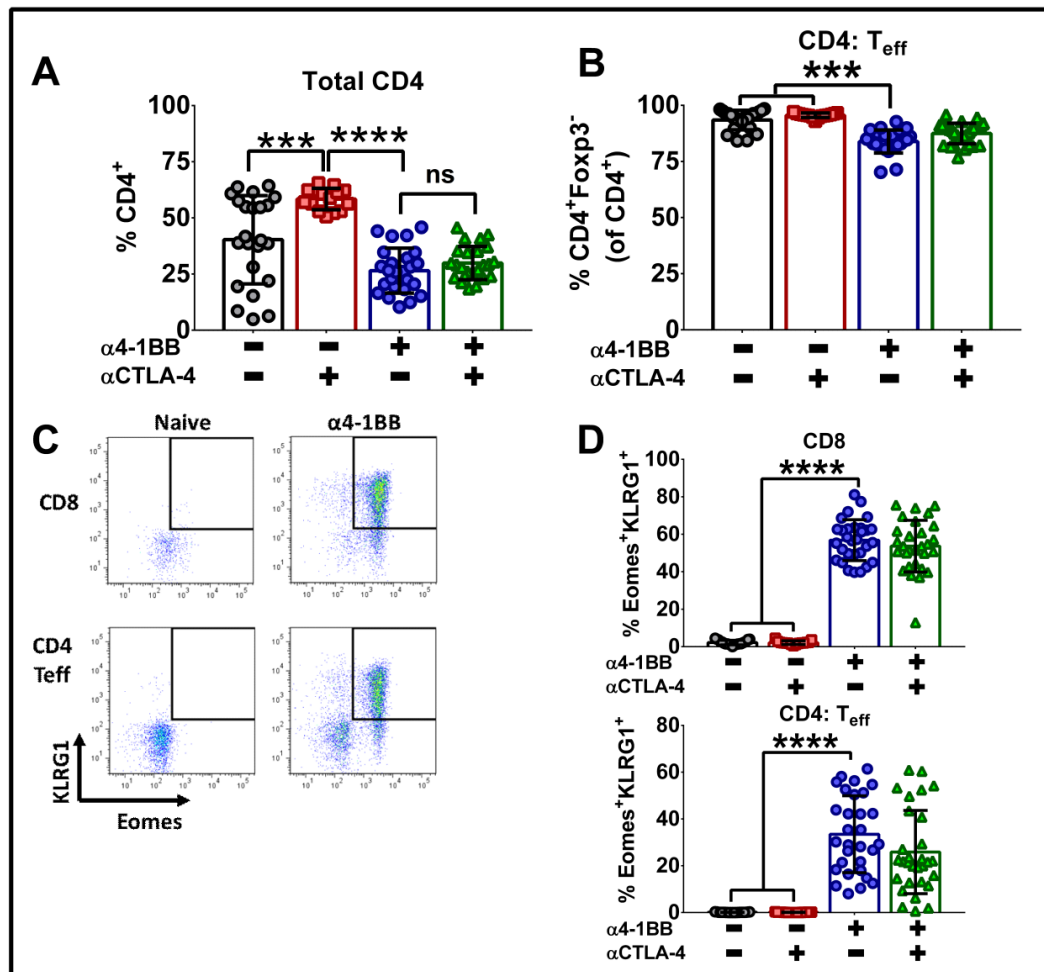
We next considered whether the chemokine receptors governing entry of hepatitis-inducing T cells into the liver, versus migration of tumor-specific T cells into melanoma tumors might be sufficiently different to separate tumor immunity from hepatotoxicity. We found that CCR2<sup>-/-</sup> mice, and to a lesser extent CXCR3<sup>-/-</sup> mice, were protected from 4-1BB agonist induced liver toxicity but were still capable of effectively combating B16-Ova tumors growing on the flank. The impact of CCR2 knockout in abrogating liver toxicity remains enticing, as both small molecule (CCX872, ChemoCentryx; PF-04136309, Pfizer) and antibody (MLN1202, Millennium) antagonists for CCR2 are currently in clinical trials. Given our findings, 4-1BB agonist antibodies administered in combination with CCR2 inhibitors may prove to be a potent combination in promoting tumor regression while inhibiting off-target liver toxicity.

## Supplemental Figure 3.1



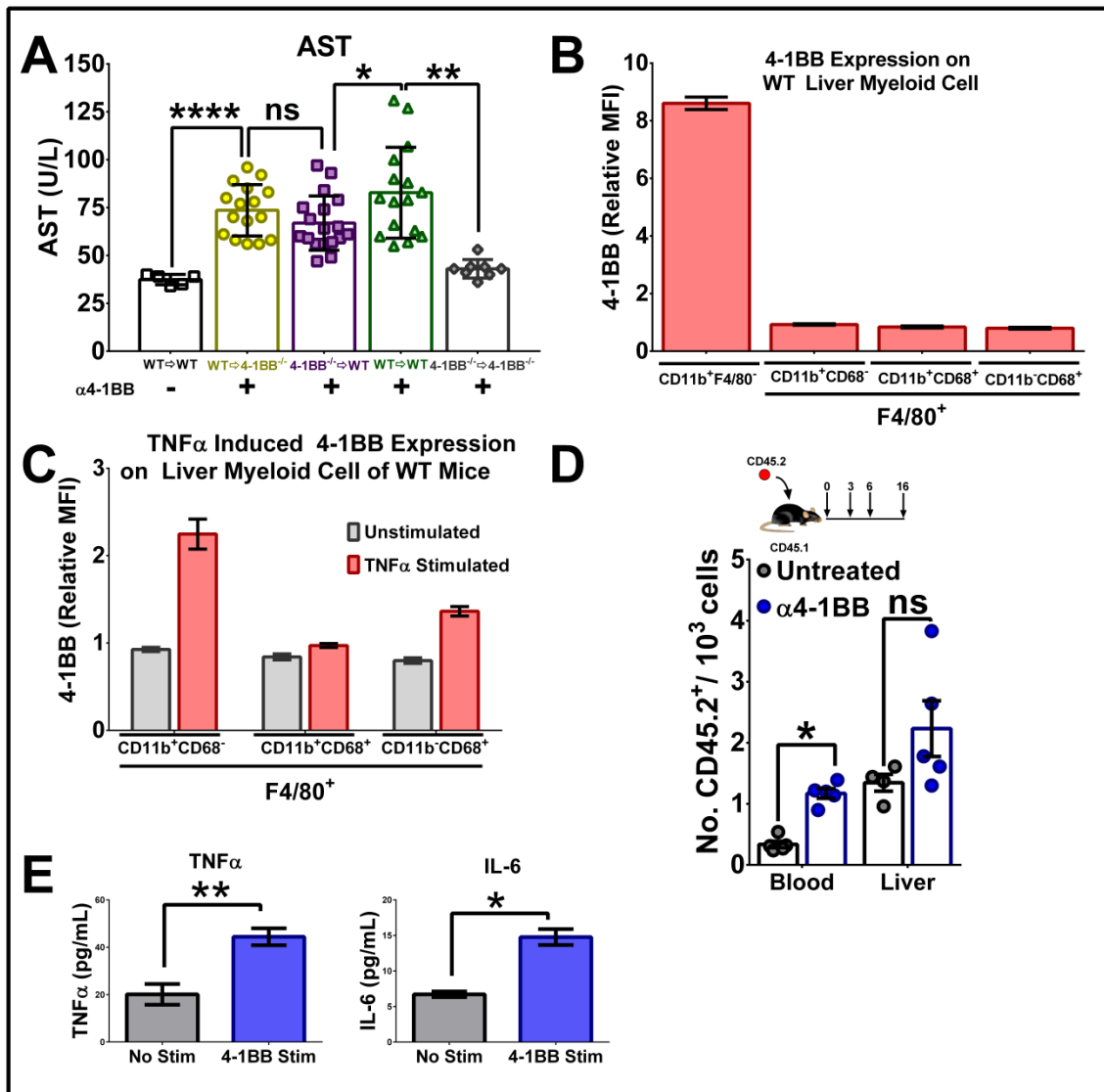
**Supplemental Figure 3.1: Peak of 4-1BB mediated liver transaminase level and gating strategy for flow cytometry analysis of liver immune infiltrates.** A) Mice were administered  $\alpha$ 4-1BB antibodies within 3 day intervals (days 0, 3, and 6) and were bled on days 7, 14 and 23 in order to assess serum transaminase levels. Each point in A represents data taken from an individual mice. B) Representative gating strategy to analyze CD8<sup>+</sup>, CD4<sup>+</sup> Teff, and CD4<sup>+</sup> Treg T cell populations as well as F4/80<sup>+</sup>CD11b<sup>+</sup>CD68<sup>-</sup>, F4/80<sup>+</sup>CD11b<sup>+</sup>CD68<sup>+</sup>, and F4/80<sup>+</sup>CD11b<sup>-</sup>CD68<sup>+</sup> myeloid populations within perfused livers.

Supplemental Figure 3.2



**Supplemental Figure 3.2: Representative flow cytometry analysis of liver immune infiltrates.** A) Frequency of total CD4 (CD4+CD3+ ) and B) CD4 Teff (CD4+CD3+ Foxp3+ ) infiltrates into the perfused livers of treated mice 16 days after initiation of therapy. C) Representative gating strategy for analysis of Eomes+KLRG1+ TcEO (top) or ThEO (bottom) phenotype cells infiltrating the livers of treated mice. D) Quantification of TcEO (top) and ThEO (bottom) phenotype cells enumerated at the percent of CD3+CD8+ Eomes+KLRG1+ or CD3+CD4+ Foxp3- Eomes+KLRG1+ cells respectively that infiltrated perfused livers. Data were pooled from  $\geq 2$  experiments with 5 mice per group. Bars represent mean  $\pm$  SD. Statistical significance was calculated using a two-sided Student's T test applying Welch's correction for unequal variance. ns, not significant; \*P < 0.05, \*\*P < 0.01, \*\*\*P < 0.001, \*\*\*\*P < 0.0001.

Supplemental Figure 3.3

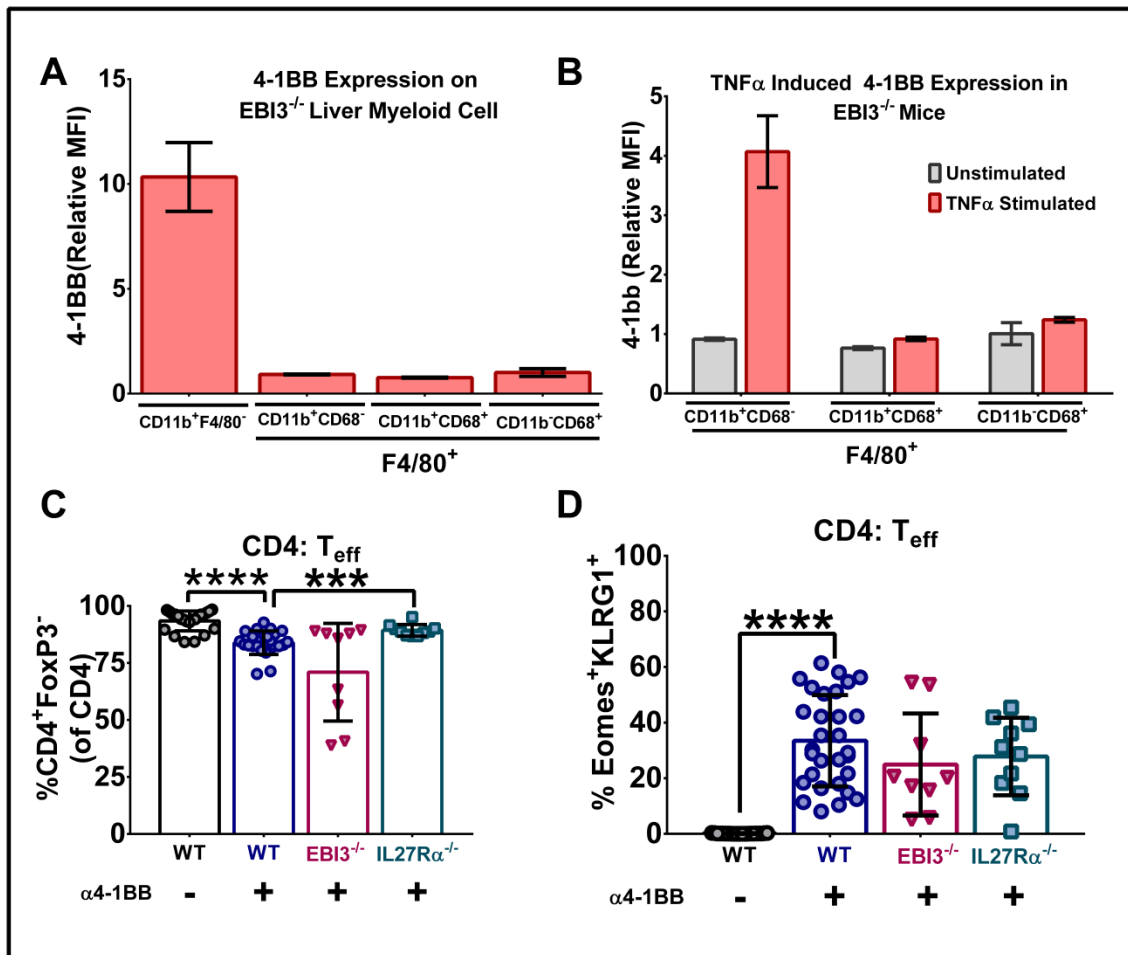


**Supplemental Figure 3.3: Administration of 4-1BB agonist antibodies initiates liver pathology through activation of liver-resident myeloid cells. A)**

Mice were sublethally irradiated (500 rads) before administration of  $2 \times 10^6$  CD90+ splenocytes. Wildtype mice either received splenocytes from wildtype mice (WT $\diamond$ WT) or from 4-1BB $^{-/-}$  mice (4-1BB $^{-/-}$  $\diamond$ WT) and 4-1BB $^{-/-}$  mice received splenocytes from wildtype mice (WT $\diamond$ 4-1BB $^{-/-}$ ) or from 4-1BB $^{-/-}$  mice (4-1BB $^{-/-}$  $\diamond$ 4-1BB $^{-/-}$ ). Mice were subsequently treated with three rounds of isotype control or  $\alpha$ 4-1BB immunotherapy. Treated mice were then bled 16 days after first administration of therapy and serum AST was measured. Quantification of 4-1BB expression on naïve mice using flow cytometry analysis on myeloid cells from perfused livers either at B) basal level or C) after induction by TNF $\alpha$  stimulation. The liver myeloid populations were categorized into bone marrow derived CD11b+ F4/80-monocytes and three subsets of F4/80+ liver-resident macrophages: CD11b+CD68- cytokine-producing Kupffer cells, CD11b+CD68+ cytokine-producing/phagocytic Kupffer cells, and CD11b-CD68+ phagocytic Kupffer cells. D) Quantification of congenically labelled and adoptively transferred bone marrow derived myeloid cells into perfused livers and blood based on flow cytometry of mice administered with  $\alpha$ 4-1BB therapy. Each point within graphs in A and D represents individual mice. C) Bone marrow derived monocytes were in vitro stimulated with  $\alpha$ 4-1BB (3H3) antibody for 48 hours and cytokine release was measured using a CBA kit. Data were pooled from  $\geq 2$  experiments with 5 mice per group. Bars represent mean  $\pm$  SD. Statistical significance was calculated using a two-sided Student's T test applying Welch's correction for unequal variance. ns, not significant; \*P < 0.05, \*\*P < 0.01, \*\*\*P < 0.001, \*\*\*\*P < 0.0001.



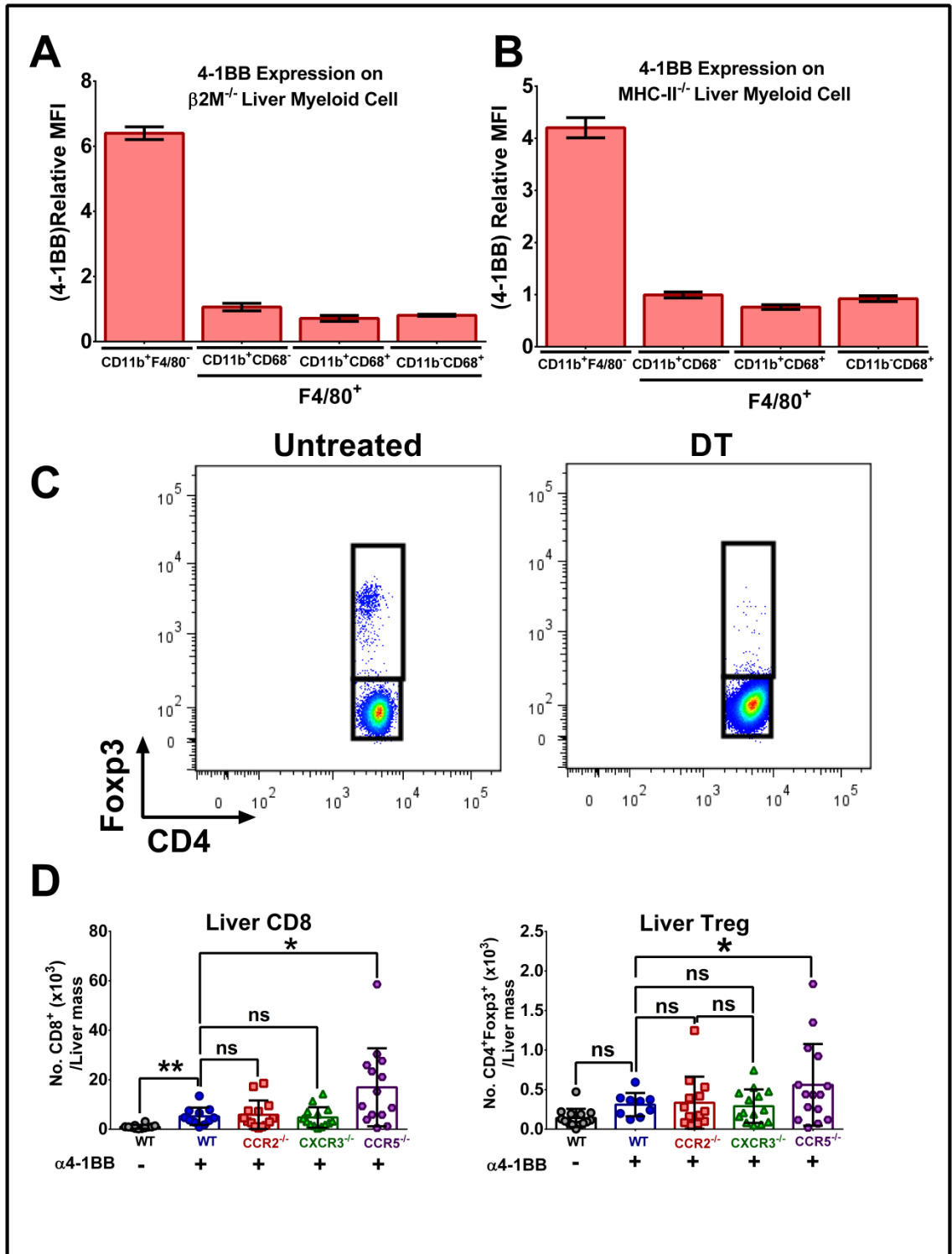
Supplemental Figure 3.4



**Supplemental Figure 4: Effects of IL-27 pathway inactivation on CD4 T cells.**

Quantification of 4-1BB expressions on EBI3<sup>-/-</sup> mice using flow cytometry analysis on myeloid cells from perfused livers at A) basal level or B) after 48 hours of TNF $\alpha$  stimulation. The liver myeloid population was categorized into bone marrow derived CD11b<sup>+</sup> F4/80<sup>-</sup> monocytes and three subsets of liver-resident macrophages: CD11b<sup>+</sup>CD68<sup>-</sup> cytokine-producing Kupffer cells, CD11b<sup>+</sup>CD68<sup>+</sup> cytokine-producing/phagocytic Kupffer cells, and CD11b<sup>-</sup>CD68<sup>+</sup> phagocytic Kupffer cells. C) Frequency of effector CD4 T cells (CD3<sup>+</sup>CD4<sup>+</sup> Foxp3<sup>-</sup>) infiltrating the perfused livers of  $\alpha$ 4-1BB treated wildtype (WT), EBI3<sup>-/-</sup>, or IL27R $\alpha$ <sup>-/-</sup> mice. D) ThEO phenotype cells (Eomes<sup>+</sup>KLRG1<sup>+</sup>) enumerated as the percent CD3<sup>+</sup>CD4<sup>+</sup> Foxp3<sup>-</sup> cells that infiltrated perfused livers. Data were pooled from  $\geq 2$  experiments with 5 mice per group. Bars represent mean  $\pm$  SD. Statistical significance was calculated using a two-sided Student's T test applying Welch's correction for unequal variance. ns, not significant; \*P < 0.05, \*\*P < 0.01, \*\*\*P < 0.001, \*\*\*\*P < 0.0001.

Supplemental Figure 3.5



**Supplemental Figure 5: Representative flow cytometry analysis of liver immune infiltrates.** A) Quantification of 4-1BB expression on liver myeloid populations within  $\beta 2M^{-/-}$  mice or B) MHC-II $^{-/-}$  mice using flow cytometry analysis on myeloid cells from perfused livers. C) Depletion of Treg cells in FoxP3 $^{-}$  DTR mice 13 days after administration of Diphtheria toxin (10 $\mu$ g/kg body weight) FACS plots are representative of one mouse bled at day 13, prior to sacrifice. D) Quantification of CD8 T cell (left) or Treg (right) infiltrates within perfused livers of  $\alpha 4$ -1BB treated mice was measured by flow cytometry. Infiltrates were calculated as the total number of cells per liver mass. Bars represent mean  $\pm$  SD. Statistical significance was calculated using a two-sided Student's T test applying Welch's correction for unequal variance. ns, not significant; \*P < 0.05, \*\*P < 0.01, \*\*\*P < 0.001, \*\*\*\*P < 0.0001.

## Chapter 4: General Discussion

### General Discussion and Future Directions

Tumor immunotherapy has shown very promising clinical benefit against an array of cancers, however, two major challenges remain unresolved in the field. First, many patients do not respond to therapy at all or relapse after a period of remission, and a number of cancers remain almost entirely refractory to current immunotherapies. Second, there are several immune-related adverse effects associated with immune-modulating therapeutic antibodies. Research in the field of tumor immunotherapy focuses on improving the efficacy of therapies to expand clinical benefit across different tumor types while eliminating unwanted side effects.

The first part of this work focuses on understanding the molecular mechanisms of acquired resistance to a triple ( $\alpha$ CTLA-4,  $\alpha$ PD-1 and  $\alpha$ PD-L1) combination of checkpoint immunotherapy. Multiple efforts are underway in the field to understand the biology of tumor immune evasion in the context of immunotherapy. Most of these studies are being conducted on human patient samples, which though clinically relevant, limits the ability to utilize genetic modification to ask specific biological questions or validate preliminary findings. In current preclinical models, it is difficult to distinguish between mice who fail to respond due to resistance from mice who fail therapy for purely stochastic reasons. Moreover, tumors contain a complex mix of both tumor cells and TME (non-tumor cells) constituting pro- and anti-tumor immunity. In current preclinical tumor models and clinical studies, it is very hard to study effects of therapeutic agents on tumor cells in isolation from their TME. Studying them separately could be very useful for understanding and disrupting the synergy between tumor cells and their tumor-supportive tumor microenvironment. We developed a novel mouse

melanoma model to address these issues. We have evolved a triple checkpoint therapy-resistant B16 melanoma through serial *in vivo* passage. These tumor cells adapted to the presence of immunotherapy over multiple passages, thereby enriching a specific genetic signature important for evasion of immunotherapeutic pressure. This reduced the signal to noise ratio, enabling the separation of immunotherapy responders and non-responders easily. Tumor cells expressed td-tomato fluorescent protein which could be used to FACS sort the tumor cells from their microenvironment.

We investigated tumor cells and TME separately and showed the metabolic and immunologic interactions between the two. In our future studies, we aim to further divide the TME into two components CD45 positive immune cells and CD45 negative non-hematopoietic cells in order to highlight the differential effects that therapy resistant tumors have on these two cell populations. CD45 positive cells in the TME can include anti-tumor CD4/CD8 effector T cells and dendritic cells, and studying them separately will help us explore the resistance mechanisms in different tumor types.

Resistant tumors have upregulated glycolysis and oxidative phosphorylation to achieve hyper-metabolic states. We believe that hyper-metabolic tumor cells deplete essential nutrients from the tumor microenvironment, thereby starving CD8 T cells. Hence, CD8 T cells lose their metabolic fitness (metabolic insufficiency) to perform effector functions. Surprisingly, MDSC and Treg are able to thrive in this unfavorable tumor microenvironment and become more immune-suppressive. It would be interesting to delineate the mechanisms

underlying the ability of MDSCs and Tregs to survive and function in this nutrient-depleted TME.

We imaged the metabolic profile of resistant tumors using a hyperpolarized pyruvate and non-invasive MRI technique, and separated resistant tumors from parental based on their metabolic signatures. The hyperpolarized pyruvate and MRI imaging technique is already in clinical trials for other indications and could be potentially applied in an immuno-oncology setting to predict responses to immunotherapy. These findings need to be further validated in a slow-growing tumor model, which is partially sensitive to immunotherapy. In slow growing tumor models, a metabolic signature could be imaged before and during therapy to predict the likelihood of response. This will help us confirm if the imaging technique can be used to predict responsiveness in clinic.

The second part of this work focuses on characterizing mechanisms of immune-related hepatotoxicity associated with 4-1BB agonist antibodies. Despite the unprecedented success of 4-1BB (CD137) agonist antibodies in preclinical studies as mono- and combination therapies, clinical development of 4-1BB agonist antibodies has been hampered by dose-limiting liver toxicity. We describe a pathway by which 4-1BB activation on liver myeloid cells initiates inflammatory cytokine production, particularly interleukin-27, and progressed towards activation of hepatotoxic CD8 T cells.

Bone marrow-derived monocytes, involved in routine immune surveillance in liver tissue, express 4-1BB on their surface at a basal level. In response to 4-1BB co-stimulation, they release inflammatory cytokines which further upregulate 4-1BB expression on resident Kupffer cells. In response to 4-1BB mediated



activation, bone marrow derived monocytes and resident Kupffer cells release interleukin-27 (IL-27), which initiates a cascade of inflammatory cytokine production. In the clinic, IRAE associated with immunomodulatory antibodies are readily managed with steroid intervention. While checkpoint blockade antibody-induced IRAE mediated by T cells can be managed with steroid interventions, 4-1BB agonist antibody-induced liver inflammation initiated by myeloid cells is difficult to control with steroids. We also demonstrated that IL-27 is a critical regulator of  $\alpha$ 4-1BB induced liver toxicity. Remarkably, genetic abrogation of IL-27 (EBI3<sup>-/-</sup>) or its receptor (IL27R $\alpha$ <sup>-/-</sup>) completely abolished the capacity for 4-1BB agonists to mediate hepatic pathology as demonstrated by reduced levels of serum AST and ALT, as well as significant reductions in T cell infiltrates in the liver. Even though IL-27 could be a potential therapeutic target to explore for controlling 4-1BB induced liver inflammation, it needs to be further characterized. Its immunoregulatory role in individual tumor types has to be elucidated since IL-27 has both pro- and anti-inflammatory functions (242).

We have confirmed the findings from earlier studies that CTLA-4 blockade reduces 4-1BB induced liver pathology (94,209). In our previous preclinical studies we have shown that combining 4-1BB agonist antibodies with CTLA-4 blockade antibodies provides synergistic survival benefit in the B16 melanoma model. Given that this combination also shows therapeutic synergy and the capacity to limit IRAE associated with  $\alpha$ CTLA-4 treatment (94,209), it would be interesting to investigate its efficacy in the clinic. In future studies, we will delineate the cellular and molecular pathways of  $\alpha$ CTLA-4 mediated reduction in liver pathology, which could serve as potential therapeutic targets.

About 75% of the blood supply in the liver comes from the portal vein (venous blood from the intestine) and is continuously exposed to food and microbial antigens from the intestine (243-245). Processing of food by the liver could produce substantial foreign antigen exposure (245,246). To prevent immune system over-activation, the liver maintains a local immune tolerant microenvironment and serves as a barrier to environmental antigens (245,246). The local and systemic tolerance to self and foreign antigens in the liver is maintained by non-parenchymal liver cells such dendritic cells (DCs), Kupffer cells (KCs), Treg, and hepatic stellate cells (HSCs) (245,246). We believe that 4-1BB agonist antibodies break this immune tolerance by activating Kupffer cells. Potentially, this could be due to the ability of 4-1BB co-stimulation to enhance antigen presentation, suggested by increased in MHC-II expression on Kupffer cells and presentation of foreign antigens to T cells. We have demonstrated that 4-1BB antibody treatment increases infiltration of CD8 T cells into the liver, where they act as primary effectors of hepatic damage. Using  $\beta 2M^{-/-}$  mice we have shown that both CD8 T cells and MHC-I antigen presentation in the liver are required for 4-1BB induced hepatotoxicity. This also suggests that the key to potent anti-tumor effects related to 4-1BB agonist antibodies lies in the ability of strong 4-1BB co-stimulation to break self-tolerance. We showed that Foxp3+ regulatory T cells, which also play a key role in maintaining liver immune tolerance (247), tried to suppress  $\alpha 4-1BB$  induced liver inflammation as a compensatory mechanism, and  $\alpha CTLA-4$  mediated amelioration of liver inflammation is due increase of Treg cells in liver parenchyma. Further work needs to be done to delineate the mechanism of  $\alpha CTLA-4$  driven increased in Treg infiltration into the liver parenchyma.

To divert therapy-induced immune responses towards tumors without causing hepatic immune inflammation, we used a chemokine modulation approach. Using knockout mice lacking individual chemokine receptors, we went on to show that T cell chemotaxis into the liver could be uncoupled from T cell trafficking into the tumor, thus maintaining anti-tumor responses generated by  $\alpha$ 4-1BB while limiting infiltration of hepatotoxic T cells into the liver. Particularly, the chemokine receptors CCR2 and CXCR3 appear to be important for T cell and/or monocyte trafficking into the liver and subsequent promotion of hepatic damage, without impacting anti-tumor responses. The impact of CCR2 knockout in abrogating liver toxicity remains enticing, as small molecule inhibitors targeting CCR2 are currently being considered as immunotherapeutic agents to inhibit the recruitment of monocytes into the tumor microenvironment. CCR2 inhibitors when combined with 4-1BB agonist antibodies may prove to be a potent combination in promoting tumor regression while inhibiting off-target liver toxicity.

In conclusion, our data demonstrate that tumors can upregulate glycolysis, oxidoreductase, and mitochondrial mediated oxidative phosphorylation to evade the response to anti-CTLA-4, anti-PD-1 and anti-PD-L1 immunotherapies. 4-1BB agonist antibodies trigger hepatitis via activation and expansion of interleukin-27-producing liver Kupffer cells and monocytes. Co-administration of CTLA-4 and/or CCR2 blockade may minimize hepatitis, while yielding equal or greater antitumor immunity.

## References:

1. Harshman, L. C., Drake, C. G., Wargo, J. A., Sharma, P., and Bhardwaj, N. (2014) Cancer immunotherapy highlights from the 2014 ASCO Meeting. *Cancer Immunol Res* **2**, 714-719
2. Burnet, F. M. (1971) Immunological Surveillance in Neoplasia. *Immunological Reviews* **7**, 3-25
3. Dunn, G. P., Bruce, A. T., Ikeda, H., Old, L. J., and Schreiber, R. D. (2002) Cancer immunoediting: from immunosurveillance to tumor escape. *Nature immunology* **3**, 991-998
4. Matsushita, H., Vesely, M. D., Koboldt, D. C., Rickert, C. G., Uppaluri, R., Magrini, V. J., Arthur, C. D., White, J. M., Chen, Y.-S., Shea, L. K., Hundal, J., Wendl, M. C., Demeter, R., Wylie, T., Allison, J. P., Smyth, M. J., Old, L. J., Mardis, E. R., and Schreiber, R. D. (2012) Cancer exome analysis reveals a T-cell-dependent mechanism of cancer immunoediting. *Nature* **482**, 400-404
5. Schreiber, R. D., Old, L. J., and Smyth, M. J. (2011) Cancer Immunoediting: Integrating Immunity's Roles in Cancer Suppression and Promotion. *Science* **331**, 1565-1570
6. Wolchok, J. D., and Saenger, Y. (2008) The Mechanism of Anti-CTLA-4 Activity and the Negative Regulation of T-Cell Activation. *The Oncologist* **13**, 2-9

7. Krummel, M. F., and Allison, J. P. (1995) CD28 and CTLA-4 have opposing effects on the response of T cells to stimulation. *The Journal of Experimental Medicine* **182**, 459-465
8. Larkin, J., Chiarion-Sileni, V., Gonzalez, R., Grob, J. J., Cowey, C. L., Lao, C. D., Schadendorf, D., Dummer, R., Smylie, M., Rutkowski, P., Ferrucci, P. F., Hill, A., Wagstaff, J., Carlino, M. S., Haanen, J. B., Maio, M., Marquez-Rodas, I., McArthur, G. A., Ascierto, P. A., Long, G. V., Callahan, M. K., Postow, M. A., Grossmann, K., Sznol, M., Dreno, B., Bastholt, L., Yang, A., Rollin, L. M., Horak, C., Hodi, F. S., and Wolchok, J. D. (2015) Combined Nivolumab and Ipilimumab or Monotherapy in Untreated Melanoma. *New England Journal of Medicine* **373**, 23-34
9. Wolchok, J. D., Chiarion-Sileni, V., Gonzalez, R., Rutkowski, P., Grob, J.-J., Cowey, C. L., Lao, C. D., Wagstaff, J., Schadendorf, D., Ferrucci, P. F., Smylie, M., Dummer, R., Hill, A., Hogg, D., Haanen, J., Carlino, M. S., Bechter, O., Maio, M., Marquez-Rodas, I., Guidoboni, M., McArthur, G., Lebbé, C., Ascierto, P. A., Long, G. V., Cebon, J., Sosman, J., Postow, M. A., Callahan, M. K., Walker, D., Rollin, L., Bhore, R., Hodi, F. S., and Larkin, J. (2017) Overall Survival with Combined Nivolumab and Ipilimumab in Advanced Melanoma. *New England Journal of Medicine* **377**, 1345-1356
10. Wolchok, J. D., Neyns, B., Linette, G., Negrier, S., Lutzky, J., Thomas, L., Waterfield, W., Schadendorf, D., Smylie, M., Guthrie Jr, T., Grob, J.-J., Chesney, J., Chin, K., Chen, K., Hoos, A., O'Day, S. J., and Lebbé, C. (2010) Ipilimumab monotherapy in patients with pretreated advanced

- melanoma: a randomised, double-blind, multicentre, phase 2, dose-ranging study. *The Lancet Oncology* **11**, 155-164
11. LaFleur, M. W., Muroyama, Y., Drake, C. G., and Sharpe, A. H. (2018) Inhibitors of the PD-1 Pathway in Tumor Therapy. *The Journal of Immunology* **200**, 375-383
  12. Chemnitz, J. M., Parry, R. V., Nichols, K. E., June, C. H., and Riley, J. L. (2004) SHP-1 and SHP-2 Associate with Immunoreceptor Tyrosine-Based Switch Motif of Programmed Death 1 upon Primary Human T Cell Stimulation, but Only Receptor Ligation Prevents T Cell Activation. *The Journal of Immunology* **173**, 945-954
  13. Ribas, A., Hamid, O., Daud, A., and et al. (2016) Association of pembrolizumab with tumor response and survival among patients with advanced melanoma. *JAMA* **315**, 1600-1609
  14. Reck, M., Rodríguez-Abreu, D., Robinson, A. G., Hui, R., Csőszi, T., Fülöp, A., Gottfried, M., Peled, N., Tafreshi, A., Cuffe, S., O'Brien, M., Rao, S., Hotta, K., Leiby, M. A., Lubiniecki, G. M., Shentu, Y., Rangwala, R., and Brahmer, J. R. (2016) Pembrolizumab versus Chemotherapy for PD-L1–Positive Non–Small-Cell Lung Cancer. *New England Journal of Medicine* **375**, 1823-1833
  15. Borghaei, H., Paz-Ares, L., Horn, L., Spigel, D. R., Steins, M., Ready, N. E., Chow, L. Q., Vokes, E. E., Felip, E., Holgado, E., Barlesi, F., Kohlhäufel, M., Arrieta, O., Burgio, M. A., Fayette, J., Lena, H., Poddubskaya, E., Gerber, D. E., Gettinger, S. N., Rudin, C. M., Rizvi, N., Crinò, L., Blumenschein, G. R. J., Antonia, S. J., Dorange, C., Harbison, C. T., Graf

- Finckenstein, F., and Brahmer, J. R. (2015) Nivolumab versus Docetaxel in Advanced Nonsquamous Non–Small-Cell Lung Cancer. *New England Journal of Medicine* **373**, 1627-1639
16. Garon, E. B., Rizvi, N. A., Hui, R., Leighl, N., Balmanoukian, A. S., Eder, J. P., Patnaik, A., Aggarwal, C., Gubens, M., Horn, L., Carcereny, E., Ahn, M.-J., Felip, E., Lee, J.-S., Hellmann, M. D., Hamid, O., Goldman, J. W., Soria, J.-C., Dolled-Filhart, M., Rutledge, R. Z., Zhang, J., Luceford, J. K., Rangwala, R., Lubiniecki, G. M., Roach, C., Emancipator, K., and Gandhi, L. (2015) Pembrolizumab for the Treatment of Non–Small-Cell Lung Cancer. *New England Journal of Medicine* **372**, 2018-2028
17. Motzer, R. J., Escudier, B., McDermott, D. F., George, S., Hammers, H. J., Srinivas, S., Tykodi, S. S., Sosman, J. A., Procopio, G., Plimack, E. R., Castellano, D., Choueiri, T. K., Gurney, H., Donskov, F., Bono, P., Wagstaff, J., Gaurer, T. C., Ueda, T., Tomita, Y., Schutz, F. A., Kollmannsberger, C., Larkin, J., Ravaud, A., Simon, J. S., Xu, L.-A., Waxman, I. M., and Sharma, P. (2015) Nivolumab versus Everolimus in Advanced Renal-Cell Carcinoma. *New England Journal of Medicine* **373**, 1803-1813
18. Ansell, S. M., Lesokhin, A. M., Borrello, I., Halwani, A., Scott, E. C., Gutierrez, M., Schuster, S. J., Millenson, M. M., Cattrly, D., Freeman, G. J., Rodig, S. J., Chapuy, B., Ligon, A. H., Zhu, L., Grosso, J. F., Kim, S. Y., Timmerman, J. M., Shipp, M. A., and Armand, P. (2015) PD-1 Blockade with Nivolumab in Relapsed or Refractory Hodgkin's Lymphoma. *New England Journal of Medicine* **372**, 311-319

19. Doni, E., Carli, G., Di Rocco, A., Sassone, M., Gandolfi, S., Patti, C., Falisi, E., Salemi, C., and Visco, C. (2017) Autoimmune haemolytic anaemia in mantle cell lymphoma : an insidious complication associated with leukemic disease. *Hematological Oncology* **35**, 135-137
20. Sharma, P., Callahan, M. K., Bono, P., Kim, J., Spiliopoulou, P., Calvo, E., Pillai, R. N., Ott, P. A., de Braud, F., Morse, M., Le, D. T., Jaeger, D., Chan, E., Harbison, C., Lin, C.-S., Tschaike, M., Azrilevich, A., and Rosenberg, J. E. (2016) Nivolumab monotherapy in recurrent metastatic urothelial carcinoma (CheckMate 032): a multicentre, open-label, two-stage, multi-arm, phase 1/2 trial. *The Lancet Oncology* **17**, 1590-1598
21. Bauml, J., Seiwert, T. Y., Pfister, D. G., Worden, F., Liu, S. V., Gilbert, J., Saba, N. F., Weiss, J., Wirth, L., Sukari, A., Kang, H., Gibson, M. K., Massarelli, E., Powell, S., Meister, A., Shu, X., Cheng, J. D., and Haddad, R. (2017) Pembrolizumab for Platinum- and Cetuximab-Refractory Head and Neck Cancer: Results From a Single-Arm, Phase II Study. *Journal of Clinical Oncology* **35**, 1542-1549
22. Kaufman, H. L., Russell, J., Hamid, O., Bhatia, S., Terheyden, P., D'Angelo, S. P., Shih, K. C., Lebbé, C., Linette, G. P., Milella, M., Brownell, I., Lewis, K. D., Lorch, J. H., Chin, K., Mahnke, L., von Heydebreck, A., Cuillerot, J.-M., and Nghiem, P. (2016) Avelumab in patients with chemotherapy-refractory metastatic Merkel cell carcinoma: a multicentre, single-group, open-label, phase 2 trial. *The Lancet Oncology* **17**, 1374-1385



23. Antonia, S. J., Vansteenkiste, J. F., and Moon, E. (2016) Immunotherapy: Beyond Anti-PD-1 and Anti-PD-L1 Therapies. *Am Soc Clin Oncol Educ Book* **35**, e450-458
24. Chen, L., and Flies, D. B. (2013) Molecular mechanisms of T cell co-stimulation and co-inhibition. *Nature Reviews Immunology* **13**, 227
25. Bartkowiak, T., Jaiswal, A. R., Ager, C. R., Chin, R., Chen, C.-H., Budhani, P., Ai, M., Reilley, M. J., Sebastian, M. M., Hong, D. S., and Curran, M. A. (2018) Activation of 4-1BB on liver myeloid cells triggers hepatitis via an interleukin-27 dependent pathway. *Clinical Cancer Research*
26. Bartkowiak, T., Singh, S., Yang, G., Galvan, G., Haria, D., Ai, M., Allison, J. P., Sastry, K. J., and Curran, M. A. (2015) Unique potential of 4-1BB agonist antibody to promote durable regression of HPV+ tumors when combined with an E6/E7 peptide vaccine. *Proceedings of the National Academy of Sciences* **112**, E5290-E5299
27. Sharpe , A. H., and Abbas , A. K. (2006) T-Cell Costimulation — Biology, Therapeutic Potential, and Challenges. *New England Journal of Medicine* **355**, 973-975
28. Postow, M. A., Sidlow, R., and Hellmann, M. D. (2018) Immune-Related Adverse Events Associated with Immune Checkpoint Blockade. *New England Journal of Medicine* **378**, 158-168
29. Comber, J. D., and Philip, R. (2014) MHC class I antigen presentation and implications for developing a new generation of therapeutic vaccines. *Ther Adv Vaccines* **2**, 77-89

30. Sade-Feldman, M., Jiao, Y. J., Chen, J. H., Rooney, M. S., Barzily-Rokni, M., Eliane, J.-P., Bjorgaard, S. L., Hammond, M. R., Vitzthum, H., Blackmon, S. M., Frederick, D. T., Hazar-Rethinam, M., Nadres, B. A., Van Seventer, E. E., Shukla, S. A., Yizhak, K., Ray, J. P., Rosebrock, D., Livitz, D., Adalsteinsson, V., Getz, G., Duncan, L. M., Li, B., Corcoran, R. B., Lawrence, D. P., Stemmer-Rachamimov, A., Boland, G. M., Landau, D. A., Flaherty, K. T., Sullivan, R. J., and Hacohen, N. (2017) Resistance to checkpoint blockade therapy through inactivation of antigen presentation. *Nature Communications* **8**, 1136
31. Giannakis, M., Mu, Xinmeng J., Shukla, Sachet A., Qian, Zhi R., Cohen, O., Nishihara, R., Bahl, S., Cao, Y., Amin-Mansour, A., Yamauchi, M., Sukawa, Y., Stewart, C., Rosenberg, M., Mima, K., Inamura, K., Noshio, K., Nowak, Jonathan A., Lawrence, Michael S., Giovannucci, Edward L., Chan, Andrew T., Ng, K., Meyerhardt, Jeffrey A., Van Allen, Eliezer M., Getz, G., Gabriel, Stacey B., Lander, Eric S., Wu, Catherine J., Fuchs, Charles S., Ogino, S., and Garraway, Levi A. (2016) Genomic Correlates of Immune-Cell Infiltrates in Colorectal Carcinoma. *Cell Reports* **15**, 857-865
32. Schumacher, T. N., and Schreiber, R. D. (2015) Neoantigens in cancer immunotherapy. *Science* **348**, 69-74
33. Rizvi, N. A., Hellmann, M. D., Snyder, A., Kvistborg, P., Makarov, V., Havel, J. J., Lee, W., Yuan, J., Wong, P., Ho, T. S., Miller, M. L., Rekhtman, N., Moreira, A. L., Ibrahim, F., Bruggeman, C., Gasmir, B., Zappasodi, R., Maeda, Y., Sander, C., Garon, E. B., Merghoub, T.,

- Wolchok, J. D., Schumacher, T. N., and Chan, T. A. (2015) Mutational landscape determines sensitivity to PD-1 blockade in non-small cell lung cancer. *Science* **348**, 124-128
34. Chabanon, R. M., Pedrero, M., Lefebvre, C., Marabelle, A., Soria, J.-C., and Postel-Vinay, S. (2016) Mutational Landscape and Sensitivity to Immune Checkpoint Blockers. *Clinical Cancer Research* **22**, 4309-4321
35. Ock, C.-Y., Hwang, J.-E., Keam, B., Kim, S.-B., Shim, J.-J., Jang, H.-J., Park, S., Sohn, B. H., Cha, M., Ajani, J. A., Kopetz, S., Lee, K.-W., Kim, T. M., Heo, D. S., and Lee, J.-S. (2017) Genomic landscape associated with potential response to anti-CTLA-4 treatment in cancers. *Nature Communications* **8**, 1050
36. Robbins, P. F., Lu, Y.-C., El-Gamil, M., Li, Y. F., Gross, C., Gartner, J., Lin, J. C., Teer, J. K., Cliften, P., Tycksen, E., Samuels, Y., and Rosenberg, S. A. (2013) Mining exomic sequencing data to identify mutated antigens recognized by adoptively transferred tumor-reactive T cells. *Nature Medicine* **19**, 747
37. McGranahan, N., Furness, A. J. S., Rosenthal, R., Ramskov, S., Lyngaa, R., Saini, S. K., Jamal-Hanjani, M., Wilson, G. A., Birkbak, N. J., Hiley, C. T., Watkins, T. B. K., Shafi, S., Murugaesu, N., Mitter, R., Akarca, A. U., Linares, J., Marafioti, T., Henry, J. Y., Van Allen, E. M., Miao, D., Schilling, B., Schadendorf, D., Garraway, L. A., Makarov, V., Rizvi, N. A., Snyder, A., Hellmann, M. D., Merghoub, T., Wolchok, J. D., Shukla, S. A., Wu, C. J., Peggs, K. S., Chan, T. A., Hadrup, S. R., Quezada, S. A., and

- Swanton, C. (2016) Clonal neoantigens elicit T cell immunoreactivity and sensitivity to immune checkpoint blockade. *Science* **351**, 1463-1469
38. Spranger, S., Luke, J. J., Bao, R., Zha, Y., Hernandez, K. M., Li, Y., Gajewski, A. P., Andrade, J., and Gajewski, T. F. (2016) Density of immunogenic antigens does not explain the presence or absence of the T-cell-inflamed tumor microenvironment in melanoma. *Proceedings of the National Academy of Sciences* **113**, E7759-E7768
39. Winograd, R., Byrne, K. T., Evans, R. A., Odorizzi, P. M., Meyer, A. R. L., Bajor, D. L., Clendenin, C., Stanger, B. Z., Furth, E. E., Wherry, E. J., and Vonderheide, R. H. (2015) Induction of T-cell Immunity Overcomes Complete Resistance to PD-1 and CTLA-4 Blockade and Improves Survival in Pancreatic Carcinoma. *Cancer Immunology Research* **3**, 399-411
40. Liu, C., Peng, W., Xu, C., Lou, Y., Zhang, M., Wargo, J. A., Chen, J. Q., Li, H. S., Watowich, S. S., Yang, Y., Tompers Frederick, D., Cooper, Z. A., Mbofung, R. M., Whittington, M., Flaherty, K. T., Woodman, S. E., Davies, M. A., Radvanyi, L. G., Overwijk, W. W., Lizee, G., and Hwu, P. (2013) BRAF inhibition increases tumor infiltration by T cells and enhances the antitumor activity of adoptive immunotherapy in mice. *Clin Cancer Res* **19**, 393-403
41. Peng, W., Chen, J. Q., Liu, C., Malu, S., Creasy, C., Tetzlaff, M. T., Xu, C., McKenzie, J. A., Zhang, C., Liang, X., Williams, L. J., Deng, W., Chen, G., Mbofung, R., Lazar, A. J., Torres-Cabala, C. A., Cooper, Z. A., Chen, P.-L., Tieu, T. N., Spranger, S., Yu, X., Bernatchez, C., Forget, M.-A.,

- Haymaker, C., Amaria, R., McQuade, J. L., Glitza, I. C., Cascone, T., Li, H. S., Kwong, L. N., Heffernan, T. P., Hu, J., Bassett, R. L., Bosenberg, M. W., Woodman, S. E., Overwijk, W. W., Lizée, G., Roszik, J., Gajewski, T. F., Wargo, J. A., Gershenwald, J. E., Radvanyi, L., Davies, M. A., and Hwu, P. (2016) Loss of PTEN Promotes Resistance to T Cell–Mediated Immunotherapy. *Cancer Discovery* **6**, 202-216
42. Spranger, S., Bao, R., and Gajewski, T. F. (2015) Melanoma-intrinsic  $\beta$ -catenin signalling prevents anti-tumour immunity. *Nature* **523**, 231
43. Keir, M. E., Butte, M. J., Freeman, G. J., and Sharpe, A. H. (2008) PD-1 and Its Ligands in Tolerance and Immunity. *Annual Review of Immunology* **26**, 677-704
44. Liakou, C. I., Kamat, A., Tang, D. N., Chen, H., Sun, J., Troncoso, P., Logothetis, C., and Sharma, P. (2008) CTLA-4 blockade increases IFN $\gamma$ -producing CD4+ICOS $^+$  cells to shift the ratio of effector to regulatory T cells in cancer patients. *Proceedings of the National Academy of Sciences* **105**, 14987-14992
45. Benci, J. L., Xu, B., Qiu, Y., Wu, T. J., Dada, H., Twyman-Saint Victor, C., Cucolo, L., Lee, D. S. M., Pauken, K. E., Huang, A. C., Gangadhar, T. C., Amaravadi, R. K., Schuchter, L. M., Feldman, M. D., Ishwaran, H., Vonderheide, R. H., Maity, A., Wherry, E. J., and Minn, A. J. Tumor Interferon Signaling Regulates a Multigenic Resistance Program to Immune Checkpoint Blockade. *Cell* **167**, 1540-1554.e1512
46. Gao, J., Shi, L. Z., Zhao, H., Chen, J., Xiong, L., He, Q., Chen, T., Roszik, J., Bernatchez, C., Woodman, S. E., Chen, P.-L., Hwu, P., Allison, J. P.,

- Futreal, A., Wargo, J. A., and Sharma, P. (2016) Loss of IFN- $\gamma$  Pathway Genes in Tumor Cells as a Mechanism of Resistance to Anti-CTLA-4 Therapy. *Cell* **167**, 397-404.e399
47. Curran, M. A., Montalvo, W., Yagita, H., and Allison, J. P. (2010) PD-1 and CTLA-4 combination blockade expands infiltrating T cells and reduces regulatory T and myeloid cells within B16 melanoma tumors. *Proceedings of the National Academy of Sciences* **107**, 4275-4280
48. Sucker, A., Zhao, F., Pieper, N., Heeke, C., Maltaner, R., Stadler, N., Real, B., Bielefeld, N., Howe, S., Weide, B., Gutzmer, R., Utikal, J., Loquai, C., Gogas, H., Klein-Hitpass, L., Zeschnigk, M., Westendorf, A. M., Trilling, M., Horn, S., Schilling, B., Schadendorf, D., Griewank, K. G., and Paschen, A. (2017) Acquired IFN $\gamma$  resistance impairs anti-tumor immunity and gives rise to T-cell-resistant melanoma lesions. *Nature Communications* **8**, 15440
49. Zaretsky, J. M., Garcia-Diaz, A., Shin, D. S., Escuin-Ordinas, H., Hugo, W., Hu-Lieskovan, S., Torrejon, D. Y., Abril-Rodriguez, G., Sandoval, S., Barthly, L., Saco, J., Homet Moreno, B., Mezzadra, R., Chmielowski, B., Ruchalski, K., Shintaku, I. P., Sanchez, P. J., Puig-Saus, C., Cherry, G., Seja, E., Kong, X., Pang, J., Berent-Maoz, B., Comin-Anduix, B., Graeber, T. G., Tume, P. C., Schumacher, T. N. M., Lo, R. S., and Ribas, A. (2016) Mutations Associated with Acquired Resistance to PD-1 Blockade in Melanoma. *New England Journal of Medicine* **375**, 819-829

50. Chouaib, S., Noman, M. Z., Kosmatopoulos, K., and Curran, M. A. (2016) Hypoxic stress: obstacles and opportunities for innovative immunotherapy of cancer. *Oncogene* **36**, 439
51. Lardner, A. (2001) The effects of extracellular pH on immune function. *J Leukoc Biol* **69**, 522-530
52. Nakagawa, Y., Negishi, Y., Shimizu, M., Takahashi, M., Ichikawa, M., and Takahashi, H. (2015) Effects of extracellular pH and hypoxia on the function and development of antigen-specific cytotoxic T lymphocytes. *Immunology Letters* **167**, 72-86
53. Redegeld, F., Filippini, A., and Sitkovsky, M. (1991) Comparative studies of the cytotoxic T lymphocyte-mediated cytotoxicity and of extracellular ATP-induced cell lysis. Different requirements in extracellular Mg<sup>2+</sup> and pH. *The Journal of Immunology* **147**, 3638-3645
54. Fischer, K., Hoffmann, P., Voelkl, S., Meidenbauer, N., Ammer, J., Edinger, M., Gottfried, E., Schwarz, S., Rothe, G., Hoves, S., Renner, K., Timischl, B., Mackensen, A., Kunz-Schughart, L., Andreesen, R., Krause, S. W., and Kreutz, M. (2007) Inhibitory effect of tumor cell-derived lactic acid on human T cells. *Blood* **109**, 3812-3819
55. Dang, Eric V., Barbi, J., Yang, H.-Y., Jinasena, D., Yu, H., Zheng, Y., Bordman, Z., Fu, J., Kim, Y., Yen, H.-R., Luo, W., Zeller, K., Shimoda, L., Topalian, Suzanne L., Semenza, Gregg L., Dang, Chi V., Pardoll, Drew M., and Pan, F. (2011) Control of TH17/Treg Balance by Hypoxia-Inducible Factor 1. *Cell* **146**, 772-784

56. Ai, M., Bartkowiak, T., Jaiswal, A. R., Shah, K., Ager, C., Lerman, B., and Curran, M. A. (2014) Abstract 629: Combination hypoxia-specific chemotherapy and immunotherapy of prostate cancer. *Cancer Research* **74**, 629-629
57. Scharping, N. E., Menk, A. V., Whetstone, R. D., Zeng, X., and Delgoffe, G. M. (2016) Efficacy of PD-1 blockade is potentiated by metformin-induced reduction of tumor hypoxia. *Cancer Immunology Research*
58. Angelin, A., Gil-de-Gómez, L., Dahiya, S., Jiao, J., Guo, L., Levine, M. H., Wang, Z., Quinn, W. J., Kopinski, P. K., Wang, L., Akimova, T., Liu, Y., Bhatti, T. R., Han, R., Laskin, B. L., Baur, J. A., Blair, I. A., Wallace, D. C., Hancock, W. W., and Beier, U. H. (2017) Foxp3 Reprograms T Cell Metabolism to Function in Low-Glucose, High-Lactate Environments. *Cell Metabolism* **25**, 1282-1293.e1287
59. Legat, A., Speiser, D., Pircher, H., Zehn, D., and Furtak, S. (2013) Inhibitory Receptor Expression Depends More Dominantly on Differentiation and Activation than “Exhaustion” of Human CD8 T Cells. *Frontiers in Immunology* **4**
60. Odorizzi, P. M., Pauken, K. E., Paley, M. A., Sharpe, A., and Wherry, E. J. (2015) Genetic absence of PD-1 promotes accumulation of terminally differentiated exhausted CD8<sup>+</sup> T cells. *The Journal of Experimental Medicine* **212**, 1125-1137
61. Chang, C.-H., Curtis, Jonathan D., Maggi, Leonard B., Faubert, B., Villarino, Alejandro V., O’Sullivan, D., Huang, Stanley C.-C., van der Windt, Gerritje J. W., Blagih, J., Qiu, J., Weber, Jason D., Pearce,



- Edward J., Jones, Russell G., and Pearce, Erika L. (2013)  
 Posttranscriptional Control of T Cell Effector Function by Aerobic  
 Glycolysis. *Cell* **153**, 1239-1251
62. Ho, P.-C., Bihuniak, Jessica D., Macintyre, Andrew N., Staron, M., Liu, X.,  
 Amezcua, R., Tsui, Y.-C., Cui, G., Micevic, G., Perales, Jose C.,  
 Kleinstein, Steven H., Abel, E. D., Insogna, Karl L., Feske, S., Locasale,  
 Jason W., Bosenberg, Marcus W., Rathmell, Jeffrey C., and Kaech,  
 Susan M. (2015) Phosphoenolpyruvate Is a Metabolic Checkpoint of Anti-  
 tumor T Cell Responses. *Cell* **162**, 1217-1228
63. Buck, M. D., O'Sullivan, D., and Pearce, E. L. (2015) T cell metabolism  
 drives immunity. *The Journal of Experimental Medicine* **212**, 1345-1360
64. Wherry, E. J., and Kurachi, M. (2015) Molecular and cellular insights into T  
 cell exhaustion. *Nature Reviews Immunology* **15**, 486
65. O'Sullivan, D., van der Windt, Gerritje J. W., Huang, Stanley C.-C., Curtis,  
 Jonathan D., Chang, C.-H., Buck, Michael D., Qiu, J., Smith, Amber M.,  
 Lam, Wing Y., DiPlato, Lisa M., Hsu, F.-F., Birnbaum, Morris J., Pearce,  
 Edward J., and Pearce, Erika L. Memory CD8<sup>+</sup> T Cells Use  
 Cell-Intrinsic Lipolysis to Support the Metabolic Programming Necessary  
 for Development. *Immunity* **41**, 75-88
66. Scharping, Nicole E., Menk, Ashley V., Moreci, Rebecca S., Whetstone,  
 Ryan D., Dadey, Rebekah E., Watkins, Simon C., Ferris, Robert L., and  
 Delgoffe, Greg M. The Tumor Microenvironment Represses T Cell  
 Mitochondrial Biogenesis to Drive Intratumoral T Cell Metabolic  
 Insufficiency and Dysfunction. *Immunity* **45**, 701-703

67. Bengsch, B., Johnson, A. L., Kurachi, M., Odorizzi, P. M., Pauken, K. E., Attanasio, J., Stelekati, E., McLane, L. M., Paley, M. A., Delgoffe, G. M., and Wherry, E. J. Bioenergetic Insufficiencies Due to Metabolic Alterations Regulated by the Inhibitory Receptor PD-1 Are an Early Driver of CD8<sup>+</sup> T Cell Exhaustion. *Immunity* **45**, 358-373
68. Cheng, W.-C., and Ho, P.-C. (2016) Metabolic tug-of-war in tumors results in diminished T cell antitumor immunity. *OncolImmunology* **5**, e1119355
69. Yang, K., and Chi, H. AMPK Helps T Cells Survive Nutrient Starvation. *Immunity* **42**, 4-6
70. Faubert, B., Boily, G., Izreig, S., Griss, T., Samborska, B., Dong, Z., Dupuy, F., Chambers, C., Fuerth, Benjamin J., Viollet, B., Mamer, Orval A., Avizonis, D., DeBerardinis, Ralph J., Siegel, Peter M., and Jones, Russell G. AMPK Is a Negative Regulator of the Warburg Effect and Suppresses Tumor Growth In Vivo. *Cell Metabolism* **17**, 113-124
71. Delgoffe, G. M., Pollizzi, K. N., Waickman, A. T., Heikamp, E., Meyers, D. J., Horton, M. R., Xiao, B., Worley, P. F., and Powell, J. D. (2011) The kinase mTOR regulates the differentiation of helper T cells through the selective activation of signaling by mTORC1 and mTORC2. *Nature immunology* **12**, 295
72. Pollizzi, K. N., Patel, C. H., Sun, I.-H., Oh, M.-H., Waickman, A. T., Wen, J., Delgoffe, G. M., and Powell, J. D. (2015) mTORC1 and mTORC2 selectively regulate CD8<sup>+</sup> T cell differentiation. *The Journal of Clinical Investigation* **125**, 2090-2108

73. Pollizzi, K. N., Sun, I.-H., Patel, C. H., Lo, Y.-C., Oh, M.-H., Waickman, A. T., Tam, A. J., Blosser, R. L., Wen, J., Delgoffe, G. M., and Powell, J. D. (2016) Asymmetric inheritance of mTORC1 kinase activity during division dictates CD8+ T cell differentiation. *Nature immunology* **17**, 704
74. Watson, M., Whetstone, R., Deshpande, R., Menk, A., Scharping, N., Morrison, B., Gellhaus, S. W., and Delgoffe, G. (2017) Lactic acid as a mediator of metabolic symbiosis between regulatory T cells and the tumor microenvironment (32nd Annual Meeting and Pre-Conference Programs of the Society for Immunotherapy of Cancer (SITC 2017): Part One. Society for Immunotherapy of Cancer's Journal for Immunotherapy of Cancer
75. Platten, M., Wick, W., and Van den Eynde, B. J. (2012) Tryptophan Catabolism in Cancer: Beyond IDO and Tryptophan Depletion. *Cancer Research* **72**, 5435-5440
76. Holmgaard, R. B., Zamarin, D., Munn, D. H., Wolchok, J. D., and Allison, J. P. (2013) Indoleamine 2,3-dioxygenase is a critical resistance mechanism in antitumor T cell immunotherapy targeting CTLA-4. *The Journal of Experimental Medicine* **210**, 1389-1402
77. Spranger, S., Koblish, H. K., Horton, B., Scherle, P. A., Newton, R., and Gajewski, T. F. (2014) Mechanism of tumor rejection with doublets of CTLA-4, PD-1/PD-L1, or IDO blockade involves restored IL-2 production and proliferation of CD8+ T cells directly within the tumor microenvironment. *Journal for Immunotherapy of Cancer* **2**, 3

78. Timosenko, E., Hadjinicolaou, A. V., and Cerundolo, V. (2017) Modulation of cancer-specific immune responses by amino acid degrading enzymes. *Immunotherapy* **9**, 83-97
79. Mussai, F., De Santo, C., Abu-Dayyeh, I., Booth, S., Quek, L., McEwen-Smith, R. M., Qureshi, A., Dazzi, F., Vyas, P., and Cerundolo, V. (2013) Acute myeloid leukemia creates an arginase-dependent immunosuppressive microenvironment. *Blood* **122**, 749-758
80. Boursi, B., Mamtani, R., Haynes, K., and Yang, Y.-X. (2015) Recurrent antibiotic exposure may promote cancer formation – Another step in understanding the role of the human microbiota? *European Journal of Cancer* **51**, 2655-2664
81. Zitvogel, L., Ayyoub, M., Routy, B., and Kroemer, G. (2016) Microbiome and Anticancer Immunosurveillance. *Cell* **165**, 276-287
82. Cotillard, A., Kennedy, S. P., Kong, L. C., Prifti, E., Pons, N., Le Chatelier, E., Almeida, M., Quinquis, B., Levenez, F., Galleron, N., Gougis, S., Rizkalla, S., Batto, J.-M., Renault, P., consortium, A. N. R. M., Doré, J., Zucker, J.-D., Clément, K., Ehrlich, S. D., and members, A. N. R. M. c. (2013) Dietary intervention impact on gut microbial gene richness. *Nature* **500**, 585
83. Burrows, M. P., Volchkov, P., Kobayashi, K. S., and Chervonsky, A. V. (2015) Microbiota regulates type 1 diabetes through Toll-like receptors. *Proceedings of the National Academy of Sciences* **112**, 9973-9977
84. Dalal, S. R., and Chang, E. B. (2014) The microbial basis of inflammatory bowel diseases. *The Journal of Clinical Investigation* **124**, 4190-4196

85. Lee, Y. K., Menezes, J. S., Umesaki, Y., and Mazmanian, S. K. (2011) Proinflammatory T-cell responses to gut microbiota promote experimental autoimmune encephalomyelitis. *Proceedings of the National Academy of Sciences* **108**, 4615-4622
86. Kamada, N., Seo, S.-U., Chen, G. Y., and Núñez, G. (2013) Role of the gut microbiota in immunity and inflammatory disease. *Nature Reviews Immunology* **13**, 321
87. Louis, P., Hold, G. L., and Flint, H. J. (2014) The gut microbiota, bacterial metabolites and colorectal cancer. *Nature Reviews Microbiology* **12**, 661
88. Garrett, W. S. (2015) Cancer and the microbiota. *Science* **348**, 80-86
89. Dapito, Dianne H., Mencin, A., Gwak, G.-Y., Pradere, J.-P., Jang, M.-K., Mederacke, I., Caviglia, Jorge M., Khiabani, H., Adeyemi, A., Bataller, R., Lefkowitz, Jay H., Bower, M., Friedman, R., Sartor, R. B., Rabadan, R., and Schwabe, Robert F. (2012) Promotion of Hepatocellular Carcinoma by the Intestinal Microbiota and TLR4. *Cancer Cell* **21**, 504-516
90. Velicer, C. M., Heckbert, S. R., Lampe, J. W., Potter, J. D., Robertson, C. A., and Taplin, S. H. (2004) Antibiotic use in relation to the risk of breast cancer. *JAMA* **291**, 827-835
91. Gopalakrishnan, V., Spencer, C. N., Nezi, L., Reuben, A., Andrews, M. C., Karpinets, T. V., Prieto, P. A., Vicente, D., Hoffman, K., Wei, S. C., Cogdill, A. P., Zhao, L., Hudgens, C. W., Hutchinson, D. S., Manzo, T., Petaccia de Macedo, M., Cotechini, T., Kumar, T., Chen, W. S., Reddy, S. M., Szczepaniak Sloane, R., Galloway-Pena, J., Jiang, H., Chen, P. L.,

- Shpall, E. J., Rezvani, K., Alousi, A. M., Chemaly, R. F., Shelburne, S., Vence, L. M., Okhuysen, P. C., Jensen, V. B., Swennes, A. G., McAllister, F., Marcelo Riquelme Sanchez, E., Zhang, Y., Le Chatelier, E., Zitvogel, L., Pons, N., Austin-Breneman, J. L., Haydu, L. E., Burton, E. M., Gardner, J. M., Sirmans, E., Hu, J., Lazar, A. J., Tsujikawa, T., Diab, A., Tawbi, H., Glitza, I. C., Hwu, W. J., Patel, S. P., Woodman, S. E., Amaria, R. N., Davies, M. A., Gershenwald, J. E., Hwu, P., Lee, J. E., Zhang, J., Coussens, L. M., Cooper, Z. A., Futreal, P. A., Daniel, C. R., Ajami, N. J., Petrosino, J. F., Tetzlaff, M. T., Sharma, P., Allison, J. P., Jenq, R. R., and Wargo, J. A. (2018) Gut microbiome modulates response to anti-PD-1 immunotherapy in melanoma patients. *Science* **359**, 97-103
92. Jobin, C. (2018) Precision medicine using microbiota. *Science* **359**, 32-34
93. Matson, V., Fessler, J., Bao, R., Chongsuwat, T., Zha, Y., Alegre, M.-L., Luke, J. J., and Gajewski, T. F. (2018) The commensal microbiome is associated with anti-PD-1 efficacy in metastatic melanoma patients. *Science* **359**, 104-108
94. Curran, M. A., Kim, M., Montalvo, W., Al-Shamkhani, A., and Allison, J. P. (2011) Combination CTLA-4 Blockade and 4-1BB Activation Enhances Tumor Rejection by Increasing T-Cell Infiltration, Proliferation, and Cytokine Production. *PLoS ONE* **6**, e19499
95. Gao, J., Ward, J. F., Pettaway, C. A., Shi, L. Z., Subudhi, S. K., Vence, L. M., Zhao, H., Chen, J., Chen, H., Efstathiou, E., Troncso, P., Allison, J. P., Logothetis, C. J., Wistuba, II, Sepulveda, M. A., Sun, J., Wargo, J., Blando, J., and Sharma, P. (2017) VISTA is an inhibitory immune

- checkpoint that is increased after ipilimumab therapy in patients with prostate cancer. *Nat Med* **23**, 551-555
96. Wolchok , J. D., Kluger , H., Callahan , M. K., Postow , M. A., Rizvi , N. A., Lesokhin , A. M., Segal , N. H., Ariyan , C. E., Gordon , R.-A., Reed , K., Burke , M. M., Caldwell , A., Kronenberg , S. A., Agunwamba , B. U., Zhang , X., Lowy , I., Inzunza , H. D., Feely , W., Horak , C. E., Hong , Q., Korman , A. J., Wigginton , J. M., Gupta , A., and Sznol , M. (2013) Nivolumab plus Ipilimumab in Advanced Melanoma. *New England Journal of Medicine* **369**, 122-133
97. Koyama, S., Akbay, E. A., Li, Y. Y., Herter-Sprie, G. S., Buczkowski, K. A., Richards, W. G., Gandhi, L., Redig, A. J., Rodig, S. J., Asahina, H., Jones, R. E., Kulkarni, M. M., Kuraguchi, M., Palakurthi, S., Fecci, P. E., Johnson, B. E., Janne, P. A., Engelman, J. A., Gangadharan, S. P., Costa, D. B., Freeman, G. J., Bueno, R., Hodi, F. S., Dranoff, G., Wong, K.-K., and Hammerman, P. S. (2016) Adaptive resistance to therapeutic PD-1 blockade is associated with upregulation of alternative immune checkpoints. *Nature Communications* **7**, 10501
98. Motz, G. T., Santoro, S. P., Wang, L.-P., Garrabrant, T., Lastra, R. R., Hagemann, I. S., Lal, P., Feldman, M. D., Benencia, F., and Coukos, G. (2014) Tumor endothelium FasL establishes a selective immune barrier promoting tolerance in tumors. *Nature Medicine* **20**, 607
99. Motz, Greg T., and Coukos, G. (2013) Deciphering and Reversing Tumor Immune Suppression. *Immunity* **39**, 61-73

100. Dirx, A. E. M., oude Egbrink, M. G. A., Kuijpers, M. J. E., van der Niet, S. T., Heijnen, V. V. T., Steege, J. C. A. B.-t., Wagstaff, J., and Griffioen, A. W. (2003) Tumor Angiogenesis Modulates Leukocyte-Vessel Wall Interactions *in Vivo* by Reducing Endothelial Adhesion Molecule Expression. *Cancer Research* **63**, 2322-2329
101. Huang, Y., Lin, L., Shanker, A., Malhotra, A., Yang, L., Dikov, M. M., and Carbone, D. P. (2011) Resuscitating Cancer Immunosurveillance: Selective Stimulation of DLL1-Notch Signaling in T cells Rescues T-cell Function and Inhibits Tumor Growth. *Cancer Research* **71**, 6122-6131
102. Gaborit, D. I., Chen, H. L., Girgis, K. R., Cunningham, H. T., Meny, G. M., Nadaf, S., Kavanaugh, D., and Carbone, D. P. (1996) Production of vascular endothelial growth factor by human tumors inhibits the functional maturation of dendritic cells. *Nature Medicine* **2**, 1096
103. Terme, M., Pernot, S., Marcheteau, E., Sandoval, F., Benhamouda, N., Colussi, O., Dubreuil, O., Carpentier, A. F., Tartour, E., and Taieb, J. (2013) VEGFA-VEGFR Pathway Blockade Inhibits Tumor-Induced Regulatory T-cell Proliferation in Colorectal Cancer. *Cancer Research* **73**, 539-549
104. Rivera, Lee B., Meyronet, D., Hervieu, V., Frederick, Mitchell J., Bergsland, E., and Bergers, G. (2015) Intratumoral Myeloid Cells Regulate Responsiveness and Resistance to Antiangiogenic Therapy. *Cell Reports* **11**, 577-591



105. De Palma, M., Venneri, M. A., Galli, R., Sergi, L. S., Politi, L. S., Sampaolesi, M., and Naldini, L. (2005) Tie2 identifies a hematopoietic lineage of proangiogenic monocytes required for tumor vessel formation and a mesenchymal population of pericyte progenitors. *Cancer Cell* **8**, 211-226
106. Rigamonti, N., Kadioglu, E., Keklikoglou, I., Wyser Rmili, C., Leow, Ching C., and De Palma, M. (2014) Role of Angiopoietin-2 in Adaptive Tumor Resistance to VEGF Signaling Blockade. *Cell Reports* **8**, 696-706
107. Shojaei, F., Wu, X., Malik, A. K., Zhong, C., Baldwin, M. E., Schanz, S., Fuh, G., Gerber, H.-P., and Ferrara, N. (2007) Tumor refractoriness to anti-VEGF treatment is mediated by CD11b+Gr1+ myeloid cells. *Nature Biotechnology* **25**, 911
108. Fischer, C., Jonckx, B., Mazzone, M., Zacchigna, S., Loges, S., Pattarini, L., Chorianopoulos, E., Liesenborghs, L., Koch, M., De Mol, M., Autiero, M., Wyns, S., Plaisance, S., Moons, L., van Rooijen, N., Giacca, M., Stassen, J.-M., Dewerchin, M., Collen, D., and Carmeliet, P. (2007) Anti-PlGF Inhibits Growth of VEGF(R)-Inhibitor-Resistant Tumors without Affecting Healthy Vessels. *Cell* **131**, 463-475
109. Schmittnaegel, M., Rigamonti, N., Kadioglu, E., Cassarà, A., Wyser Rmili, C., Kiialainen, A., Kienast, Y., Mueller, H.-J., Ooi, C.-H., Laoui, D., and De Palma, M. (2017) Dual angiopoietin-2 and VEGFA inhibition elicits antitumor immunity that is enhanced by PD-1 checkpoint blockade. *Science Translational Medicine* **9**

110. Allen, E., Jabouille, A., Rivera, L. B., Lodewijckx, I., Missiaen, R., Steri, V., Feyen, K., Tawney, J., Hanahan, D., Michael, I. P., and Bergers, G. (2017) Combined antiangiogenic and anti-PD-L1 therapy stimulates tumor immunity through HEV formation. *Science Translational Medicine* **9**
111. Hugo, W., Zaretsky, J. M., Sun, L., Song, C., Moreno, B. H., Hui-Lieskovan, S., Berent-Maoz, B., Pang, J., Chmielowski, B., Cherry, G., Seja, E., Lomeli, S., Kong, X., Kelley, M. C., Sosman, J. A., Johnson, D. B., Ribas, A., and Lo, R. S. (2016) Genomic and Transcriptomic Features of Response to Anti-PD-1 Therapy in Metastatic Melanoma. *Cell* **165**, 35-44
112. Van Allen, E. M., Wagle, N., Stojanov, P., Perrin, D. L., Cibulskis, K., Marlow, S., Jane-Valbuena, J., Friedrich, D. C., Kryukov, G., Carter, S. L., McKenna, A., Sivachenko, A., Rosenberg, M., Kiezun, A., Voet, D., Lawrence, M., Lichtenstein, L. T., Gentry, J. G., Huang, F. W., Fostel, J., Farlow, D., Barbie, D., Gandhi, L., Lander, E. S., Gray, S. W., Joffe, S., Janne, P., Garber, J., MacConaill, L., Lindeman, N., Rollins, B., Kantoff, P., Fisher, S. A., Gabriel, S., Getz, G., and Garraway, L. A. (2014) Whole-exome sequencing and clinical interpretation of formalin-fixed, paraffin-embedded tumor samples to guide precision cancer medicine. *Nature Medicine* **20**, 682
113. Wolchok, J. D., Kluger, H., Callahan, M. K., Postow, M. A., Rizvi, N. A., Lesokhin, A. M., Segal, N. H., Ariyan, C. E., Gordon, R.-A., Reed, K., Burke, M. M., Caldwell, A., Kronenberg, S. A., Agunwamba, B. U., Zhang, X., Lowy, I., Inzunza, H. D., Feely, W., Horak, C. E., Hong, Q., Korman, A.

- J., Wigginton, J. M., Gupta, A., and Sznol, M. (2013) Nivolumab plus Ipilimumab in Advanced Melanoma. *New England Journal of Medicine* **369**, 122-133
114. Carreno, B. M., Magrini, V., Becker-Hapak, M., Kaabinejadian, S., Hundal, J., Petti, A. A., Ly, A., Lie, W.-R., Hildebrand, W. H., Mardis, E. R., and Linette, G. P. (2015) A dendritic cell vaccine increases the breadth and diversity of melanoma neoantigen-specific T cells. *Science* **348**, 803-808
115. Ott, P. A., Hu, Z., Keskin, D. B., Shukla, S. A., Sun, J., Bozym, D. J., Zhang, W., Luoma, A., Giobbie-Hurder, A., Peter, L., Chen, C., Olive, O., Carter, T. A., Li, S., Lieb, D. J., Eisenhaure, T., Gjini, E., Stevens, J., Lane, W. J., Javeri, I., Nellaiappan, K., Salazar, A. M., Daley, H., Seaman, M., Buchbinder, E. I., Yoon, C. H., Harden, M., Lennon, N., Gabriel, S., Rodig, S. J., Barouch, D. H., Aster, J. C., Getz, G., Wucherpfennig, K., Neubergh, D., Ritz, J., Lander, E. S., Fritsch, E. F., Hacohen, N., and Wu, C. J. (2017) An immunogenic personal neoantigen vaccine for patients with melanoma. *Nature* **547**, 217
116. Sahin, U., Derhovanessian, E., Miller, M., Kloke, B.-P., Simon, P., Löwer, M., Bukur, V., Tadmor, A. D., Luxemburger, U., Schrörs, B., Omokoko, T., Vormehr, M., Albrecht, C., Paruzynski, A., Kuhn, A. N., Buck, J., Heesch, S., Schreeb, K. H., Müller, F., Ortseifer, I., Vogler, I., Godehardt, E., Attig, S., Rae, R., Breitkreuz, A., Tolliver, C., Suchan, M., Martic, G., Hohberger, A., Sorn, P., Diekmann, J., Ciesla, J., Waksman, O., Brück, A.-K., Witt, M., Zillgen, M., Rothermel, A., Kasemann, B., Langer, D., Bolte, S., Diken, M., Kreiter, S., Nemecek, R., Gebhardt, C., Grabbe, S., Höller, C., Utikal,

- J., Huber, C., Loquai, C., and Türeci, Ö. (2017) Personalized RNA mutanome vaccines mobilize poly-specific therapeutic immunity against cancer. *Nature* **547**, 222
117. Hiniker, S. M., Reddy, S. A., Maecker, H. T., Subrahmanyam, P. B., Rosenberg-Hasson, Y., Swetter, S. M., Saha, S., Shura, L., and Knox, S. J. (2016) A Prospective Clinical Trial Combining Radiation Therapy With Systemic Immunotherapy in Metastatic Melanoma. *International Journal of Radiation Oncology\*Biography\*Physics* **96**, 578-588
118. Barker, C. A., Postow, M. A., Khan, S. A., Beal, K., Parhar, P. K., Yamada, Y., Lee, N. Y., and Wolchok, J. D. (2013) Concurrent Radiotherapy and Ipilimumab Immunotherapy for Patients with Melanoma. *Cancer Immunology Research* **1**, 92-98
119. Zamarin, D., Holmgaard, R. B., Subudhi, S. K., Park, J. S., Mansour, M., Palese, P., Merghoub, T., Wolchok, J. D., and Allison, J. P. (2014) Localized Oncolytic Virotherapy Overcomes Systemic Tumor Resistance to Immune Checkpoint Blockade Immunotherapy. *Science Translational Medicine* **6**, 226ra232-226ra232
120. De Henau, O., Rausch, M., Winkler, D., Campesato, L. F., Liu, C., Cymerman, D. H., Budhu, S., Ghosh, A., Pink, M., Tchaicha, J., Douglas, M., Tibbitts, T., Sharma, S., Proctor, J., Kosmider, N., White, K., Stern, H., Soglia, J., Adams, J., Palombella, V. J., McGovern, K., Kutok, J. L., Wolchok, J. D., and Merghoub, T. (2016) Overcoming resistance to checkpoint blockade therapy by targeting PI3K $\gamma$  in myeloid cells. *Nature* **539**, 443

121. Cannarile, M. A., Weisser, M., Jacob, W., Jegg, A.-M., Ries, C. H., and Rüttinger, D. (2017) Colony-stimulating factor 1 receptor (CSF1R) inhibitors in cancer therapy. *Journal for ImmunoTherapy of Cancer* **5**, 53
122. Iversen, T. Z., Engell-Noerregaard, L., Ellebaek, E., Andersen, R., Larsen, S. K., Bjoern, J., Zeyher, C., Gouttefangeas, C., Thomsen, B. M., Holm, B., thor Straten, P., Mellempgaard, A., Andersen, M. H., and Svane, I. M. (2014) Long-lasting Disease Stabilization in the Absence of Toxicity in Metastatic Lung Cancer Patients Vaccinated with an Epitope Derived from Indoleamine 2,3 Dioxygenase. *Clinical Cancer Research* **20**, 221-232
123. Andersen, M. H. (2012) The specific targeting of immune regulation: T-cell responses against Indoleamine 2,3-dioxygenase. *Cancer Immunology, Immunotherapy* **61**, 1289-1297
124. Ager, C. R., Reilley, M. J., Nicholas, C., Bartkowiak, T., Jaiswal, A. R., and Curran, M. A. (2017) **Intratumoral STING activation with T cell checkpoint modulation generates systemic antitumor immunity**. *Cancer Immunology Research*
125. Steggerda, S. M., Bennett, M. K., Chen, J., Emberley, E., Huang, T., Janes, J. R., Li, W., MacKinnon, A. L., Makkouk, A., Marguier, G., Murray, P. J., Neou, S., Pan, A., Parlati, F., Rodriguez, M. L. M., Van de Velde, L.-A., Wang, T., Works, M., Zhang, J., Zhang, W., and Gross, M. I. (2017) Inhibition of arginase by CB-1158 blocks myeloid cell-mediated immune suppression in the tumor microenvironment. *Journal for ImmunoTherapy of Cancer* **5**, 101

126. Gross, M., Chen, J., Englert, J., Janes, J., Leone, R., MacKinnon, A., Parlati, F., Rodriguez, M., Shwonek, P., and Powell, J. (2016) Abstract 2329: Glutaminase inhibition with CB-839 enhances anti-tumor activity of PD-1 and PD-L1 antibodies by overcoming a metabolic checkpoint blocking T cell activation. *Cancer Research* **76**, 2329-2329
127. Ueda, H., Howson, J. M. M., Esposito, L., Heward, J., Snook, Chamberlain, G., Rainbow, D. B., Hunter, K. M. D., Smith, A. N., Di Genova, G., Herr, M. H., Dahlman, I., Payne, F., Smyth, D., Lowe, C., Twells, R. C. J., Howlett, S., Healy, B., Nutland, S., Rance, H. E., Everett, V., Smink, L. J., Lam, A. C., Cordell, H. J., Walker, N. M., Bordin, C., Hulme, J., Motzo, C., Cucca, F., Hess, J. F., Metzker, M. L., Rogers, J., Gregory, S., Allahabadia, A., Nithiyananthan, R., Tuomilehto-Wolf, E., Tuomilehto, J., Bingley, P., Gillespie, K. M., Undlien, D. E., Rønningen, K. S., Guja, C., Ionescu-Tîrgoviște, C., Savage, D. A., Maxwell, A. P., Carson, D. J., Patterson, C. C., Franklyn, J. A., Clayton, D. G., Peterson, L. B., Wicker, L. S., Todd, J. A., and Gough, S. C. L. (2003) Association of the T-cell regulatory gene CTLA4 with susceptibility to autoimmune disease. *Nature* **423**, 506
128. Vaidya, B., Pearce, S. H. S., Charlton, S., Marshall, N., Rowan, A. D., Griffiths, I. D., Kendall-Taylor, P., Cawston, T. E., and Young-Min, S. (2002) An association between the CTLA4 exon 1 polymorphism and early rheumatoid arthritis with autoimmune endocrinopathies. *Rheumatology* **41**, 180-183

129. Zhernakova, A., Eerligh, P., Barrera, P., Weseloy, J. Z., Huizinga, T. W. J., Roep, B. O., Wijmenga, C., and Koeleman, B. P. C. (2005) CTLA4 is differentially associated with autoimmune diseases in the Dutch population. *Human Genetics* **118**, 58-66
130. Jin, P., Xiang, B., Huang, G., and Zhou, Z. (2015) The association of cytotoxic T-lymphocyte antigen-4 + 49A/G and CT60 polymorphisms with type 1 diabetes and latent autoimmune diabetes in Chinese adults. *Journal of Endocrinological Investigation* **38**, 149-154
131. Song, G. G., Kim, J.-H., Kim, Y. H., and Lee, Y. H. (2013) Association between CTLA-4 polymorphisms and susceptibility to Celiac disease: A meta-analysis. *Human Immunology* **74**, 1214-1218
132. Fernández-Mestre, M., Sánchez, K., Balbás, O., Gendzekhzadze, K., Ogando, V., Cabrera, M., and Layrisse, Z. (2009) Influence of CTLA-4 gene polymorphism in autoimmune and infectious diseases. *Human Immunology* **70**, 532-535
133. Prokunina, L., Castillejo-López, C., Öberg, F., Gunnarsson, I., Berg, L., Magnusson, V., Brookes, A. J., Tentler, D., Kristjansdóttir, H., Gröndal, G., Bolstad, A. I., Svenungsson, E., Lundberg, I., Sturfelt, G., Jönssen, A., Truedsson, L., Lima, G., Alcocer-Varela, J., Jonsson, R., Gyllensten, U. B., Harley, J. B., Alarcón-Segovia, D., Steinsson, K., and Alarcón-Riquelme, M. E. (2002) A regulatory polymorphism in PDCD1 is associated with susceptibility to systemic lupus erythematosus in humans. *Nature Genetics* **32**, 666

134. Hudson, L. L., Rocca, K., Song, Y. W., and Pandey, J. P. (2002) CTLA-4 gene polymorphisms in systemic lupus erythematosus: a highly significant association with a determinant in the promoter region. *Human Genetics* **111**, 452-455
135. Bertsias, G. K., Nakou, M., Choulaki, C., Raptopoulou, A., Papadimitraki, E., Goulielmos, G., Kritikos, H., Sidiropoulos, P., Tzardi, M., Kardassis, D., Mamalaki, C., and Boumpas, D. T. (2009) Genetic, immunologic, and immunohistochemical analysis of the programmed death 1/programmed death ligand 1 pathway in human systemic lupus erythematosus. *Arthritis & Rheumatism* **60**, 207-218
136. Bertrand, A., Kostine, M., Barnetche, T., Truchetet, M.-E., and Schaeffer, T. (2015) Immune related adverse events associated with anti-CTLA-4 antibodies: systematic review and meta-analysis. *BMC Medicine* **13**, 211
137. Weber, J. S., Antonia, S. J., Topalian, S. L., Schadendorf, D., Larkin, J. M. G., Sznol, M., Liu, H. Y., Waxman, I., and Robert, C. (2015) Safety profile of nivolumab (NIVO) in patients (pts) with advanced melanoma (MEL): A pooled analysis. *Journal of Clinical Oncology* **33**, 9018-9018
138. Robert, C., Schachter, J., Long, G. V., Arance, A., Grob, J. J., Mortier, L., Daud, A., Carlino, M. S., McNeil, C., Lotem, M., Larkin, J., Lorigan, P., Neyns, B., Blank, C. U., Hamid, O., Mateus, C., Shapira-Frommer, R., Kosh, M., Zhou, H., Ibrahim, N., Ebbinghaus, S., and Ribas, A. (2015) Pembrolizumab versus Ipilimumab in Advanced Melanoma. *New England Journal of Medicine* **372**, 2521-2532



139. Postow, M. A. (2015) Managing immune checkpoint-blocking antibody side effects. *Am Soc Clin Oncol Educ Book*, 76-83
140. Juszczak, A., Gupta, A., Karavitaki, N., Middleton, M. R., and Grossman, A. B. (2012) Ipilimumab: a novel immunomodulating therapy causing autoimmune hypophysitis: a case report and review. *Eur J Endocrinol* **167**, 1-5
141. Michot, J. M., Bigenwald, C., Champiat, S., Collins, M., Carbonnel, F., Postel-Vinay, S., Berdelou, A., Varga, A., Bahleda, R., Hollebecque, A., Massard, C., Fuerea, A., Ribrag, V., Gazzah, A., Armand, J. P., Amellal, N., Angevin, E., Noel, N., Boutros, C., Mateus, C., Robert, C., Soria, J. C., Marabelle, A., and Lambotte, O. (2016) Immune-related adverse events with immune checkpoint blockade: a comprehensive review. *European Journal of Cancer* **54**, 139-148
142. Beck, K. E., Blansfield, J. A., Tran, K. Q., Feldman, A. L., Hughes, M. S., Royal, R. E., Kammula, U. S., Topalian, S. L., Sherry, R. M., Kleiner, D., Quezado, M., Lowy, I., Yellin, M., Rosenberg, S. A., and Yang, J. C. (2006) Enterocolitis in Patients With Cancer After Antibody Blockade of Cytotoxic T-Lymphocyte–Associated Antigen 4. *Journal of Clinical Oncology* **24**, 2283-2289
143. Hodi, F. S., O'Day, S. J., McDermott, D. F., Weber, R. W., Sosman, J. A., Haanen, J. B., Gonzalez, R., Robert, C., Schadendorf, D., Hassel, J. C., Akerley, W., van den Eertwegh, A. J. M., Lutzky, J., Lorigan, P., Vaubel, J. M., Linette, G. P., Hogg, D., Ottensmeier, C. H., Lebbé, C., Peschel, C., Quirt, I., Clark, J. I., Wolchok, J. D., Weber, J. S., Tian, J.,

- Yellin , M. J., Nichol , G. M., Hoos , A., and Urba , W. J. (2010) Improved Survival with Ipilimumab in Patients with Metastatic Melanoma. *New England Journal of Medicine* **363**, 711-723
144. Brahmer, J., Reckamp, K. L., Baas, P., Crinò, L., Eberhardt, W. E. E., Poddubskaya, E., Antonia, S., Pluzanski, A., Vokes, E. E., Holgado, E., Waterhouse, D., Ready, N., Gainor, J., Arén Frontera, O., Havel, L., Steins, M., Garassino, M. C., Aerts, J. G., Domine, M., Paz-Ares, L., Reck, M., Baudelet, C., Harbison, C. T., Lestini, B., and Spigel, D. R. (2015) Nivolumab versus Docetaxel in Advanced Squamous-Cell Non–Small-Cell Lung Cancer. *New England Journal of Medicine* **373**, 123-135
145. Hamid , O., Robert , C., Daud , A., Hodi , F. S., Hwu , W.-J., Kefford , R., Wolchok , J. D., Hersey , P., Joseph , R. W., Weber , J. S., Dronca , R., Gangadhar , T. C., Patnaik , A., Zarour , H., Joshua , A. M., Gergich , K., Elassaiss-Schaap , J., Algazi , A., Mateus , C., Boasberg , P., Tumeah , P. C., Chmielowski , B., Ebbinghaus , S. W., Li , X. N., Kang , S. P., and Ribas , A. (2013) Safety and Tumor Responses with Lambrolizumab (Anti–PD-1) in Melanoma. *New England Journal of Medicine* **369**, 134-144
146. Johnston, R. L., Lutzky, J., Chodhry, A., and Barkin, J. S. (2008) Cytotoxic T-Lymphocyte-Associated Antigen 4 Antibody-Induced Colitis and Its Management with Infliximab. *Digestive Diseases and Sciences* **54**, 2538
147. Bernardo, S. G., Moskalenko, M., Pan, M., Shah, S., Sidhu, H. K., Sicular, S., Harcharik, S., Chang, R., Friedlander, P., and Saenger, Y. M. (2013) Elevated rates of transaminitis during ipilimumab therapy for metastatic melanoma. *Melanoma Research* **23**, 47-54

148. Wolchok, J. D., Neyns, B., Linette, G., Negrier, S., Lutzky, J., Thomas, L., Waterfield, W., Schadendorf, D., Smylie, M., Guthrie, T., Grob, J.-J., Chesney, J., Chin, K., Chen, K., Hoos, A., O'Day, S. J., and Lebbé, C. (2010) Ipilimumab monotherapy in patients with pretreated advanced melanoma: a randomised, double-blind, multicentre, phase 2, dose-ranging study. *The Lancet Oncology* **11**, 155-164
149. Ribas, A., Kefford, R., Marshall, M. A., Punt, C. J. A., Haanen, J. B., Marmol, M., Garbe, C., Gogas, H., Schachter, J., Linette, G., Lorigan, P., Kendra, K. L., Maio, M., Trefzer, U., Smylie, M., McArthur, G. A., Dreno, B., Nathan, P. D., Mackiewicz, J., Kirkwood, J. M., Gomez-Navarro, J., Huang, B., Pavlov, D., and Hauschild, A. (2013) Phase III Randomized Clinical Trial Comparing Tremelimumab With Standard-of-Care Chemotherapy in Patients With Advanced Melanoma. *Journal of Clinical Oncology* **31**, 616-622
150. El-Khoueiry, A. B., Melero, I., Crocenzi, T. S., Welling, T. H., Yau, T. C., Yeo, W., Chopra, A., Grosso, J., Lang, L., Anderson, J., Cruz, C. M. D., and Sangro, B. (2015) Phase I/II safety and antitumor activity of nivolumab in patients with advanced hepatocellular carcinoma (HCC): CA209-040. *Journal of Clinical Oncology* **33**, LBA101-LBA101
151. Herbst, R. S., Soria, J.-C., Kowanetz, M., Fine, G. D., Hamid, O., Gordon, M. S., Sosman, J. A., McDermott, D. F., Powderly, J. D., Gettinger, S. N., Kohrt, H. E. K., Horn, L., Lawrence, D. P., Rost, S., Leabman, M., Xiao, Y., Mokatrín, A., Koeppen, H., Hegde, P. S., Mellman, I., Chen, D. S., and

- Hodi, F. S. (2014) Predictive correlates of response to the anti-PD-L1 antibody MPDL3280A in cancer patients. *Nature* **515**, 563
152. Ascierto, P. A., Simeone, E., Sznol, M., Fu, Y.-X., and Melero, I. (2010) Clinical Experiences With Anti-CD137 and Anti-PD1 Therapeutic Antibodies. *Seminars in Oncology* **37**, 508-516
153. Bartkowiak, T., and Curran, M. A. (2015) 4-1BB Agonists: Multi-Potent Potentiators of Tumor Immunity. *Front Oncol* **5**, 117
154. Ryder, M., Callahan, M., Postow, M. A., Wolchok, J., and Fagin, J. A. (2014) Endocrine-related adverse events following ipilimumab in patients with advanced melanoma: a comprehensive retrospective review from a single institution. *Endocr Relat Cancer* **21**, 371-381
155. Corsello, S. M., Barnabei, A., Marchetti, P., De Vecchis, L., Salvatori, R., and Torino, F. (2013) Endocrine side effects induced by immune checkpoint inhibitors. *J Clin Endocrinol Metab* **98**, 1361-1375
156. Blansfield, J. A., Beck, K. E., Tran, K., Yang, J. C., Hughes, M. S., Kammula, U. S., Royal, R. E., Topalian, S. L., Haworth, L. R., Levy, C., Rosenberg, S. A., and Sherry, R. M. (2005) Cytotoxic T-lymphocyte-associated antigen-4 blockage can induce autoimmune hypophysitis in patients with metastatic melanoma and renal cancer. *J Immunother* **28**, 593-598
157. Dillard, T., Yedinak, C. G., Alumkal, J., and Fleseriu, M. (2010) Anti-CTLA-4 antibody therapy associated autoimmune hypophysitis: serious immune related adverse events across a spectrum of cancer subtypes. *Pituitary* **13**, 29-38

158. Iwama, S., De Remigis, A., Callahan, M. K., Slovin, S. F., Wolchok, J. D., and Caturegli, P. (2014) Pituitary Expression of CTLA-4 Mediates Hypophysitis Secondary to Administration of CTLA-4 Blocking Antibody. *Science Translational Medicine* **6**, 230ra245-230ra245
159. Naidoo, J., Page, D. B., Li, B. T., Connell, L. C., Schindler, K., Lacouture, M. E., Postow, M. A., and Wolchok, J. D. (2015) Toxicities of the anti-PD-1 and anti-PD-L1 immune checkpoint antibodies. *Annals of Oncology* **26**, 2375-2391
160. Caturegli, P., Di Dalmazi, G., Lombardi, M., Grosso, F., Larman, H. B., Larman, T., Taverna, G., Cosottini, M., and Lupi, I. (2016) Hypophysitis Secondary to Cytotoxic T-Lymphocyte-Associated Protein 4 Blockade: Insights into Pathogenesis from an Autopsy Series. *Am J Pathol* **186**, 3225-3235
161. Topalian, S. L., Hodi, F. S., Brahmer, J. R., Gettinger, S. N., Smith, D. C., McDermott, D. F., Powderly, J. D., Carvajal, R. D., Sosman, J. A., Atkins, M. B., Leming, P. D., Spigel, D. R., Antonia, S. J., Horn, L., Drake, C. G., Pardoll, D. M., Chen, L., Sharfman, W. H., Anders, R. A., Taube, J. M., McMiller, T. L., Xu, H., Korman, A. J., Jure-Kunkel, M., Agrawal, S., McDonald, D., Kollia, G. D., Gupta, A., Wigginton, J. M., and Sznol, M. (2012) Safety, Activity, and Immune Correlates of Anti-PD-1 Antibody in Cancer. *New England Journal of Medicine* **366**, 2443-2454
162. O'Day, S. J., Maio, M., Chiarion-Sileni, V., Gajewski, T. F., Pehamberger, H., Bondarenko, I. N., Queirolo, P., Lundgren, L., Mikhailov, S., Roman, L., Verschraegen, C., Humphrey, R., Ibrahim, R., de Pril, V., Hoos, A., and

- Wolchok, J. D. (2010) Efficacy and safety of ipilimumab monotherapy in patients with pretreated advanced melanoma: a multicenter single-arm phase II study. *Annals of Oncology* **21**, 1712-1717
163. Eckert, A., Schoeffler, A., Dalle, S., Phan, A., Kiakouama, L., and Thomas, L. (2009) Anti-CTLA4 Monoclonal Antibody Induced Sarcoidosis in a Metastatic Melanoma Patient. *Dermatology* **218**, 69-70
164. Robinson, M. R., Chan, C. C., Yang, J. C., Rubin, B. I., Gracia, G. J., Sen, H. N., Csaky, K. G., and Rosenberg, S. A. (2004) Cytotoxic T lymphocyte-associated antigen 4 blockade in patients with metastatic melanoma: a new cause of uveitis. *J Immunother* **27**, 478-479
165. Fadel , F., Karoui , K. E., and Knebelmann , B. (2009) Anti-CTLA4 Antibody–Induced Lupus Nephritis. *New England Journal of Medicine* **361**, 211-212
166. Izzedine, H., Gueutin, V., Gharbi, C., Mateus, C., Robert, C., Routier, E., Thomas, M., Baumelou, A., and Rouvier, P. (2014) Kidney injuries related to ipilimumab. *Invest New Drugs* **32**, 769-773
167. Bot, I., Blank, C. U., Boogerd, W., and Brandsma, D. (2013) Neurological immune-related adverse events of ipilimumab. *Pract Neurol* **13**, 278-280
168. Loochtan, A. I., Nickolich, M. S., and Hobson-Webb, L. D. (2015) Myasthenia gravis associated with ipilimumab and nivolumab in the treatment of small cell lung cancer. *Muscle Nerve* **52**, 307-308
169. Riaz, N., Havel, J. J., Makarov, V., Desrichard, A., Urba, W. J., Sims, J. S., Hodi, F. S., Martín-Algarra, S., Mandal, R., Sharfman, W. H., Bhatia, S., Hwu, W.-J., Gajewski, T. F., Slingluff, C. L., Chowell, D., Kendall, S.

- M., Chang, H., Shah, R., Kuo, F., Morris, L. G. T., Sidhom, J.-W., Schneck, J. P., Horak, C. E., Weinhold, N., and Chan, T. A. (2017) Tumor and Microenvironment Evolution during Immunotherapy with Nivolumab. *Cell* **171**, 934-949.e915
170. Vesely, M. D., and Schreiber, R. D. (2013) Cancer immunoediting: antigens, mechanisms, and implications to cancer immunotherapy. *Annals of the New York Academy of Sciences* **1284**, 1-5
171. O'Sullivan, T., Saddawi-Konefka, R., Vermi, W., Koebel, C. M., Arthur, C., White, J. M., Uppaluri, R., Andrews, D. M., Ngiow, S. F., Teng, M. W. L., Smyth, M. J., Schreiber, R. D., and Bui, J. D. (2012) Cancer immunoediting by the innate immune system in the absence of adaptive immunity. *The Journal of Experimental Medicine* **209**, 1869-1882
172. Anderson, Ana C., Joller, N., and Kuchroo, Vijay K. (2016) Lag-3, Tim-3, and TIGIT: Co-inhibitory Receptors with Specialized Functions in Immune Regulation. *Immunity* **44**, 989-1004
173. Chen, P. L., Roh, W., Reuben, A., Cooper, Z. A., Spencer, C. N., Prieto, P. A., Miller, J. P., Bassett, R. L., Gopalakrishnan, V., Wani, K., De Macedo, M. P., Austin-Breneman, J. L., Jiang, H., Chang, Q., Reddy, S. M., Chen, W. S., Tetzlaff, M. T., Broaddus, R. J., Davies, M. A., Gershenwald, J. E., Haydu, L., Lazar, A. J., Patel, S. P., Hwu, P., Hwu, W. J., Diab, A., Glitza, I. C., Woodman, S. E., Vence, L. M., Wistuba, II, Amaria, R. N., Kwong, L. N., Prieto, V., Davis, R. E., Ma, W., Overwijk, W. W., Sharpe, A. H., Hu, J., Futreal, P. A., Blando, J., Sharma, P., Allison, J. P., Chin, L., and Wargo, J. A. (2016) Analysis of Immune Signatures in

Longitudinal Tumor Samples Yields Insight into Biomarkers of Response and Mechanisms of Resistance to Immune Checkpoint Blockade. *Cancer Discov* **6**, 827-837

174. Roh, W., Chen, P. L., Reuben, A., Spencer, C. N., Prieto, P. A., Miller, J. P., Gopalakrishnan, V., Wang, F., Cooper, Z. A., Reddy, S. M., Gumbs, C., Little, L., Chang, Q., Chen, W. S., Wani, K., De Macedo, M. P., Chen, E., Austin-Breneman, J. L., Jiang, H., Roszik, J., Tetzlaff, M. T., Davies, M. A., Gershenwald, J. E., Tawbi, H., Lazar, A. J., Hwu, P., Hwu, W. J., Diab, A., Glitza, I. C., Patel, S. P., Woodman, S. E., Amaria, R. N., Prieto, V. G., Hu, J., Sharma, P., Allison, J. P., Chin, L., Zhang, J., Wargo, J. A., and Futreal, P. A. (2017) Integrated molecular analysis of tumor biopsies on sequential CTLA-4 and PD-1 blockade reveals markers of response and resistance. *Sci Transl Med* **9**
175. Fidler, I. J. (1973) Selection of successive tumour lines for metastasis. *Nature: New biology* **242**, 148-149
176. Fidler, I. J., Gersten, D. M., and Budmen, M. B. (1976) Characterization in Vivo and in Vitro of Tumor Cells Selected for Resistance to Syngeneic Lymphocyte-mediated Cytotoxicity. *Cancer Research* **36**, 3160-3165
177. Fidler, I. J., and Kripke, M. L. (1980) Tumor cell antigenicity, host immunity, and cancer metastasis. *Cancer Immunol Immunother* **7**, 201-205
178. Eisenhauer, E. A., Therasse, P., Bogaerts, J., Schwartz, L. H., Sargent, D., Ford, R., Dancey, J., Arbuck, S., Gwyther, S., Mooney, M., Rubinstein, L., Shankar, L., Dodd, L., Kaplan, R., Lacombe, D., and Verweij, J. (2009)



- New response evaluation criteria in solid tumours: Revised RECIST guideline (version 1.1). *European Journal of Cancer* **45**, 228-247
179. Dutta, P., Le, A., Vander Jagt, D. L., Tsukamoto, T., Martinez, G. V., Dang, C. V., and Gillies, R. J. (2013) Evaluation of LDH-A and Glutaminase Inhibition *In Vivo* by Hyperpolarized <sup>13</sup>C-Pyruvate Magnetic Resonance Spectroscopy of Tumors. *Cancer Research* **73**, 4190-4195
180. Curran, M. A., and Allison, J. P. (2009) Tumor vaccines expressing flt3 ligand synergize with ctla-4 blockade to reject preimplanted tumors. *Cancer Res* **69**, 7747-7755
181. Kelderman, S., Heemskerk, B., van Tinteren, H., van den Brom, R. R. H., Hospers, G. A. P., van den Eertwegh, A. J. M., Kapiteijn, E. W., de Groot, J. W. B., Soetekouw, P., Jansen, R. L., Fiets, E., Furness, A. J. S., Renn, A., Krzystanek, M., Szallasi, Z., Lorigan, P., Gore, M. E., Schumacher, T. N. M., Haanen, J. B. A. G., Larkin, J. M. G., and Blank, C. U. (2014) Lactate dehydrogenase as a selection criterion for ipilimumab treatment in metastatic melanoma. *Cancer Immunol Immunother* **63**, 449-458
182. Dick, J., Lang, N., Slynko, A., Kopp-Schneider, A., Schulz, C., Dimitrakopoulou-Strauss, A., Enk, A. H., and Hassel, J. C. (2016) Use of LDH and autoimmune side effects to predict response to ipilimumab treatment. *Immunotherapy* **8**, 1033-1044
183. Jain, N., Nguyen, H., Chambers, C., and Kang, J. (2010) Dual function of CTLA-4 in regulatory T cells and conventional T cells to prevent

- multiorgan autoimmunity. *Proceedings of the National Academy of Sciences* **107**, 1524-1528
184. Billiard, J., Dennison, J. B., Briand, J., Annan, R. S., Chai, D., Colón, M., Dodson, C. S., Gilbert, S. A., Greshock, J., Jing, J., Lu, H., McSurdy-Freed, J. E., Orband-Miller, L. A., Mills, G. B., Quinn, C. J., Schneck, J. L., Scott, G. F., Shaw, A. N., Waitt, G. M., Wooster, R. F., and Duffy, K. J. (2013) Quinoline 3-sulfonamides inhibit lactate dehydrogenase A and reverse aerobic glycolysis in cancer cells. *Cancer & Metabolism* **1**, 19
185. Xie, H., Hanai, J.-i., Ren, J.-G., Kats, L., Burgess, K., Bhargava, P., Signoretti, S., Billiard, J., Duffy, Kevin J., Grant, A., Wang, X., Lorkiewicz, Pawel K., Schatzman, S., Bousamra, M., II, Lane, Andrew N., Higashi, Richard M., Fan, Teresa W. M., Pandolfi, Pier P., Sukhatme, Vikas P., and Seth, P. Targeting Lactate Dehydrogenase-A Inhibits Tumorigenesis and Tumor Progression in Mouse Models of Lung Cancer and Impacts Tumor-Initiating Cells. *Cell Metabolism* **19**, 795-809
186. Liu, Y., Bell, T., Zhang, H., Sun, Y., Li, C. J., Feng, N., Huang, S., Guo, H., Wang, J., Ahmed, M., Zhang, V., Lam, L. T., Nomie, K., Zhang, L., Di Francesco, M. E., Marszalek, J., and Wang, M. (2016) Targeting Oxphos Pathway Against Ibrutinib Resistance to Mantle Cell Lymphoma. *Blood* **128**, 290-290
187. Moreira, D., Zhao, X., Won, H., Duttagupta, P., Pal, S., and Kortylewski, M. 261. Gain-of-Function Effect Augments Therapeutic Efficacy of CpG-STAT3 Anti-Sense Oligonucleotide Against Castration-Resistant Prostate Cancers. *Molecular Therapy* **24**, S103

188. Choi, B. K., Lee, D. Y., Lee, D. G., Kim, Y. H., Kim, S.-H., Oh, H. S., Han, C., and Kwon, B. S. (2016) 4-1BB signaling activates glucose and fatty acid metabolism to enhance CD8<sup>+</sup> T cell proliferation. *Cellular & Molecular Immunology* **14**, 748
189. Williams, J. B., Horton, B. L., Zheng, Y., Duan, Y., Powell, J. D., and Gajewski, T. F. (2017) The EGR2 targets LAG-3 and 4-1BB describe and regulate dysfunctional antigen-specific CD8<sup>+</sup> T cells in the tumor microenvironment. *The Journal of Experimental Medicine*
190. Xu, Y., Li, F., Lv, L., Li, T., Zhou, X., Deng, C.-X., Guan, K.-L., Lei, Q.-Y., and Xiong, Y. (2014) Oxidative Stress Activates SIRT2 to Deacetylate and Stimulate Phosphoglycerate Mutase. *Cancer Research* **74**, 3630-3642
191. Singh, S., Brocker, C., Koppaka, V., Chen, Y., Jackson, B. C., Matsumoto, A., Thompson, D. C., and Vasiliou, V. (2013) Aldehyde dehydrogenases in cellular responses to oxidative/electrophilic stress. *Free Radical Biology and Medicine* **56**, 89-101
192. Hartley, D. P., Ruth, J. A., and Petersen, D. R. (1995) The Hepatocellular Metabolism of 4-Hydroxynonenal by Alcohol Dehydrogenase, Aldehyde Dehydrogenase, and Glutathione S-Transferase. *Archives of Biochemistry and Biophysics* **316**, 197-205
193. Tarasenko, T. N., Pacheco, S. E., Koenig, M. K., Gomez-Rodriguez, J., Kapnick, S. M., Diaz, F., Zervas, P. M., Barca, E., Sudderth, J., DeBerardinis, R. J., Covian, R., Balaban, R. S., DiMauro, S., and McGuire, P. J. (2017) Cytochrome c Oxidase Activity Is a Metabolic

- Checkpoint that Regulates Cell Fate Decisions During T Cell Activation and Differentiation. *Cell Metabolism* **25**, 1254-1268.e1257
194. Wang, R., and Green, D. R. (2012) Metabolic checkpoints in activated T cells. *Nature immunology* **13**, 907
195. Chang, C.-H., Qiu, J., O'Sullivan, D., Buck, Michael D., Noguchi, T., Curtis, Jonathan D., Chen, Q., Gindin, M., Gubin, Matthew M., van der Windt, Gerritje J. W., Tonc, E., Schreiber, Robert D., Pearce, Edward J., and Pearce, Erika L. (2015) Metabolic Competition in the Tumor Microenvironment Is a Driver of Cancer Progression. *Cell* **162**, 1229-1241
196. Sukumar, M., Roychoudhuri, R., and Restifo, Nicholas P. (2015) Nutrient Competition: A New Axis of Tumor Immunosuppression. *Cell* **162**, 1206-1208
197. Huber, V., Camisaschi, C., Berzi, A., Ferro, S., Lugini, L., Triulzi, T., Tuccitto, A., Tagliabue, E., Castelli, C., and Rivoltini, L. (2017) Cancer acidity: An ultimate frontier of tumor immune escape and a novel target of immunomodulation. *Seminars in Cancer Biology* **43**, 74-89
198. Garcia-Diaz, A., Shin, D. S., Moreno, B. H., Saco, J., Escuin-Ordinas, H., Rodriguez, G. A., Zaretsky, J. M., Sun, L., Hugo, W., Wang, X., Parisi, G., Saus, C. P., Torrejon, D. Y., Graeber, T. G., Comin-Anduix, B., Hu-Lieskovan, S., Damoiseaux, R., Lo, R. S., and Ribas, A. Interferon Receptor Signaling Pathways Regulating PD-L1 and PD-L2 Expression. *Cell Reports* **19**, 1189-1201

199. Serrao, E. M., and Brindle, K. M. (2016) Potential Clinical Roles for Metabolic Imaging with Hyperpolarized [1-(13)C]Pyruvate. *Front Oncol* **6**, 59
200. Wilson, D. M., and Kurhanewicz, J. (2014) Hyperpolarized 13C MR for molecular imaging of prostate cancer. *J Nucl Med* **55**, 1567-1572
201. Buck, M. D., Sowell, R. T., Kaech, S. M., and Pearce, E. L. (2017) Metabolic Instruction of Immunity. *Cell* **169**, 570-586
202. Ai, M., and Curran, M. A. (2015) Immune checkpoint combinations from mouse to man. *Cancer immunology, immunotherapy : CII*
203. Pardoll, D. M. (2012) The blockade of immune checkpoints in cancer immunotherapy. *Nat Rev Cancer* **12**, 252-264
204. Schaer, D. A., Hirschhorn-Cymerman, D., and Wolchok, J. D. (2014) Targeting tumor-necrosis factor receptor pathways for tumor immunotherapy. *J Immunother Cancer* **2**, 7
205. Bartkowiak, T., and Curran, M. A. (2015) Accelerating Cancer Immunotherapy Through 4-1BB Activation. *Frontiers in Oncology* **5**
206. Segal, N. H., Gopal, A. K., Bhatia, S., Kohrt, H. E., Levy, R., Pishvaian, M. J., Houot, R., Bartlett, N., Nghiem, P., Kronenberg, S. A., Thall, A. D., Mugundu, G., Huang, B., and Davis, C. (2014) A phase 1 study of PF-05082566 (anti-4-1BB) in patients with advanced cancer. *Journal of Clinical Oncology* **32**, 3007-3007
207. Michot, J. M., Bigenwald, C., Champiat, S., Collins, M., Carbonnel, F., Postel-Vinay, S., Berdelou, A., Varga, A., Bahleda, R., Hollebecque, A., Massard, C., Fuerea, A., Ribrag, V., Gazzah, A., Armand, J. P., Amellal,

- N., Angevin, E., Noel, N., Boutros, C., Mateus, C., Robert, C., Soria, J. C., Marabelle, A., and Lambotte, O. (2016) Immune-related adverse events with immune checkpoint blockade: a comprehensive review. *Eur J Cancer* **54**, 139-148
208. Sun, Y., Lin, X., Chen, H. M., Wu, Q., Subudhi, S. K., Chen, L., and Fu, Y. X. (2002) Administration of agonistic anti-4-1BB monoclonal antibody leads to the amelioration of experimental autoimmune encephalomyelitis. *J Immunol* **168**, 1457-1465
209. Kocak, E., Lute, K., Chang, X., May, K. F., Jr., Exten, K. R., Zhang, H., Abdessalam, S. F., Lehman, A. M., Jarjoura, D., Zheng, P., and Liu, Y. (2006) Combination therapy with anti-CTL antigen-4 and anti-4-1BB antibodies enhances cancer immunity and reduces autoimmunity. *Cancer Res* **66**, 7276-7284
210. Dubrot, J., Milheiro, F., Alfaro, C., Palazon, A., Martinez-Forero, I., Perez-Gracia, J. L., Morales-Kastresana, A., Romero-Trevejo, J. L., Ochoa, M. C., Hervas-Stubbs, S., Prieto, J., Jure-Kunkel, M., Chen, L., and Melero, I. (2010) Treatment with anti-CD137 mAbs causes intense accumulations of liver T cells without selective antitumor immunotherapeutic effects in this organ. *Cancer immunology, immunotherapy : CII* **59**, 1223-1233
211. Segal, N. H., Logan, T. F., Hodi, F. S., McDermott, D. F., Melero, I., Hamid, O., Schmidt, H., Robert, C., Chiarion-Sileni, V., Ascierto, P. A., Maio, M., Urba, W. J., Gangadhar, T. C., Suryawanshi, S., Neely, J., Jure-Kunkel, M., Krishnan, S., Kohrt, H. E., Sznol, M., and Levy, R. (2016)

Results From an Integrated Safety Analysis of Urelumab, an Agonist Anti-CD137 Monoclonal Antibody. *Clin Cancer Res*

212. Bartkowiak, T., Singh, S., Yang, G., Galvan, G., Haria, D., Ai, M., Allison, J. P., Sastry, K. J., and Curran, M. A. (2015) Unique potential of 4-1BB agonist antibody to promote durable regression of HPV+ tumors when combined with an E6/E7 peptide vaccine. *Proc Natl Acad Sci U S A* **112**, E5290-5299
213. Curran, M. A., Geiger, T. L., Montalvo, W., Kim, M., Reiner, S. L., Al-Shamkhani, A., Sun, J. C., and Allison, J. P. (2013) Systemic 4-1BB activation induces a novel T cell phenotype driven by high expression of Eomesodermin. *J Exp Med* **210**, 743-755
214. Peng, J., Hamanishi, J., Matsumura, N., Abiko, K., Murat, K., Baba, T., Yamaguchi, K., Horikawa, N., Hosoe, Y., Murphy, S. K., Konishi, I., and Mandai, M. (2015) Chemotherapy Induces Programmed Cell Death-Ligand 1 Overexpression via the Nuclear Factor-kappaB to Foster an Immunosuppressive Tumor Microenvironment in Ovarian Cancer. *Cancer Res* **75**, 5034-5045
215. Zhou, X., and Hansson, G. K. (2004) Effect of sex and age on serum biochemical reference ranges in C57BL/6J mice. *Comp Med* **54**, 176-178
216. Chen, S., Lee, L. F., Fisher, T. S., Jessen, B., Elliott, M., Evering, W., Logronio, K., Tu, G. H., Tsaparikos, K., Li, X., Wang, H., Ying, C., Xiong, M., VanArsdale, T., and Lin, J. C. (2015) Combination of 4-1BB agonist and PD-1 antagonist promotes antitumor effector/memory CD8 T cells in a poorly immunogenic tumor model. *Cancer Immunol Res* **3**, 149-160

217. Qui, H. Z., Hagymasi, A. T., Bandyopadhyay, S., St Rose, M. C., Ramanarasimhaiah, R., Menoret, A., Mittler, R. S., Gordon, S. M., Reiner, S. L., Vella, A. T., and Adler, A. J. (2011) CD134 Plus CD137 Dual Costimulation Induces Eomesodermin in CD4 T Cells To Program Cytotoxic Th1 Differentiation. *J Immunol* **187**, 3555-3564
218. Song, C., Sadashivaiah, K., Furusawa, A., Davila, E., Tamada, K., and Banerjee, A. (2014) Eomesodermin is required for antitumor immunity mediated by 4-1BB-agonist immunotherapy. *Oncoimmunology* **3**, e27680
219. Akhmetzyanova, I., Zelinsky, G., Littwitz-Salomon, E., Malyshkina, A., Dietze, K. K., Streeck, H., Brandau, S., and Dittmer, U. (2016) CD137 Agonist Therapy Can Reprogram Regulatory T Cells into Cytotoxic CD4+ T Cells with Antitumor Activity. *J Immunol* **196**, 484-492
220. Banchereau, J., Bazan, F., Blanchard, D., Briere, F., Galizzi, J. P., van Kooten, C., Liu, Y. J., Rousset, F., and Saeland, S. (1994) The CD40 antigen and its ligand. *Annu Rev Immunol* **12**, 881-922
221. Futagawa, T., Akiba, H., Kodama, T., Takeda, K., Hosoda, Y., Yagita, H., and Okumura, K. (2002) Expression and function of 4-1BB and 4-1BB ligand on murine dendritic cells. *Int Immunol* **14**, 275-286
222. Kienzle, G., and von Kempis, J. (2000) CD137 (ILA/4-1BB), expressed by primary human monocytes, induces monocyte activation and apoptosis of B lymphocytes. *Int Immunol* **12**, 73-82
223. Liaskou, E., Wilson, D. V., and Oo, Y. H. (2012) Innate immune cells in liver inflammation. *Mediators Inflamm* **2012**, 949157



224. Kinoshita, M., Uchida, T., Sato, A., Nakashima, M., Nakashima, H., Shono, S., Habu, Y., Miyazaki, H., Hiroi, S., and Seki, S. (2010) Characterization of two F4/80-positive Kupffer cell subsets by their function and phenotype in mice. *J Hepatol* **53**, 903-910
225. Gomez Perdiguero, E., Klapproth, K., Schulz, C., Busch, K., Azzoni, E., Crozet, L., Garner, H., Trouillet, C., de Bruijn, M. F., Geissmann, F., and Rodewald, H. R. (2015) Tissue-resident macrophages originate from yolk-sac-derived erythro-myeloid progenitors. *Nature* **518**, 547-551
226. Dixon, L. J., Barnes, M., Tang, H., Pritchard, M. T., and Nagy, L. E. (2013) Kupffer cells in the liver. *Compr Physiol* **3**, 785-797
227. Heydtmann, M., and Adams, D. H. (2009) Chemokines in the immunopathogenesis of hepatitis C infection. *Hepatology* **49**, 676-688
228. Oo, Y. H., Shetty, S., and Adams, D. H. (2010) The role of chemokines in the recruitment of lymphocytes to the liver. *Dig Dis* **28**, 31-44
229. Huber, M., Steinwald, V., Guralnik, A., Brustle, A., Kleemann, P., Rosenplanter, C., Decker, T., and Lohoff, M. (2008) IL-27 inhibits the development of regulatory T cells via STAT3. *Int Immunol* **20**, 223-234
230. Morishima, N., Owaki, T., Asakawa, M., Kamiya, S., Mizuguchi, J., and Yoshimoto, T. (2005) Augmentation of effector CD8+ T cell generation with enhanced granzyme B expression by IL-27. *J Immunol* **175**, 1686-1693
231. Siebler, J., Wirtz, S., Frenzel, C., Schuchmann, M., Lohse, A. W., Galle, P. R., and Neurath, M. F. (2008) Cutting edge: a key pathogenic role of IL-27 in T cell- mediated hepatitis. *J Immunol* **180**, 30-33

232. Simpson, T. R., Li, F., Montalvo-Ortiz, W., Sepulveda, M. A., Bergerhoff, K., Arce, F., Roddie, C., Henry, J. Y., Yagita, H., Wolchok, J. D., Peggs, K. S., Ravetch, J. V., Allison, J. P., and Quezada, S. A. (2013) Fc-dependent depletion of tumor-infiltrating regulatory T cells co-defines the efficacy of anti-CTLA-4 therapy against melanoma. *J Exp Med* **210**, 1695-1710
233. Airoidi, I., and Ribatti, D. (2011) Regulation of angiostatic chemokines driven by IL-12 and IL-27 in human tumors. *J Leukoc Biol* **90**, 875-882
234. Shimizu, M., Shimamura, M., Owaki, T., Asakawa, M., Fujita, K., Kudo, M., Iwakura, Y., Takeda, Y., Luster, A. D., Mizuguchi, J., and Yoshimoto, T. (2006) Antiangiogenic and antitumor activities of IL-27. *J Immunol* **176**, 7317-7324
235. Melero, I., Rouzaut, A., Motz, G. T., and Coukos, G. (2014) T-cell and NK-cell infiltration into solid tumors: a key limiting factor for efficacious cancer immunotherapy. *Cancer Discov* **4**, 522-526
236. Boisvert, J., Kunkel, E. J., Campbell, J. J., Keeffe, E. B., Butcher, E. C., and Greenberg, H. B. (2003) Liver-infiltrating lymphocytes in end-stage hepatitis C virus: subsets, activation status, and chemokine receptor phenotypes. *J Hepatol* **38**, 67-75
237. Curran, M. A., Montalvo, W., Yagita, H., and Allison, J. P. (2010) PD-1 and CTLA-4 combination blockade expands infiltrating T cells and reduces regulatory T and myeloid cells within B16 melanoma tumors. *Proc Natl Acad Sci U S A* **107**, 4275-4280
238. Quezada, S. A., Peggs, K. S., Curran, M. A., and Allison, J. P. (2006) CTLA4 blockade and GM-CSF combination immunotherapy alters the

- intratumor balance of effector and regulatory T cells. *J Clin Invest* **116**, 1935-1945
239. Cocco, C., Giuliani, N., Di Carlo, E., Ognio, E., Storti, P., Abeltino, M., Sorrentino, C., Ponzoni, M., Ribatti, D., and Airoidi, I. (2010) Interleukin-27 acts as multifunctional antitumor agent in multiple myeloma. *Clin Cancer Res* **16**, 4188-4197
240. Fabbi, M., Carbotti, G., and Ferrini, S. (2017) Dual Roles of IL-27 in Cancer Biology and Immunotherapy. *Mediators Inflamm* **2017**, 3958069
241. Wang, W., Lau, R., Yu, D., Zhu, W., Korman, A., and Weber, J. (2009) PD1 blockade reverses the suppression of melanoma antigen-specific CTL by CD4+ CD25(Hi) regulatory T cells. *Int Immunol* **21**, 1065-1077
242. Fabbi, M., Carbotti, G., and Ferrini, S. (2017) Dual Roles of IL-27 in Cancer Biology and Immunotherapy. *Mediators of Inflammation* **2017**, 14
243. Wohlleber, D., and Knolle, P. A. The Liver as an Immune-Privileged Site. in *Infection, Immune Homeostasis and Immune Privilege* (Stein-Streilein, J. ed.), Springer, Basel, 2012. pp
244. Oldhafer, F., Bock, M., Falk, C. S., and Vondran, F. W. (2016) Immunological aspects of liver cell transplantation. *World J Transplant* **6**, 42-53
245. Tiegs, G., and Lohse, A. W. (2010) Immune tolerance: What is unique about the liver. *Journal of Autoimmunity* **34**, 1-6
246. Horst, A. K., Neumann, K., Diehl, L., and Tiegs, G. (2016) Modulation of liver tolerance by conventional and nonconventional antigen-presenting

cells and regulatory immune cells. *Cellular & Molecular Immunology* **13**, 277

247. Li, F., and Tian, Z. (2013) The liver works as a school to educate regulatory immune cells. *Cellular And Molecular Immunology* **10**, 292

## VITA

Ashvin Rameshlal Jaiswal was born in Amravati, Maharashtra, India on September, 03, 1982, the son of Suman Jaiswal and Rameshlal Jaiswal. After completing high school at Shri Shivaji Science College Amravati, India in 2000, he entered his undergraduate studies at Amravati University. He received the degree of Bachelor of Pharmacy from Amravati University in May 2004. For the next four years, he worked as a sales officer at Sun Pharmaceutical Industries Limited in Mumbai, India before entering a Master's program in Pharmaceutical Sciences at Idaho State University. He received his MS in Pharmaceutical Sciences in May 2011. He worked for a year as a research associate in IQuum Inc. (Roche) and Ipsen Bioscience, Inc (Baxter). In August 2012 he began his PhD studies at The University of Texas MD Anderson Cancer Center UTHHealth Graduate School of Biomedical Sciences.